Bralower, T.J., Premoli Silva, I., and Malone, M.J. (Eds.)
Proceedings of the Ocean Drilling Program, Scientific Results Volume 198

7. Early to Mid-Cretaceous Calcareous Nannoplankton from the Northwest Pacific Ocean, Leg 198, Shatsky Rise[1]

Paul R. Bown[2]

ABSTRACT

During Ocean Drilling Program Leg 198, Sites 1207, 1208, 1212, 1213, and 1214 were drilled on Shatsky Rise, coring Lower to mid-Cretaceous successions of nannofossil chalk, porcellanite, and chert. Although recovery was poor, these sites yielded an outstanding record of calcareous nannoplankton, providing valuable data concerning the evolutionary succession and paleobiogeography of the largest Cretaceous marine habitat. Mid-Cretaceous sections (Aptian–Cenomanian) were recovered at all sites, and Site 1213 includes an apparently complete Berriasian–Hauterivian section. Biostratigraphic dating is problematic in places because of the absence or rarity of zonal fossils of both Boreal and Tethyan affinity. The majority of nannofossil assemblages are relatively typical of this age, but there are clear differences that set them apart from coeval epicontinental assemblages: for example, *Lithraphidites carniolensis* is common to abundant throughout and was most likely an oceanic-adapted taxon; the cold- to temperate-water species *Crucibiscutum salebrosum*, *Repagulum parvidentatum,* and *Seribiscutum primitivum* are entirely absent, indicating the persistence of tropical, warm surface water temperatures; and the warm-water species *Hayesites irregularis* is common. Most striking, however, is the virtual absence of *Nannoconus* and *Micrantholithus*, both taxa that were conspicuous and often common components of many Tethyan and Atlantic nannofloras. These forms were almost certainly neritic adapted and usually absent in deep open-ocean settings away from guyots and plat-

[1]Bown, P.R., 2005. Early to mid-Cretaceous calcareous nannoplankton from the northwest Pacific Ocean, ODP Leg 198, Shatsky Rise. *In* Bralower, T.J., Premoli Silva, I., and Malone, M.J. (Eds.), *Proc. ODP, Sci. Results*, 198, 1–82 [Online]. Available from World Wide Web: <http://www-odp.tamu.edu/publications/198_SR/VOLUME/CHAPTERS/103.PDF>. [Cited YYYY-MM-DD]
[2]Department of Earth Sciences, University College London, Gower Street, London WC1E 6BT, United Kingdom. **p.bown@ucl.ac.uk**

Initial receipt: 22 February 2004
Acceptance: 19 February 2005
Web publication: 14 December 2005
Ms 198SR-103

forms. Other Tethyan taxa are also absent or rare and sporadically distributed (e.g., *Calcicalathina oblongata*, *Conusphaera* spp., *Tubodiscus verenae,* and *Lithraphidites bollii*), and factors related to neritic environments presumably controlled their distribution. Site 1213 also records extended Early Cretaceous ranges for species previously thought to have become extinct during the Late Jurassic (e.g., *Axopodorhabdus cylindratus*, *Hexapodorhabdus cuvillieri,* and *Biscutum dorsetensis*), suggesting these species became Pacific-restricted prior to their extinction. *Watznaueria britannica* may also have been a species with Pacific affinities before reexpansion of its biogeography in the early Aptian.

One new genus (*Mattiolia*) and thirteen new species (*Zeugrhabdotus clarus, Zeugrhabdotus petrizzoae, Helicolithus leckiei, Rhagodiscus amplus, Rhagodiscus robustus, Rhagodiscus sageri, Rhagodiscus adinfinitus, Tubodiscus bellii, Tubodiscus frankiae, Gartnerago ponticula, Haqius peltatus, Mattiolia furva,* and *Kokia stellata*) are described from the Shatsky Rise Lower Cretaceous section.

INTRODUCTION

Five sites (1207, 1208, 1212, 1213, and 1214) drilled during Ocean Drilling Program (ODP) Leg 198 (September–October 2001) on Shatsky Rise (northwest Pacific Ocean) cored Lower to mid-Cretaceous successions of nannofossil chalk, porcellanite, and chert, which, although poorly recovered, yielded an outstanding record of calcareous nannoplankton. Nannoplankton appeared in the Late Triassic (~225 Ma) and diversified rapidly in the Early Jurassic (205–188 Ma), but much of the remainder of the Mesozoic was characterized by steady increases in diversity and background evolutionary rates (Bown et al., 2004). The Jurassic/Cretaceous boundary interval saw considerable taxonomic reorganization of nannoplankton, with high turnover rates at species level, the appearance of several important new nannolith groups (e.g., nannoconids), the putative first record of widespread nannofossil-generated carbonates, and the onset of significant paleobiogeographic differentiation (Bown and Cooper, 1999; Bornemann et al., 2003; Bown et al., 2004). The exact nature and timing of events through this interval, in particular, have been difficult to determine precisely due to the absence of stratigraphically complete nannofossil-bearing sections. Continental shelf sections of this age are frequently incomplete as a result of sea level lowstands; only a small number of nannofossil-bearing oceanic sections have been recovered, and these are virtually restricted to the Atlantic (e.g., Bralower et al., 1989).

Nannofossil assemblages from the Leg 198 sections provide an excellent record of the final stages of the Jurassic–Cretaceous evolutionary transition and their subsequent history through the Early to mid-Cretaceous, including oceanic anoxic events (OAEs) 1a and 1b (early Aptian and early Albian, respectively). The sites, crucially, represent a record of truly oceanic nannoplankton from by far the largest Cretaceous marine habitat, the Pacific Ocean. These findings can be compared to the better known epicontinental shelf assemblages, which form the basis for much of our understanding of paleoecology (and resulting paleoceanographic proxies) and evolution (and resulting biostratigraphic events). This paper includes a discussion of the biostratigraphic analysis, which was problematic in places due to missing marker species. We also discuss the paleobiogeographic and paleoceanographic implications of these Lower Cretaceous tropical coccolithophore assemblages and shed

light on the debate concerning the paleoecologically enigmatic nannolith groups, the nannoconids and braarudosphaerids (*Micrantholithus* and *Braarudosphaera*).

MATERIAL AND GEOLOGICAL SETTING

Shatsky Rise is a moderately sized large igneous province that was erupted episodically at a hotspot triple junction intersection between 146 and 133 Ma (Tithonian–Valanginian) at equatorial latitudes. Subsidence of the rise occurred soon after its construction, and Early Cretaceous water depths were probably on the order of 1.0–2.3 km. The sites were thus above the calcite compensation depth throughout the Cretaceous (Bralower, Premoli Silva, Malone, et al., 2002). Shatsky Rise was located close to the equator through the entire Early Cretaceous interval, drifting around 8° from a slightly northerly location between 140 and 120 Ma and maintaining an equatorial position between 120 and 100 Ma (Bralower, Premoli Silva, Malone, et al., 2002; **Sager et al.,** this volume; Robinson et al., 2004).

Site 1207 is located on the northernmost high, Site 1208 on the Central High, and Sites 1212–1214 (the latter is equivalent to Deep Sea Drilling Project [DSDP] Site 306) on the Southern High of Shatsky Rise (Fig. **F1**). The Northern and Southern Highs are currently separated by 5° of latitude. The Cretaceous sections recovered at all three sites are characterized by ubiquitous and abundant chert that greatly affected core recovery, which was poor throughout (7%–13%) (Bralower, Premoli Silva, Malone, et al., 2002). Nevertheless, every core produced some sediment, usually chert or porcellanite, accompanied by layers or vugs of variably lithified nannofossil-rich carbonate. We were able to generate a continuous calcareous nannoplankton record, but sample spacing is often limited to 9–10 m and the small amount of carbonate sediment available generally prohibited the recovery of foraminifers (Bralower, Premoli Silva, Malone, et al., 2002).

Hole 1208A was terminated after recovery of one Albian core, and Site 1212 recovered only four Albian cores (10 m), but both are included here for completeness.

F1. Bathymetric map of Shatsky Rise, p. 43.

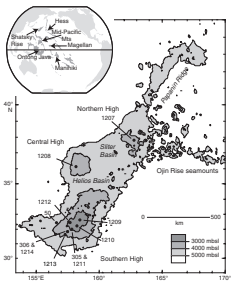

T1. Calcareous nannofossils, Site 1213, p. 48.

METHODS

Calcareous nannofossils were analyzed using simple smear slides and standard light microscope techniques (Bown and Young, 1998). Samples were analyzed semiquantitatively; abundance and preservation categories are given in Table **T1.** Biostratigraphy is described with reference to the lowermost Cretaceous NK zones of Bralower et al. (1989), Lower Cretaceous NC zones of Roth (1978, 1983) with subzones after Bralower (1987) and Bralower et al. (1993), and Upper Cretaceous zones of Burnett (1998). The biostratigraphic zones, chronostratigraphy, and timescale correlations are after Shipboard Scientific Party (2002a).

NANNOFOSSIL RESULTS

Site 1213

Smear slides were produced from 61 sample intervals of Site 1213. All but four yielded nannofossils; the four barren samples came from an organic-rich interval (OAE1a, see below) in Core 198-1213B-8R. Nannofossil abundance was usually high and preservation consistently moderate to good. The stratigraphic distribution of nannoplankton is shown in Table **T1,** an age-depth plot in Figure **F2,** and selected datum events, zonal boundaries, and chronostratigraphic interpretations in Figure **F3.** The assemblages are largely composed of cosmopolitan species, but there are a number of distinctive features that most likely reflect the position and paleoceanography of the Shatsky Rise area. There are two striking absences from the Lower Cretaceous assemblages: first the total absence of *Micrantholithus* and second the almost total absence of *Nannoconus* (trace amounts occur in several upper Albian samples). Both these nannofossil genera are often numerically significant assemblage components, *Micrantholithus* across a wide range of latitudes and *Nannoconus* particularly in the western Tethys–proto-Atlantic–Caribbean region (Street and Bown, 2000). *Braarudosphaera*, a close relative of *Micrantholithus* and a conspicuous component of many Aptian–Cenomanian epicontinental assemblages, was found in only two upper Albian samples.

Other significant absences or trace occurrences only include *Calcicalathina oblongata*, *Conusphaera mexicana*, *Conusphaera rothii*, *Tubodiscus verenae*, and *Lithraphidites bollii*, all Tethyan marker taxa. *Eiffellithus primus*, *Eiffellithus striatus*, and *Eiffellithus windii* are rare and present in only a few samples.

Notable occurrences include the presence of *Podorhabdus grassei* and *Axopodorhabdus cylindratus*, not previously recorded above the Tithonian (Upper Jurassic) (Bralower et al., 1989; Bown and Cooper, 1998), the presence of the Tethyan taxa *Haqius ellipticus*, *Umbria granulosa*, and *Rucinolithus wisei*, and the putative high-latitude taxa *Stradnerlithus silvaradius* and *Kokia*. *Lithraphidites carniolensis* is conspicuously abundant throughout.

Nannofossil biostratigraphy of the lowermost cores could not always be achieved by straightforward application of existing biostratigraphic schemes because of the absence or sporadic occurrence of many standard marker species of both Tethyan and Boreal affinity. However, there appears to be a relatively continuous Berriasian–Hauterivian section but an unconformity between the Hauterivian and lower Aptian. Cores 198-1213B-9R through 7R are mid-Cretaceous in age (lower Aptian–Cenomanian) and the nannofossil biostratigraphy is relatively straightforward. The biostratigraphic results are summarized below, and datum and zone details are provided in **"Lower to Mid-Cretaceous Biostratigraphy,"** p. 6, and Figure **F3.**

The deepest core (Core 198-1213B-27R) is assigned to Zone NK1 (Berriasian) based on the presence of *Helenea chiastia*, *L. carniolensis*, *Tubodiscus*, and *Rotelapillus laffittei*. Cores 198-1213B-26R through 16R are correlated with Zone NK2 (Berriasian) based on the presence of the marker species *Retecapsa angustiforata* and *Percivalia fenestrata* and supported by first occurrences (FOs) of *Assipetra infracretacea* and *R. wisei*. Cores 198-1213B-15R and 14R are assigned to Subzone NK3a (lower Valanginian) based on the FO of *Rhagodiscus dekaenelii* (see **"Lower to Mid-Cretaceous Biostratigraphy,"** p. 6). Interval 198-1213B-13R-1, 5

F2. Age-depth plot, Site 1213, p. 44.

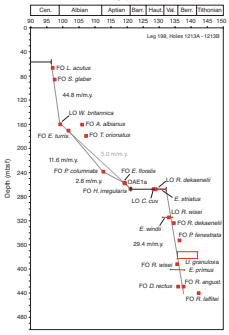

F3. Biostratigraphy/chronostratigraphy, Sites 1207, 1213, 1214, p. 45.

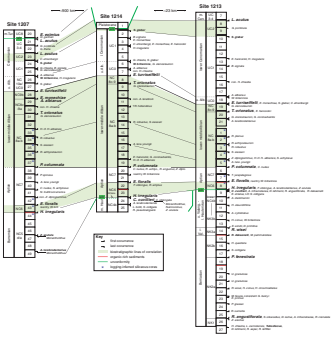

cm, to 9R-1, 47 cm, falls within Subzones NK3b–NC4b (mid-Valanginian through lower Hauterivian) based on the last occurrence (LO) of *R. wisei* and the LO of *R. dekaenelii*. A marked change in nannofossil assemblages in Core 198-1213B-9R indicates a significant stratigraphic gap, incorporating much of Subzone NC4b and all of Zone NC5 (upper lower Hauterivian–uppermost Barremian). Above this there is a relatively straightforward succession of nannofossil marker species (FOs of *Hayesites irregularis*, *Eprolithus floralis*, *Prediscosphaera columnata*, *Tranolithus orionatus*, *Eiffellithus turriseiffelii*, and *Lithraphidites acutus*) that define Zones NC6–NC11 (uppermost Barremian–middle Cenomanian). Not all subzones can be recognized because of missing or anomalous ranges of subzonal markers (see **"Lower to Mid-Cretaceous Biostratigraphy,"** p. 6). The organic-rich, noncalcareous sediments recovered in Core 198-1214-8R occur between the FOs of *H. irregularis* and *E. floralis* (Zone NC6) and strongly indicate a correlation with the Selli event (OAE1a).

Site 1214

Smear slides were prepared from 38 levels of Site 1214. All but three samples yielded nannofossils; the three barren samples came from an organic-rich interval in Core 198-1214A-23R (OAE1a, see below). Nannofossil abundance was usually high. The stratigraphic distribution of nannoplankton is shown in Table **T2,** an age-depth plot in Figure **F4,** and selected datum events, zonal boundaries, and chronstratigraphic interpretations in Figure **F3.** The assemblages are largely made up of cosmopolitan nannofossil species, but samples from the lowermost cores, 198-1214A-24R and 25R, contain a number of interesting features, specifically, rare occurrences of the typically Tethyan taxa *Nannoconus*, *C. oblongata*, *L. bollii*, and the abundant presence of *Micrantholithus*.

Much of Hole 1214A (22 of 25 cores) is Aptian–Albian, and the nannofossil biostratigraphy is comparable with that recorded at Sites 1213 and 1207. The lowermost two cores are upper Hauterivian and contain a number of interesting nannofloral elements. Details of the biostratigraphic analysis are given below and summarized in Figure **F2.**

Interval 198-1214A-25R-1, 22 cm, to 24R-1, 72–75 cm, falls within nannofossil Subzone NC4b based primarily on the co-occurrence of *L. bollii* and *Cruciellipsis cuvillieri* and supported by the presence of *C. oblongata* and *Speetonia colligata*. This short interval is also notable for the presence of rare nannoconids and very abundant disaggregated *Micrantholithus* liths; the sediment is essentially a *Micrantholithus* chalk. Sediments of this age were not recovered at Site 1213, and the older Lower Cretaceous sediments from that site did not yield *Nannoconus* or *Micrantholithus*. Sample 198-1214A-24R-1, 46–47 cm, does not contain age-diagnostic species, but the absence of *C. oblongata* and *H. irregularis* and the relatively common occurrence of *Zeugrhabdotus scutula* indicate correlation with Barremian Subzones NC5d–NC5e (see **"Lower to Mid-Cretaceous Biostratigraphy,"** p. 6). This part of the section includes a hiatus that comprises much of the Barremian or is extremely condensed.

Site 1214 yielded the same Aptian–Cenomanian zonal succession as Sites 1213 and 1207. Zone NC9 and subzones within Zones NC6 and NC7 were not recognized (see **"Lower to Mid-Cretaceous Biostratigraphy,"** p. 6).

T2. Calcareous nannofossils, Site 1214, p. 49.

F4. Age-depth plot, Site 1214, p. 46.

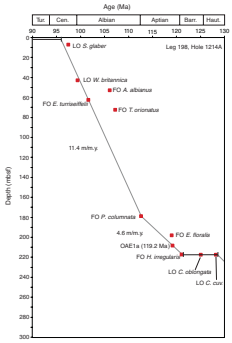

Organic-rich noncalcareous sediments recovered in Core 198-1214A-23R occur between the FOs of *H. irregularis* and *E. floralis* (Zone NC6), strongly indicating a correlation with the Selli event (OAE1a).

Site 1207

Smear slides were prepared from 35 levels of Site 1207. All but two samples yielded nannofossils; the two barren samples came from an organic-rich interval in Core 198-1207B-44R (OAE1a). Nannofossil abundance was usually high. The stratigraphic distribution of nannoplankton is shown in Table **T3** an age-depth plot in Figure **F5,** and selected datum events, zonal boundaries, and chronstratigraphic interpretations in Figure **F3.** The assemblages are largely made up of cosmopolitan nannofossil species.

Cores 198-1207B-21R through 44R are mid-Cretaceous in age, and the nannofossil biostratigraphy is comparable with that recorded at Sites 1213 and 1214. Details of the biostratigraphic analysis are given below and summarized in Figure **F3.**

Organic-rich noncalcareous sediments recovered in Core 198-1207B-44R occur between the FOs of *H. irregularis* and *E. floralis* (Zone NC6) and strongly indicate a correlation with the Selli event (OAE1a). The lowermost cores, 198-1207B-45R through 49R, lack diagnostic marker taxa but are assigned to Subzones NC5d–NC5e (Barremian) (see **"Lower to Mid-Cretaceous Biostratigraphy,"** p. 6).

Site 1208

Smear slides were prepared from one core catcher (Section 198-1208A-42X-CC); drilling was terminated at this level due to problems related to abundant chert. The sample yielded a well-preserved, abundant, diverse assemblage (Table **T4**) that could be assigned to Subzones NC8a–NC9b (middle Albian) based on the presence of *T. orionatus* and the absence of *E. turriseiffelii*. The absence of *Axopodorhabdus albianus* was not used to infer a more refined Subzone NC8a designation because it occurred anomalously high in other more complete sections (Sites 1207, 1214, and 1213).

Site 1212

Smear slides were prepared from four cores (198-1212B-24H through 27H), and samples yielded well-preserved, common to abundant, diverse assemblages (Table **T5**). The samples are assigned to Subzone NC10a (upper Albian) based on the presence of *E. turriseiffelii*, *H. irregularis*, and *Gartnerago stenostaurion* (see **"Lower to Mid-Cretaceous Biostratigraphy,"** below).

LOWER TO MID-CRETACEOUS BIOSTRATIGRAPHY

Sites 1207, 1208, 1212, 1213, and 1214

Lower Cretaceous nannofossil biostratigraphy was first established in low-latitude, Tethyan, onshore sections (Thierstein, 1971, 1973; Sissingh, 1977, with modifications by Perch-Nielsen, 1979, 1985; Applegate and Bergen, 1988) and later DSDP oceanic sections, mainly from the

T3. Calcareous nannofossils, Site 1207, p. 50.

F5. Age-depth plot, Site 1207, p. 47.

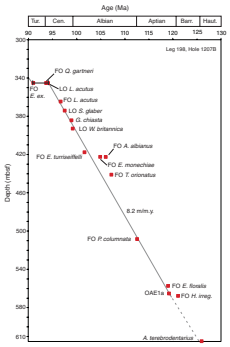

T4. Calcareous nannofossils, Site 1208, p. 51.

T5. Calcareous nannofossils, Site 1212, p. 52.

low-latitude central Atlantic (Roth, 1978, 1983, with modifications by Bralower, 1987; Bralower et al., 1993). Perch-Nielsen (1979) recognized the (bio)geographic limitations of these schemes and incorporated data from high-latitude Boreal sections (northern Europe and the North Sea Basin), although more recently separate high-resolution schemes have been developed for these areas (see reviews in Bown et al., 1998; Jeremiah, 2001). More recent studies on Tethyan sections have yielded particularly good correlations with paleomagnetic and stable isotope stratigraphies (e.g., Bralower et al., 1989; Channell et al., 1993, 1995) and have improved resolution and integration with ammonite biostratigraphy (Bergen, 1994; Gardin et al., 2000). The Jurassic/Cretaceous boundary interval is particularly problematic because of the paucity of stratigraphically complete nannofossil-productive sections with good preservation. Boreal sections are largely in nonmarine or transitional facies with stratigraphic gaps (Bown and Cooper, 1998) and Tethyan Mediterranean–Caribbean sections in massive carbonates with poor nannofossil preservation (Bralower et al., 1989). High-quality data are almost entirely restricted to two DSDP sites from the Central Atlantic Ocean (Sites 391 and 534) (Roth, 1983; Bralower et al., 1989; Bergen, 1994; but see also de Kaenel and Bergen, 1996).

The NK and NC zones and subzones of Roth (1978, 1983), Bralower et al. (1989), and Bralower (1987) were used to provide the biostratigraphic framework for Sites 1207, 1213, and 1214, but the Shatsky region is far removed from the source areas of these schemes and thus the differences observed are not surprising and will be discussed further below.

The zones and zonal boundaries were identified as follows.

Zone NK1; Berriasian (Site 1213)

The Jurassic/Cretaceous boundary interval zonation of Bralower et al. (1989) is based on a distinctive succession of nannolith appearances, notably *Conusphaera* and *Nannoconus*; however, these taxa were absent in this part of the section and the former was absent throughout. In addition, a number of important marker species of the family Cretarhabdaceae (*C. cuvillieri*, *R. angustiforata*, and *Retecapsa octofenestrata*) and genus *Eiffellithus* (*E. primus*, *E. windii*, and *E. striatus*), although present, are rare and restricted to a small number of samples, and their first and last occurrences may not be biostratigraphically reliable. The lowest Cretaceous zones are thus identified using marker species, where present, together with alternative datum events and aspects of the entire assemblages.

The lowermost productive samples (Core 198-1213B-27R) yielded *H. chiastia*, *L. carniolensis*, *Tubodiscus bellii*, and *R. laffittei*, indicating Subzone NJKc or younger. The nannofossils do not unambiguously indicate a Cretaceous age, but correlation with Zone NK1 is inferred based on the presence of the genus *Tubodiscus* and absence of *R. angustiforata*, *P. fenestrata*, and *R. wisei* (Bralower et al., 1989). Support for this interpretation also comes from radiolarian fauna that also indicate a Berriasian age for the lowermost cores (H. Kano, pers. comm., 2003).

Subzone NK2a; Berriasian (Site 1213)

The subzone base is marked by the FO of *R. angustiforata* (Sample 198-1213B-26R-1, 17–18 cm), although this is an isolated trace occurrence and thus of questionable reliability. The FO of *A. infracretacea* is

also recorded in this sample (FO indicates Subzone NJKd [lower Berriasian] after Bralower et al., 1989), along with a number of unambiguously Cretaceous species (e.g., *S. silvaradius* and *Diadorhombus rectus*). The FO of *R. wisei*, an intra-Subzone NK2a event (upper Berriasian) (Bralower et al., 1989), is recorded in Sample 198-1213B-22R-1, 58–60 cm. An interesting feature of these lowermost Cretaceous assemblages is the consistent presence of a number of taxa that were previously thought to have had LOs in the Upper Jurassic, notably *P. grassei*, *A. cylindratus*, and *Biscutum dorsetensis*. It is unlikely that these are reworked specimens, as no other Upper Jurassic taxa are present, and, in any case, a Jurassic sediment source may not have been present in the Shatsky area. These species may have been overlooked due to low numbers in previously described sections or, more likely, may have had a distinctive Pacific paleobiogeography, and survived longer in this region.

Subzone NK2b, Berriasian (Site 1213)

The FO of the zonal marker *P. fenestrata* occurs in Sample 198-1213B-18R-1, 1 cm, although this is an isolated trace occurrence and thus of questionable reliability. The LOs of *Helenea quadrata* and *U. granulosa* were also recorded in this interval and have been previously noted in Zone NK2 (Bralower et al., 1989; Bergen, 1994).

Subzone NK3a; lower Valanginian (Site 1213)

The zonal marker *C. oblongata* is absent, but the FO of *R. dekaenelii* has been recorded at a similar stratigraphic level (lower Valanginian) (Bergen, 1994) and is used here as a proxy marker for the NK3 zonal boundary. *R. dekaenelii* is distinctive, relatively common, and consistently present throughout its range at Site 1213.

Subzones NK3b to lower NC4b; upper Valanginian–lower Hauterivian (Site 1213)

The LO of the subzonal marker *R. wisei* occurs in Sample 198-1213B-14R-1, 12 cm, and the co-occurrence of *E. windii* in Core 14R indicates a well-constrained age of mid-Valanginian (Bralower et al., 1989; Bergen, 1994; Gardin et al., 2000).

The stratigraphy of this interval cannot be further subdivided because of the absence of *T. verenae*, *L. bollii*, and nannoconids and only a trace occurrence of *E. striatus*. The LO of *Helenea conus*, recorded in Core 198-1213B-13R, has previously been observed in the upper Valanginian (Bergen, 1994).

The upper part of this interval in Hole 1213B (lower part of Section 198-1213B-9R-1) cannot be younger than lower Subzone NC4b (lower Hauterivian) due to the continued presence of *C. cuvillieri* and *R. dekaenelii* (Bergen, 1994).

Upper Subzone NC4b; upper Hauterivian (Site 1214)

The co-occurrence of *Z. scutula*, *C. cuvillieri*, *C. oblongata*, and *L. bollii* in Sample 198-1214-24R-1, 72 cm, infers correlation with a short interval within the upper part of Subzone NC4b (upper Hauterivian) (Bergen, 1994; Gardin et al., 2000). The latter two species were not recorded at Sites 1207 and 1213, suggesting this interval was only recovered at Site 1214. This is further indicated by the absence of *R. dekaenelii*, the

rare but consistent presence of *Nannoconus* (three samples, the only persistent occurrence of the genus observed during Leg 198), and abundant *Micrantholithus* fragments, although the latter was also observed in Subzones NC5d–NC5e at Site 1207 (see below).

The FO of *Assipetra terebrodentarius,* recorded at Site 1214 within this interval, has previously been recorded at a higher stratigraphic level (Zone NC5), close to the Hauterivian/Barremian boundary, and not overlapping with the range of *C. cuvillieri* (Bralower, 1987; Bergen, 1994; Channell et al., 1995; Gardin et al., 2000).

Subzones NC5d–NC5e; Barremian (Sites 1207 and 1214)

Subzone NC5d is defined by the LO of *C. oblongata* and is a widely used event. Subzone NC5e has been variously defined by the LO of *Nannoconus steinmannii* (Bralower, 1987) and FO of *Flabellites oblongus* (Bralower et al., 1995). The former event is unreliable or stratigraphically higher, and the latter event usually lies very close to the base of the overlying zone, defined by the FO of *H. irregularis*. Thus, the two subzones are merged in this study.

This interval was recovered in Sites 1207 and 1213 but lacks age-diagnostic taxa. The absence of *C. cuvillieri*, *C. oblongata*, and *H. irregularis* and presence of *A. terebrodentarius* and *Z. scutula* were used to infer a correlation with Subzones NC5d–NC5e (Barremian). The common occurrence of *Z. scutula* was utilized as a Barremian acme subzone by Bown et al. (1998) and Jeremiah (2001), and this may be a widespread, correlatable feature.

Zone NC6; lower Aptian (Sites 1207, 1213, and 1214)

This zone is defined by the FO of *H. irregularis*. The FO of *F. oblongus* is also recorded at or just above this level. All three sites recovered noncalcareous black shale intervals bracketed by the FOs of *H. irregularis* and *E. floralis*, defining the extent of the lower Aptian Zone NC6. This strongly indicates that the black shales are stratigraphically equivalent to the Selli event and OAE1a.

Zone NC7; Aptian (Sites 1207, 1213, and 1214)

This zone is defined by the FO of *E. floralis*. Zone NC7 could not be further subdivided due to the absence of *Micrantholithus* and *Rhagodiscus achlyostaurion*. The latter species does occur higher in the sections, in the lower Albian, and has previously been recorded at similar levels (Erba, 1988).

Zone NC8; uppermost Aptian–lower Albian (Sites 1207, 1213, and 1214)

This zone is defined by the FO of small, rare *P. columnata*. Subzone NC8b could not be reliably recognized due to absence of *Hayesites albiensis* (see "Appendix A," p. 24, and discussion in Kennedy et al., 2000). The FO of *P. columnata* is recorded in the uppermost Aptian (plesiotypica/jacobi ammonite zone) (Bown in Kennedy et al., 2000) but is often used as a proxy marker for the Aptian/Albian boundary. The LO of large *A. terebrodentarius* (ssp. *youngii*) was recorded just above the FO of *P. columnata* by Tremolada and Erba (2002), and although this subspecies extends to higher stratigraphic levels, its last common, consistent oc-

currence may provide an alternative approximation for this stage boundary level.

Robinson et al. (2004) inferred the presence of OAE1b within this interval, expressed as more silica-rich sediments, identified using ODP downhole logging data.

Subzone NC8c–Zone NC9; Albian (Sites 1207, 1212, 1213, and 1214)

The middle and upper Albian marker species *T. orionatus*, *A. albianus*, and *E. turriseiffelii* were all identified at each site, but their stratigraphic spacing and order is atypical. *T. orionatus* and *A. albianus* are recorded anomalously high at all three sites (i.e., close to the FO of *E. turriseiffelii*), and *A. albianus* is recorded out of sequence, above the FO of *E. turriseiffelii*, at Sites 1213 and 1214. The clustering of these events (see age-depth plots in Fig. F3) perhaps indicate low sedimentation rates and/or a possible mid-Albian hiatus, but the out-of-sequence ordering indicates problems with the range of at least *A. albianus* in this area. The problem may also be exacerbated by datum/timescale correlation problems. The extent of the mismatch can be most clearly seen on the age-depth plots (Fig. F3), where no single straight line can be fitted to the mid-Albian datum points.

The NC9b subzonal marker, *Eiffellithus monechiae,* is present in correct stratigraphic position at Site 1207 but is rare at Site 1214 and is not recorded at Site 1213.

Subzone NC10a/Zone UC0; upper Albian (Sites 1207, 1212, 1213, and 1214)

This subzone is defined by the FO of *E. turriseiffelii*; this, and the overlying Subzone NC10b, are relatively thick at Sites 1207, 1213, and 1214, indicating a relatively complete section across the Albian/Cenomanian boundary.

Subzone NC10b/Zones UC1–UC2; lower Cenomanian (Sites 1207, 1213, and 1214)

Due to the absence of *Corollithion kennedyi*, this subzone cannot be recognized by its primary marker species; however, a number of other boundary interval events are present, including the LO of *G. stenostaurion*, the LO of *Watznaueria britannica*, the FO and LO of *Gartnerago chiasta*, the FO of *Gartnerago ponticulus* (= *nanum* of many authors), the FO of *Gartnerago theta*, and the LO of *Staurolithites glaber*. According to Burnett (1999), the LO of *W. britannica* lies closest to the Albian/Cenomanian boundary, and we have used this event as a proxy for the base of Subzone NC10b (Zone UC1). The younger event, the LO of *S. glaber*, occurs in upper Zone UC1 (Burnett, 1999), and we use this as an approximation for the base of Zone UC2 in the absence of *Gartnerago segmentatum*.

Zone NC11/UC3 (Sites 1207 and 1213)

This zone is marked by the FO of *L. acutus*.

NANNOPLANKTON BIOGEOGRAPHY

Extant coccolithophores are widespread in all marine photic zone environments, but the most familiar typically oceanic taxa are not found at latitudes higher than 70° and populations are most diverse at low latitudes in warm, stratified, oligotrophic, open-ocean environments. Oceanic coccolithophore biogeography defines broad latitudinal belts or zones (McIntyre and Bé, 1967; Okada and Honjo, 1973; Winter et al., 1994) distinguished by variations in assemblage composition, rather than high endemicity, as many coccolithophore species are virtually cosmopolitan. These distributions reflect the temperature and nutrient characteristics of watermasses and oceanographic features such as divergence and upwelling zones, ocean gyres, and seasonal mixing. Coastal and estuarine environments usually support different taxa, many of which are small and weakly calcified and therefore without a fossil record.

Our understanding of Early Cretaceous nannoplankton biogeography is largely based on records from the European Boreal and Tethyan epicontinental basins and Atlantic Ocean DSDP/ODP sites (Roth and Bowdler, 1981; Roth and Krumbach, 1986; Bralower et al., 1989; Mutterlose, 1992a; Mutterlose and Kessels, 2000; Street and Bown, 2000). More limited data are available for the Indian (Proto Decima, 1974; Thierstein, 1974; Bralower and Siesser, 1992; Mutterlose, 1992a; Bown, 1992), Southern (Mutterlose and Wise, 1990), and Pacific (Roth, 1973, 1981; Thierstein, 1976; Erba, 1992; Erba et al., 1995; Lozar and Tremolada, 2003) oceans. The Pacific (or Panthalassa) Ocean was the largest contiguous marine habitat on the Cretaceous Earth, but much of the seafloor has since been lost through subduction.

Street and Bown (2000) concluded that Early Cretaceous nannoplankton biogeography was characterized by a wide, low- to mid-latitude zone (50°N–50°S) of relatively stable assemblage composition and diversity, flanked in both hemispheres by distinct high-latitude zones significantly lower in diversity and dominated by typically bipolar taxa (see also Mutterlose and Kessels, 2000). Further differentiation is apparent based on the distribution of rare taxa, many of which have been labeled Boreal or Tethyan based on their distributions in the European–Atlantic area.

Neritic vs. oceanic differentiation is often acknowledged but rarely unequivocally demonstrated in Cretaceous studies (Thierstein, 1976; Roth and Krumbach, 1986; Applegate et al., 1989). Most authors agree that *Nannoconus* and *Micrantholithus* were marginal or neritic taxa that were scarce or absent in oceanic settings (Table **T6**). Street and Bown (2000) suggested neritic assemblages were characterized by lower diversity, high unevenness, and common to dominant taxa that varied with latitude and that were essentially absent in oceanic settings, citing *Nannoconus* and *Micrantholithus* as the two most important neritic groups. These observations are particularly germane to this study, from which these two taxa are practically absent; however, their paleoecology remains contentious and will be discussed further below (see ***"Nannoconus,"*** p. 13). As yet, there has been no explicit recognition of coastal nannoplankton in the Cretaceous, due, in no small part, to the paucity of data from such settings, itself a reflection of the poor preservation typical of such facies and the reticence to study such material.

This discussion will focus particularly on *Nannoconus* and *Micrantholithus,* as both represent major assemblage components with distinc-

T6. Early Cretaceous marginal sea/neritic taxa, p. 53.

tive biogeography and their virtual absence at the Shatsky sites requires an explanation. In addition, they may provide important paleoceanographic information that has yet to be fully realized (but see discussion in Erba, 1994; Street and Bown, 2000; Herrle, 2003).

Shatsky Nannoplankton Assemblages: A Tropical, Open-Ocean Assemblage

Site 1213 provides the most continuous Early Cretaceous nannoplankton record from the Pacific Ocean and gives particularly valuable insight into the Berriasian–Hauterivian evolutionary succession and paleobiogeography, an interval that followed a period of considerable taxonomic turnover at the Jurassic/Cretaceous boundary. Sites 1207, 1213, and 1214 also provide rich, well-preserved mid-Cretaceous nannofossil successions.

The great majority of nannofossil assemblages recorded from Shatsky Rise include taxa that are typical of this age; however, there are clear differences that set them apart from coeval Atlantic Ocean and European epicontinental assemblages. In terms of common assemblage components, *L. carniolensis* is consistently abundant, a feature that appears to be a characteristic of oceanic assemblages (Thierstein, 1976; Roth and Krumbach, 1986). Applegate et al. (1989) noted that *Lithraphidites* was associated with neritic taxa (*Nannoconus* and *Micrantholithus*) in Central Atlantic assemblages, but they appear to have been referring to the species *L. bollii* and *Lithraphidites alatus* and not to the most abundant and cosmopolitan species, *L. carniolensis*.

The absence of rare taxa is a subtle paleobiogeographic signal but significant nevertheless, as many of these species have been utilized in Boreal or Tethyan biostratigraphic schemes and their distribution attributed to Boreal/Tethyan biogeographic differentiation (e.g., Mutterlose, 1992a). The rarity or complete absence of many of these taxa from the Pacific (and actually much of the eastern Tethyan–Indian Ocean) suggests that these taxa may have been practically neritic in distribution and largely excluded from the expansive Cretaceous oceanic areas (Table T7) (see also Thierstein, 1976).

T7. Early Cretaceous nannoplankton rare/absent at Shatsky Rise, p. 54.

Almost certainly a number of taxa that have previously been labeled Boreal or Tethyan had truly oceanic distributions, controlled to some extent by temperature, and are better termed tropical or temperate/high-latitude taxa. The most restricted biogeographies are easiest to recognize in the fossil record, and these include the temperate species *Repagulum parvidentatum*, *Crucibiscutum salebrosum*, *Seribiscutum primitivum*, and *Ceratolithina* spp. and the tropical taxon *H. irregularis*. These interpretations are beautifully demonstrated on Shatsky Rise, where cold-water taxa were totally absent and the warm-water *H. irregularis* was periodically common to abundant.

Site 1213 also records unusual stratigraphically extended Early Cretaceous ranges for *A. cylindratus*, *Hexapodorhabdus cuvillieri*, and *B. dorsetensis,* species previously thought to have become extinct during the Late Jurassic (Tithonian) (see Bown and Cooper, 1998). Such observations suggest that these species withdrew to the Pacific Ocean prior to their final extinction. In addition, *W. britannica*, which, after the Late Jurassic, declined to trace levels in other areas, is recorded consistently and relatively commonly through much of the Berriasian–Valanginian. Again, this suggests that *W. britannica* became primarily a Pacific-restricted species during this interval before its Lazarus-taxon-like reexpansion of biogeographic range in the Aptian.

However, arguably the most striking aspect of the Shatsky assemblages, when compared with coeval sections in the Atlantic Ocean in particular, is the complete absence of *Conusphaera* and near absence of *Nannoconus* and *Micrantholithus*. The latter two genera are abundant and conspicuous components of many Atlantic and western Tethyan assemblages.

Nannoconus

Nannoconus is a noncoccolith nannofossil group that appeared cryptically in the Tithonian and was a conspicuous component of Tethyan Early Cretaceous assemblages until a numerical decline in the Aptian (the "nannoconid crisis" of Erba [1994]). The genus survived until the Campanian but was rarely common after the Albian. They were abundantly present only in certain marine settings, notably the marginal basins of the circum-western Tethys, proto-Atlantic, and Caribbean, where they may be rock forming. There is also evidence from the Barremian of the North Sea for the occurrence of endemic nannoconid species adapted to temperate epicontinental waters (*Nannoconus abundans* and *Nannoconus borealis*) (e.g., Street and Bown, 2000). However, most of the more widespread geographic occurrences appear to have been temporally restricted (Mutterlose, 1989, 1992a) and limited to neritic settings or deep-sea settings adjacent to carbonate platforms. The claim that nannoconids were cosmopolitan, without qualification, is highly misleading.

A compilation of DSDP/ODP presence/absence data from the Pacific and Indian oceans, presented here in Table **T8,** shows that nannoconids were practically absent from these oceans, which made up ~80% of the Early Cretaceous marine ecosystem. Of the 48 DSDP and ODP sites that have recovered nannofossiliferous Lower to mid-Cretaceous sections, only two (Sites 463 and 465) recovered nannoconids in more than five samples. Both these occurrences are associated with allochthonous material sourced from shallow-water platforms or guyots, an observation previously made more broadly by Thierstein (1976). Many of the other, more sporadic, occurrences are similarly associated with transported shallow-water-sourced material (e.g., Sites 766, 800–802, 872, 878, and 879). Of the many hundreds of Indian Ocean samples that have been studied, only four have yielded nannoconids (pers. observ.). We are confident that this record is robust because nannoconids are highly distinctive nannofossils and many authors have made specific reference to the absence of the group (Bukry, 1971, 1973a, 1973b; Hekel, 1973; Thierstein, 1976; Erba and Covington, 1992; Bown, 1992). Nannoconids are far more frequently found in Atlantic Ocean sites, but this ocean was a narrow intra-Pangean basin in the Early Cretaceous, and sediment transport from surrounding shelves appears to have been common. Applegate et al. (1989) clearly document Atlantic Ocean sections of shelf-sourced turbidites with common *Nannoconus* and *Micrantholithus* interbedded with pelagic carbonates in which these taxa are rare or absent. Latitude also appears to have played an important part in the biogeography of nannoconids, and, in general, they were rarer or absent at latitudes >30° (Street and Bown, 2000).

This puzzling distribution pattern has led to a range of explanations concerning their biology and paleoecology, but most have noted the link with low-latitude (tropical), sediment-starved epicontinental basins and the association with braarudosphaerids (Roth and Krumbach, 1986; Mutterlose, 1989; Street and Bown, 2000). Busson and Noël

T8. *Nannoconus*, *Micrantholithus*, and *Braarudosphaera* presence/absence, p. 55.

(1991) went further and suggested nannoconids may have been meroplanktonic calcareous dinoflagellates, excluded from deep and anoxic settings by the water-depth constraints on cyst viability but which dominated in neritic environments during red-tide-like blooms. Erba (1994) postulated a deep photic zone paleoecology comparable to the extant *Florisphaera profunda* with abundance related to nutricline depth, although, contrastingly, *F. profunda* is a strictly open-ocean, "blue-water" species.

The reasonably comprehensive Early to mid-Cretaceous biogeographic data suggest there is now little doubt that the paleoecology of nannoconids was in some way related to water depth and latitude. Abundant nannoconid occurrences are generally limited to tropical to subtropical carbonate platforms and epicontinental basins around western Tethys and the Central Atlantic, a paleobiogeography highly unusual among calcareous nannoplankton but, interestingly, comparable to the incertae sedis protozoan calpionellids (Remane, 1985). Latitudinal control is most easily explained by temperature, but, notably, coeval tropical deep-sea sites do not yield nannoconids (Table **T8;** and see Applegate et al., 1989). Migration events may have occurred during warmer climate intervals (e.g., Mutterlose, 1989), but dispersal appears to have been prevented by large oceans such as the eastern Tethys, Indian, and Pacific. Extra-Tethyan occurrences of nannoconids were linked by shallow-water migration routes via epicontinental basins or across the narrow Atlantic Ocean (e.g., Mutterlose, 1989; Bown and Concheyro, 2004). The more exotic oceanic occurrences, such as the mid-Pacific Mountains, can be explained by island-hopping migration routes more typically associated with marine benthic invertebrates and not problematic for planktonic organisms. Furthermore, the Pacific distribution data (Table **T8**), which indicate a strong association with shallow carbonate platforms, suggest that nannoconids may have been living above and around certain Pacific atolls and guyots. The rare and sporadic occurrences at other truly oceanic sites were probably drifted or transported specimens. The almost total absence of nannoconids in the Indian Ocean may reflect the presence of fewer oceanic rises and guyots (Table **T8**).

The limiting role of water depth may be explained by a number of interrelated neritic factors including environmental stability, turbulence, transparency, salinity, and nutrients or even water depth itself if the organism had a benthic life-cycle stage (Busson and Noël, 1991), as do a number of extant coastal coccolithophores (e.g., *Pleurochrysis*). The fact that nannoconids flourished in detrital-free, tropical, carbonate shelf settings suggests water column transparency may well have been important and lends support to the deep photic-zone ecology suggested by Erba (1994). If water depth did exert a direct control on nannoconid distribution, then the effect of sea level change on nannoconid records should not be overlooked. Declines in nannoconid abundance in epicontinental settings may have been associated with sea level rises in much the same way as carbonate platform drowning suppressed carbonate-producing invertebrates. This interpretation is somewhat supported by records of platform drowning episodes that coincide with nannoconid "crisis" events previously reported by Weissert et al. (1998) but explained therein by climate-driven eutrophication.

The relationship between nannoconids and trophic resources has been discussed by a number of authors, and most have suggested that they were adapted to oligotrophic environments (Busson and Noël, 1991; Coccioni et al., 1992; Erba, 1994). This is based largely on their

decline prior to black shale intervals, particularly OAE1a, that are interpreted by these authors as the product of high productivity but also the apparently inverse relationship between nannoconid and coccolith abundances. However, the black shales of the upper Albian OAE1b in southern France are considerably enriched in nannoconids relative to adjacent sediments (Kennedy et al., 2000; Herrle, 2002; Nagai et al., 2002), and the relationship between organic-rich sediments, productivity, and nannoconids is clearly not so straightforward (Herrle, 2002).

Micrantholithus

The Early Cretaceous *Micrantholithus* appears to have had a similar abundant neritic distribution to the nannoconids but over a broader latitudinal range (50°N–50°S) (Applegate et al., 1989; Street and Bown, 2000). Table T8 shows that *Micrantholithus* was practically absent from the Pacific and Indian oceans, and, when present, most of the records are sporadic trace occurrences of Albian *Braarudosphaera,* often associated with transported shallow-water material. The extant *Braarudosphaera* replaced *Micrantholithus* in the Aptian but was never as consistently abundant in the remaining Cretaceous and appears to have retained a similar eccentric ecology for much of its considerable history (Aptian–Holocene; 119 m.y.) (Roth and Bowdler, 1981; Parker et al., 1985; Siesser et al., 1992; Paleo-Alampay et al., 1999; Kelly et al., 2003). Living *Braarudosphaera bigelowii* is most common in neritic environments (Gran and Braarud, 1935) and fossil distributions are comparable, although anomalous occurrences are revealing, most notably abundant occurrences in post-Cretaceous/Tertiary boundary extinction assemblages and *Braarudosphaera* chalk occurrences in temperate to subtropical (20°–35°C) open-ocean sites, best documented for the Oligocene South Atlantic (Parker et al., 1985; Kelly et al., 2003) but also known from the Upper Cretaceous (Scarparo and Shimabukuro, 1997). These suggest *Braarudosphaera* is and was an opportunistic taxon whose oceanic occurrence may be limited to unusual neritic or oceanic conditions related to the upwelling of cool, nutrient-enriched, and/or low-salinity waters (Siesser et al., 1992).

Nannoconus, *Micrantholithus*, and the Siliceous Pacific Paradigm

Nannoconids and *Micrantholithus* are practically absent throughout the Cretaceous at the Shatsky Rise sites and are rare or absent in coeval Indian and Southern ocean sections (Table T8). The most obvious explanation for their absence at Shatsky is primary ecological exclusion by some aspect of water depth, as discussed above, and that the Pacific presented a barrier to their dispersal and habitation. This also best fits the observation of absence from the majority of Early Cretaceous deep ocean settings.

Alternatively, if these organisms were oligotrophic adapted (e.g., Erba, 1994) then it could be argued that they were excluded from the Shatsky area by high productivity that was associated with equatorial upwelling or the topography of the rise itself. Most preserved Early Cretaceous Pacific crust was close to, or drifting toward, equatorial regions, and the ubiquitous presence of chert in the Shatsky Cretaceous sections has been explained by the presence of a very broad (>30°) zone of equatorial divergence (Bralower, Premoli Silva, Malone, et al., 2002). The exclusion of nannoconids at Shatsky would have required a period of

sustained upwelling and high productivity for at least 50 m.y. through >10° latitude. The presence of abundant chert and timing of chert deposition cessation does lend some support to this hypothesis; however, the interpretation of radiolarian-sourced chert as a proxy for high productivity is based on comparison with the modern ocean where diatoms dominate primary productivity and the silica cycle. This modern plankton system was probably not established until the late Eocene, and possibly as late as the Neogene, and thus the interpretation of chert as a high-productivity proxy is highly questionable when applied to pre-Modern ocean systems and especially so for the chert-dominated Mesozoic Pacific Ocean and margins (Baumgartner, 1987; Racki and Cordey, 2000; Shipboard Scientific Party, 2002b [p. 16]; Robinson et al., 2004). In addition, the relatively high diversity nannoplankton assemblages do not indicate long-term high productivity, and high-fertility nannofossil proxy species, such as *Biscutum constans*, are virtually absent through most of the interval in question.

There is also little evidence to suggest that *Micrantholithus* and *Braarudosphaera* would have been excluded by high productivity. The biogeography and paleoecology of the extant species *B. bigelowii* is undoubtedly enigmatic, but its occurrence and abundance is definitely not controlled by productivity alone. At present it appears to exhibit preferences for neritic environments but has occasionally flourished in open-ocean settings in the past (Kelly et al., 2003).

Finally, the absence of nannoconids and braarudosphaerids in all mature Cretaceous ocean basins is compelling evidence that productivity alone was not responsible for their exclusion. Rather, it appears likely that they were excluded from deep blue-water environments, living most abundantly in marginal ocean basins, epicontinental shelves, and shallow-water oceanic platforms and guyots.

CONCLUSIONS

ODP Leg 198 Sites 1207, 1208, 1212, 1213, and 1214 on Shatsky Rise yielded the most continuous Early Cretaceous nannoplankton record yet retrieved from the Pacific Ocean and provide valuable data concerning the evolutionary succession and paleobiogeography of the largest Cretaceous marine habitat (Table T9).

T9. Datum events, p. 57.

Mid-Cretaceous sections (Aptian–Cenomanian) were recovered at all sites, and biostratigraphy is relatively straightforward for Zones NC6–NC11. Site 1213 included an apparently complete Berriasian–Hauterivian section, but biostratigraphic dating is problematic due to the absence or rarity of zonal fossils of both Boreal and Tethyan affinity (e.g., nannoconids, *C. oblongata*, *T. verenae*, *Eiffellithus* spp., etc.); Zone NK1–Subzone NC4b were identified. Short Hauterivian (Subzone NC4b) and Barremian (Subzones NC5d–NC5e) sections were also identified at Sites 1214 and 1207, respectively.

Organic-rich claystones and porcellanites dated as Zone NC6 (Aptian) were recovered at Sites 1207, 1213, and 1214 and represent Pacific expressions of OAE1a (Selli event). Older organic-rich claystones at Site 1213, in Sections 198-1213B-15R-1 and 19R-1, are assigned to Zones NK3a (lower Valanginian) and NK2a (Berriasian), respectively, and may be equivalent to organic-rich intervals from the Tethyan area (Mattioli et al., 2000; Bersezio et al., 2002; Brassell et al., 2004).

L. carniolensis is common to abundant throughout and most likely represents an oceanic-adapted taxon. Cold- to temperate-water species

such as *C. salebrosum*, *R. parvidentatum*, and *S. primitivum* are entirely absent, indicating the persistence of tropical, warm surface water temperatures. The clearest indication of warm water is provided by the common occurrence of *H. irregularis* in the mid-Cretaceous, although the putative warm-water taxon, *Rhagodiscus asper,* is consistently present and often frequent to common. Other Tethyan taxa are absent or rare and sporadically distributed (e.g., *C. oblongata*, *Conusphaera* spp., *T. verenae,* and *L. bollii*), and other factors, probably related to neritic environments, presumably controlled their distribution. *Watznaueria* is almost always the most abundant coccolith in these assemblages, as it was globally at this time (Street and Bown, 2000).

Site 1213 records extended Early Cretaceous ranges for species previously thought to have become extinct during the Late Jurassic (e.g., *A. cylindratus*, *P. grassei,* and *B. dorsetensis*), suggesting these species became Pacific restricted prior to their extinction, significantly later than their disappearance elsewhere. *W. britannica* may also have been a species with Pacific affinities before reexpansion of its biogeography in the early Aptian.

The most striking feature of the Shatsky Rise Cretaceous assemblages, however, is the virtual absence of *Nannoconus* and *Micrantholithus*, both taxa that are conspicuous and often common components of many Tethyan and Atlantic nannofloras. These forms were almost certainly neritic adapted and usually absent in open-ocean settings. Their dispersal and habitation was prevented by oceanic environments, and the distribution of nannoconids in particular may have been directly controlled by water depth itself, perhaps by the presence of a benthic life cycle stage. Discussion of the global biogeochemical significance of declines in this group should be tempered by the fact that they were absent from much of the Cretaceous marine ecosystem. *Micrantholithus* and other typically Tethyan taxa (*C. oblongata*, *Conusphaera* spp., *T. verenae,* and *L. bollii*) may also have been neritic adapted, excluded from most truly oceanic environments away from guyots and atolls.

One new genus (*Mattiolia*) and thirteen new species (*Zeugrhabdotus clarus, Zeugrhabdotus petrizzoae, Helicolithus leckiei, Rhagodiscus amplus, Rhagodiscus robustus, Rhagodiscus sageri, Rhagodiscus adinfinitus, Tubodiscus bellii, Tubodiscus frankiae, Gartnerago ponticula, Haqius peltatus, Mattiolia furva*, and *Kokia stellata*) are described from the Shatsky Rise Lower Cretaceous.

ACKNOWLEDGMENTS

This research used samples provided by the Ocean Drilling Program (ODP). The ODP is funded by the U.S. National Science Foundation (NSF) and participating countries under management of the Joint Oceanographic Institutions (JOI), Inc. Funding for ODP participation was provided by the Natural Environment Research Council (NERC), United Kingdom. The author would also like to acknowledge the contributions made by the other ODP Leg 198 shipboard palaeontologists, namely, Mark Leckie, Maria Rose Petrizzo, Jason Eleson, Isabella Premoli Silva, Tim Bralower, and Kotaro Takeda, and the science party in general, who made the leg so productive and enjoyable. The manuscript was greatly aided by the ODP editors and reviews by Jörg Mutterlose and Elisabetta Erba.

REFERENCES

Applegate, J.L., and Bergen, J.A., 1988. Cretaceous calcareous nannofossil biostratigraphy of sediments recovered from the Galicia Margin, ODP Leg 103. *In* Boillot, G., Winterer, E.L., et al., *Proc. ODP, Sci. Results,* 103: College Station, TX (Ocean Drilling Program), 293–348.

Applegate, J.L., Bergen, J.A., Covington, J.M., and Wise, S.S., 1989. Lower Cretaceous calcareous nannofossils from continental margin drill sites off North Carolina (DSDP Leg 93) and Portugal (ODP Leg 103): a comparison. *In* Crux, J.A., and Van Heck, S.E. (Eds.), *Nannofossils and their Applications:* Chichester (Ellis Horwood), 212–222.

Baumgartner, P.O., 1987. Age and genesis of Tethyan Jurassic Radiolarites. *Eclogae Geol. Helv.,* 80:831–879.

Bergen, J.A., 1994. Berriasian to early Aptian calcareous nannofossils from the Vocontian Trough (SE France) and Deep Sea Drilling Site 534: new nannofossil taxa and a summary of low-latitude biostratigraphic events. *J. Nannoplankton Res.,* 16:59–69.

Bersezio, R., Erba., E., Gorza, M., and Riva, A., 2002. Berriasian-Aptian black shales of the Maiolica formation (Lombardian Basin, Southern Alps, Northern Italy): local to global events. *Palaeogeogr., Palaeoclimatol., Palaeoecol.,* 180:253–275.

Black, M., 1971. Coccoliths of the Speeton Clay and Sutterby Marl. *Proc. Yorks. Geol. Soc.,* 38:381–424.

Bornemann, A., Aschwer, U., and Mutterlose, J., 2003. The impact of calcareous nannofossils on the pelagic carbonate accumulation across the Jurassic-Cretaceous boundary. *Palaeogeogr., Palaeoclimatol., Palaeoecol.,* 199:187–228.

Bown, P.R., 1987. Taxonomy, evolution, and biostratigraphy of late Triassic–early Jurassic calcareous nannofossils. *Spec. Pap.—Palaeontol. Assoc.,* 38:1–118.

Bown, P.R., 1992. New calcareous nannofossil taxa from the Jurassic/Cretaceous boundary interval of Site 765 and 261, Argo Abyssal Plain. *In* Gradstein, F.M., Ludden, J.N., et al., *Proc. ODP, Sci. Results,* 123: College Station, TX (Ocean Drilling Program), 369–379.

Bown, P.R. (Ed.), 1998. *Calcareous Nannofossil Biostratigraphy:* Dordrecht, The Netherlands (Kluwer Academic Publ.).

Bown, P.R., 2001. Calcareous nannofossils of the gault, upper greensand and glauconitic marl (middle Albian–lower Cenomanian) from the BGS Selborne boreholes, Hampshire. *Proc. Geol. Assoc.,* 112:223–236.

Bown, P.R., and Concheyro, A., 2004. Lower Cretaceous calcareous nannoplankton from the Neuquén Basin, Argentina. *Mar. Micropaleontol.,* 52:51–84.

Bown, P.R., and Cooper, M.K.E., 1998. Jurassic. *In* Bown, P.R. (Ed.), *Calcareous Nannofossil Biostratigraphy:* Dordrecht, The Netherlands (Kluwer Academic Publ.), 34–85.

Bown, P.R., Lees, J.A., and Young, J.R., 2004. Calcareous nannofossil evolution and diversity through time. *In* Thierstein, H.R., and Young, J.R. (Eds.), *Coccolithophores: From Molecular Process to Global Impact:* Berlin (Springer-Verlag).

Bown, P.R., Rutledge, D.C., Crux, J.A., and Gallagher, L.T., 1998. Lower Cretaceous. *In* Bown, P.R. (Ed.), *Calcareous Nannofossil Biostratigraphy:* Dordrecht, The Netherlands (Kluwer Academic Publ.), 86–131.

Bown, P.R., and Young, J.R., 1997. Mesozoic calcareous nannoplankton classification. *J. Nannoplankton Res.,* 19:21–36.

Bown, P.R., and Young, J.R., 1998. Techniques. *In* Bown, P.R. (Ed.), *Calcareous Nannofossil Biostratigraphy:* Dordrecht, The Netherlands (Kluwer Academic Publ.), 16–28.

Bralower, T.J., 1987. Valanginian to Aptian calcareous nannofossil stratigraphy and correlation with the upper M-sequence magnetic anomalies. *Mar. Micropaleontol.,* 11:293–310.

Bralower, T.J., 1992. Stable isotopic, assemblage, and paleoenvironmental investigations of juvenile-ocean sediments recovered on Leg 122, Wombat Plateau, north-

west Australia. *In* von Rad, U., Haq, B.U., et al., *Proc. ODP, Sci. Results,* 122: College Station, TX (Ocean Drilling Program), 569–585.

Bralower, T.J., and Bergen, J.A., 1998. Cenomanian–Santonian calcareous nannofossil biostratigraphy of a transect of cores drilled across the western interior seaway. *SEPM Concepts in Sedimentology and Paleontology,* 6:59–577.

Bralower, T.J., Leckie, R.M., Sliter, W.V., and Thierstein, H.R., 1995. An integrated Cretaceous microfossil biostratigraphy. *In* Berggren, W.A., Kent, D.V., Aubry, M.-P., and Hardenbol, J. (Eds.), *Geochronology, Time Scales, and Global Stratigraphic Correlation.* Spec. Publ.—SEPM (Soc. Sediment. Geol.), 54:65–79.

Bralower, T.J., Monechi, S., and Thierstein, H.R., 1989. Calcareous nannofossil zonation of the Jurassic–Cretaceous boundary interval and correlation with the geomagnetic polarity timescale. *Mar. Micropaleontol.,* 14:153–235.

Bralower, T.J., Premoli Silva, I., Malone, M.J., et al., 2002. *Proc. ODP, Init. Repts.,* 198 [CD-ROM]. Available from: Ocean Drilling Program, Texas A&M University, College Station TX 77845-9547, USA.

Bralower, T.J., and Siesser, W.G., 1992. Cretaceous calcareous nannofossil biostratigraphy of Sites 761, 762, and 763, Exmouth and Wombat Plateaus, northwest Australia. *In* von Rad, U., Haq, B.U., et al., *Proc. ODP, Sci. Results,* 122: College Station, TX (Ocean Drilling Program), 529–556.

Bralower, T.J., Sliter, W.V., Arthur, M.A., Leckie, R.M., Allard, D.J., and Schlanger, S.O., 1993. Dysoxic/anoxic episodes in the Aptian–Albian (Early Cretaceous). *In* Pringle, M.S., Sager, W.W., Sliter, W.V., and Stein, S. (Eds.), *The Mesozoic Pacific: Geology, Tectonics, and Volcanism.* Geophys. Monogr., 77:5–37.

Brassell, S.C., Dumitrescu, M., and the ODP Leg 198 Shipboard Scientific Party, 2004. Recognition of alkenones in a lower Aptian porcellanite from the west-central Pacific. *Org. Geochem.,* 35:181–188.

Bukry, D., 1971. Coccolith stratigraphy Leg 6, DSDP. *In* Fischer, A.G., Heezen, B.C., et al., *Init. Repts. DSDP,* 6: Washington (U.S. Govt. Printing Office), 965–1004.

Bukry, D., 1973a. Phytoplankton stratigraphy, Central Pacific Ocean, Deep Sea Drilling Project Leg 17. *In* Winterer, E.L., Ewing, J.I., et al., *Init. Repts. DSDP,* 17: Washington (U.S. Govt. Printing Office), 871-889.

Bukry, D., 1973b. Phytoplankton stratigraphy, Deep Sea Drilling Project Leg 20, western Pacific Ocean. *In* Heezen, B.C., MacGregor, I.D., et al., *Init. Repts. DSDP,* 20: Washington (U.S. Govt. Printing Office), 307–317.

Bukry, D., 1975a. Coccolith and silicoflagellate stratigraphy, northwestern Pacific Ocean, Deep Sea Drilling Project Leg 32. *In* Larson, R.L., Moberly, R., et al., *Init. Repts. DSDP,* 32: Washington (U.S. Govt. Printing Office), 677–701.

Bukry, D., 1975b. Phytoplankton stratigraphy, southwest Pacific, Deep Sea Drilling Project, Leg 30. *In* Andrews, J.E., Packham, G., et al., *Init. Repts. DSDP,* 30: Washington (U.S. Govt. Printing Office), 539–547.

Bukry, D., 1976. Coccolith stratigraphy of Manihiki Plateau, Central Pacific, Deep Sea Drilling Project Site 317. *In* Schlanger, S.O., Jackson, E.D., et al., *Init. Repts. DSDP,* 33: Washington (U.S. Govt. Printing Office), 493-501.

Burnett, J.A., 1998. Upper Cretaceous. *In* Bown, P.R. (Ed.), *Calcareous Nannofossil Biostratigraphy:* Dordrecht, The Netherlands (Kluwer Academic Publ.), 132–199.

Busson, G., and Noël, D., 1991. Les nannoconidés indicateurs environnementaux des oceans et mers épicontinentales du Jurassique terminal et du Crétacé inférieur. *Oceanol. Acta,* 14:333–356.

Cepek, P., 1981. Mesozoic calcareous-nannoplankton stratigraphy of the central North Pacific (Mid-Pacific Mountains and Hess Rise), Deep Sea Drilling Project Leg 62. *In* Thiede, J., Vallier, T.L., et al., *Init. Repts. DSDP,* 62: Washington (U.S. Govt. Printing Office), 397–418.

Channell, J.E.T., Erba, E., and Lini, A., 1993. Magnetostratigraphic calibration of the late Valenginian carbon isotope event in pelagic limestones from northern Italy and Switzerland. *Earth Planet. Sci. Lett.,* 118:145–166.

Channell, J.E.T., Erba, E., Nakanishi, M., and Tamaki, K., 1995. Late Jurassic–Early Cretaceous time scales and oceanic magnetic anomaly block models. *In* Berggren, W.A., Kent, D.V., Aubry, M.-P., and Hardenbol, J. (Eds.), *Geochronology, Time Scales, and Global Stratigraphic Correlation.* Spec. Publ.—SEPM (Soc. Sediment. Geol.), 54:51–63.

Coccioni, R., Erba, E., and Premoli Silva, I., 1992. Barremian–Aptian calcareous plankton biostratigraphy from the Gorgo Cerbara section (Marche, central Italy) and implications for plankton evolution. *Cretaceous Res.,* 13:517–537.

Covington, J.M., and Wise, S.W., Jr., 1987. Calcareous nannofossil biostratigraphy of a Lower Cretaceous deep-sea fan: Deep Sea Drilling Project Leg 93 Site 603, lower continental rise off Cape Hatteras. *In* van Hinte, J.E., Wise, S.W., Jr., et al., *Init. Repts. DSDP,* 93: Washington (U.S. Govt. Printing Office), 617–660.

Crux, J.A., 1982. Upper Cretaceous (Cenomanian to Campanian) calcareous nannofossils. *In* Lord, A.R. (Ed.), *A Stratigraphical Index of Calcareous Nannofossils:* Chichester (Ellis Horwood), 81–135.

de Kaenel, E., and Bergen, J.A., 1996. Mesozoic calcareous nannofossil biostratigraphy from Sites 897, 899, and 901, Iberia Abyssal Plain: new biostratigraphic evidence. *In* Whitmarsh, R.B., Sawyer, D.S., Klaus, A., and Masson, D.G. (Eds.), *Proc. ODP, Sci. Results,* 149: College Station, TX (Ocean Drilling Program), 27–59.

Deres, F., and Achéritéguy, 1980. Biostratigraphie des nannoconidés. *Bull. Cent. Rech. Explor.—Prod. Elf-Aquitaine,* 4:1–53.

Erba, E., 1988. Aptian-Albian calcareous nannofossil biostratigraphy of the Scisti a Fucoidi cored at Piobbico (central Italy). *Riv. Ital. Paleontol. Stratigr.,* 94:249–284.

Erba, E., 1992. Middle Cretaceous calcareous nannofossils from the western Pacific (Leg 129): evidence for paleoequatorial crossings. *In* Larson, R.L., Lancelot, Y., et al., *Proc. ODP, Sci. Results,* 129: College Station, TX (Ocean Drilling Program), 189–201.

Erba, E., 1994. Nannofossils and superplumes: the early Aptian "nannoconids crisis." *Paleoceanography,* 9:483–501.

Erba, E., Channell, J.E.T., Claps, M., Jones, C., Larson, R., Opdyke, B., Premoli Silva, I., Riva, A., Salvini, G., and Torricelli, S., 1999. Integrated stratigraphy of the Cismon APTICORE (southern Alps, Italy): a "reference section" for the Barremian–Aptian interval at low latitudes. *J. Foraminiferal Res.,* 29:371–391.

Erba, E., and Covington, J.M., 1992. Calcareous nannofossil biostratigraphy of Mesozoic sediments recovered from the Western Pacific, Leg 129. *In* Larson, R.L., Lancelot, Y., et al., *Proc. ODP, Sci. Results,* 129: College Station, TX (Ocean Drilling Program), 179–187.

Erba, E., Premoli Silva, I., and Watkins, D.K., 1995. Cretaceous calcareous plankton biostratigraphy of Sites 872 through 879. *In* Haggerty, J.A., Premoli Silva, I., Rack, F., and McNutt, M.K. (Eds.), *Proc. ODP, Sci. Results,* 144: College Station, TX (Ocean Drilling Program), 157–169.

Gale, A.S., Kennedy, W.J., Burnett, J.A., Caron, M., and Kidd, B.E., 1996. The Late Albian to Early Cenomanian succession at Mont Risou near Rosans (Drôme, SE France): an integrated study (ammonites, inoceramids, planktonic foraminifera, nannofossils, oxygen and carbon isotopes). *Cretaceous Res.,* 17:515–606.

Gardin, S., Bulot, L.G., Coccioni, R., de Wever, P., Hishida, K., and Lambert, E., 2000. The Valanginian to Hauterivian hemipelagic successions of the Vocontian Basin (SE France): new high resolution integrated stratigraphical data. *Sixth Int. Cretaceous Symp., Vienna, Austria,* 34. (Abstract)

Gran, H.H., and Braarud, T., 1935. A quantitative study of the phytoplankton in the Bay of Fundy and the Gulf of Maine (including observations of the hydrogeology, chemistry and turbidity). *J. Biol. Board Can.,* 1:279–467.

Hay, W.W., 1971. Preliminary dating by fossil calcareous nannoplankton, Deep Sea Drilling Project, Leg 6. *In* Fischer, A.G., Heezen, B.C., et al., *Init. Repts. DSDP,* 6: Washington (U.S. Govt. Printing Office), 1005–1012.

Hekel, H., 1973. Nannofossil biostratigraphy, Leg 20, Deep Sea Drilling Project. *In* Heezen, B.C., MacGregor, I.D., et al., *Init. Repts. DSDP,* 20: Washington (U.S. Govt. Printing Office), 221–247.

Herrle, J.O., 2002. Paleoceanographic and paleoclimatic implications on mid-Cretaceous black shale formation in the Vocontian Basin and the Atlantic: evidence from calcareous nannofossils and stable isotopes [Ph.D. dissert.]. Univ. Tubingen, Federal Republic of Germany.

Herrle, J.O., 2003. Reconstructing nutricline dynamics of mid-Cretaceous oceans: evidence from calcareous nannofossils from the Niveau Pacquier black shale (SE France). *Mar. Micropaleontol.,* 47(3–4):307–321.

Hill, M.E., 1976. Lower Cretaceous calcareous nannofossils from Texas and Oklahoma. *Palaeontographica, Abt. B,* 156:103–179.

Jeremiah, J., 2001. A Lower Cretaceous nannofossil zonation for the North Sea Basin. *J. Micropaleontol.,* 20: 45-80.

Kelly, R.K., Norris, R.D., and Zachos, J.C., 2003. Deciphering the paleoceanographic significance of early Oligocene *Braarudosphaera* chalks in the South Atlantic. *Mar. Micropaleontol.,* 49:49–63.

Kennedy, W.J., Gale, A.S., Bown, P.R., Caron, M., Davey, R.J., Gröcke, D., and Wray, D.S., 2000. Integrated stratigraphy across the Aptian-Albian boundary in the Marnes Bleues, at the Col de Pré-Guitterd, Arnayon (Drôme), and at Tortonne (Alpes-de-Haute-Provence), France: a candidate global boundary stratotype section and boundary point for the base of the Albian Stage. *Cretaceous Res.,* 21:591–720.

Klaus, A., and Sager, W.W., 2002. Data report: High-resolution site survey seismic reflection data for ODP Leg 198 drilling on Shatsky Rise, northwest Pacific. *In* Bralower, T.J., Premoli Silva, I., Malone, M.J., et al., *Proc. ODP, Init. Repts.,* 198, 1–21 [CD-ROM]. Available from: Ocean Drilling Program, Texas A&M University, College Station TX 77845-9547, USA.

Lambert, B., 1986. La notion d'espéce chez le genre *Braarudosphaera* Deflandre, 1947: myth et réalité. *Rev. Micropaleontol.,* 28:255–264.

Larson, R.L., Lancelot, Y., et al., 1992. *Proc. ODP, Sci. Results,* 129: College Station, TX (Ocean Drilling Program).

Lozar, F., and Tremolada, F., 2003. Calcareous nannofossil biostratigraphy of Cretaceous sediments recovered at ODP Site 1149 (Leg 185, Nadezhda Basin, western Pacific). *Proc. ODP, Sci. Results,* 185 [Online]: Available from World Wide Web: <http://www-odp.tamu.edu/publications/185_SR/003/003.htm>.

Mao, S., and Wise, S.W., Jr., 1993. Mesozoic calcareous nannofossils from Leg 130. *In* Berger, W.H., Kroenke, L.W., Mayer, L.A., et al., *Proc. ODP, Sci. Results,* 130: College Station, TX (Ocean Drilling Program), 85–92.

Martini, E., 1976. Cretaceous to Recent calcareous nannoplankton from the Central Pacific Ocean (DSDP Leg 33). *In* Schlanger, S.O., Jackson, E.D., et al., *Init. Repts. DSDP,* 33: Washington (U.S. Govt. Printing Office), 383–423.

Mattioli, E., Reboulet, S., Pittet, B., Proux, O., and Baudin, F., 2000. Calcareous nannoplankton and ammonoid abundance in Valanginian limestone-marl couplets: a dominance of carbonate dilution or productivity? *J. Nannoplankton Res.,* 22:123–124. (Abstract)

McIntyre, A., and Bé, A.W.H., 1967. Modern coccolithophoridae of the Atlantic Ocean. I: placoliths and cyrtoliths. *Deep-Sea Res. Part A,* 14:561–597.

Mutterlose, J., 1989. Temperature-controlled migration of calcareous nannofossils in the north-west European Aptian. *In* Crux, J.A., and van Heck, S.E. (Eds.), *Nannofossils and Their Applications:* Chichester (Ellis Horwood), 122–142.

Mutterlose, J., 1992a. Biostratigraphy and palaeobiogeography of Early Cretaceous calcareous nannofossils. *Cretaceous Res.,* 13:157–189.

Mutterlose, J., 1992b. Lower Cretaceous nannofossil biostratigraphy off northwestern Australia (Leg 123). *In* Gradstein, F.M., Ludden, J.N., et al., *Proc. ODP, Sci. Results,* 123: College Station, TX (Ocean Drilling Program), 343–368.

Mutterlose, J., and Kessels, K., 2000. Early Cretaceous calcareous nannofossils from the high latitudes: implications for palaeobiogeography and palaeoclimate. *Palaeogeogr., Palaeoclimatol., Palaeoecol.,* 160: 347–372.

Mutterlose, J., and Wise, S.W., Jr., 1990. Lower Cretaceous nannofossil biostratigraphy of ODP Leg 113 Holes 692B and 693A, continental slope off East Antarctica, Weddell Sea. *In* Barker, P.F., Kennett, J.P., et al., *Proc. ODP, Sci. Results,* 113: College Station, TX (Ocean Drilling Program), 325–351.

Nagai, K., Furukawa, M., Yoshiyama, T., Yoshida, T., Giraud, F., Inagaki, F., Nishi, H., Sakamoto, T., and Okada, H., 2002. High-resolution analysis of calcareous nannofossils from OAE1 sequences exposed in SE France. *J. Nannoplankton. Res.,* 24:141. (Abstract)

Okada, H., and Honjo, S., 1973. The distribution of oceanic coccolithophorids in the Pacific. *Deep-Sea Res. Part A,* 20:355–374.

Paleo-Alampay, A.M., Mead, G.A., and Wei, W., 1999. Unusual Oligocene *Braarudosphaera*-rich layers of the South Atlantic and their palaeoceanographic implications. *J. Nannoplankton Res.,* 21:17–26.

Parker, M.E., Clark, M., and Wise, S.W., Jr., 1985. Calcareous nannofossils of Deep Sea Drilling Project Sites 558 and 563, North Atlantic Ocean: biostratigraphy and the distribution of Oligocene braarudosphaerids. *In* Bougault, H., Cande, S.C., et al., *Init. Repts. DSDP,* 82: Washington (U.S. Govt. Printing Office), 559–589.

Perch-Nielsen, K., 1979. Calcareous nannofossils from the Cretaceous between the North Sea and the Mediterranean. *In* Wiedmann, J. (Ed.), *Aspekte der Kreide Europas*. Int. Union Geol. Sci. Ser. A, 6:223–272.

Perch-Nielsen, K., 1985. Mesozoic calcareous nannofossils. *In* Bolli, H.M., Saunders, J.B., and Perch-Nielsen, K. (Eds.), *Plankton Stratigraphy:* Cambridge (Cambridge Univ. Press), 329–426.

Proto Decima, F., 1974. Leg 27 calcareous nannoplankton. *In* Veevers, J.J., Heirtzler, J.R., et al., *Init. Repts. DSDP,* 27: Washington (U.S. Govt. Printing Office), 589–621.

Racki, G., and Cordey, F., 2000. Radiolarian paleoecology and radiolarites: is the present the key to the past? *Earth Sci. Rev.,* 52:83–120.

Remane, J., 1985. Calpionellids. *In* Bolli, H., Saunders, J., and Perch-Nielsen, K. (Eds.), *Plankton Stratigraphy.* Cambridge (Cambridge Univ. Press), 555–572.

Robinson, S.A., Williams, T., and Bown, P.R., 2004. Fluctuations in biosiliceous production and the generation of Early Cretaceous oceanic anoxic events in the Pacific Ocean (Shatsky Rise, ODP Leg 198). *Paleoceanography,* 19:PA4024:10.1029/2004PA001010.

Roth, P.H., 1973. Calcareous nannofossils—Leg 17, Deep Sea Drilling Project. *In* Winterer, E.L., Ewing, J.I., et al., *Init. Repts. DSDP,* 17: Washington (U.S. Govt. Printing Office), 695–795.

Roth, P.H., 1978. Cretaceous nannoplankton biostratigraphy and oceanography of the northwestern Atlantic Ocean. *In* Benson, W.E., Sheridan, R.E., et al., *Init. Repts. DSDP,* 44: Washington (U.S. Govt. Printing Office), 731–759.

Roth, P.H., 1981. Mid-Cretaceous calcareous nannoplankton from the central Pacific: implication for paleoceanography. *In* Thiede, J., Vallier, T.L., et al., *Init. Repts. DSDP,* 62: Washington (U.S. Govt. Printing Office), 471–489.

Roth, P.H., 1983. Jurassic and Lower Cretaceous calcareous nannofossils in the western North Atlantic (Site 534): biostratigraphy, preservation, and some observations on biogeography and paleoceanography. *In* Sheridan, R.E., Gradstein, F.M., et al., *Init. Repts. DSDP,* 76: Washington (U.S. Govt. Printing Office), 587–621.

Roth, P.H., and Bowdler, J., 1981. Middle Cretaceous calcareous nannoplankton biogeography and oceanography of the Atlantic Ocean. *In* Warme, J.E., Douglas, R.G., and Winterer, E.L. (Eds.), *The Deep Sea Drilling Project: a Decade of Progress*. Spec. Publ.—Soc. Econ. Paleontol. Mineral., 32:517–546.

Roth, P.H., and Krumbach, K.R., 1986. Middle Cretaceous calcareous nannofossil biogeography and preservation in the Atlantic and Indian Oceans: implications for paleoceanography. *Mar. Micropaleontol.,* 10:235–266.

Scarparo, A.A., and Shimabukaro, S., 1997. *Braarudosphaera* blooms and anomalous enrichment of *Nannoconus:* evidence from the Turonian South Atlantic, Santos Basin, Brazil. *J. Nannoplankton Res.,* 19:51–55.

Siesser, W.G., Bralower, T.J., and De Carlo, E.H., 1992. Mid-Tertiary *Braarudosphaera*-rich sediments on the Exmouth Plateau. *In* von Rad, U., Haq, B.U., et al., *Proc. ODP, Sci. Results,* 122: College Station, TX (Ocean Drilling Program), 653–663.

Shafik, S., 1975. Nannofossil biostratigraphy of the southwest Pacific, Deep Sea Drilling Project, Leg 30. *In* Andrews, J.E., Packham, G., et al., *Init. Repts. DSDP,* 30: Washington (U.S. Govt. Printing Office), 549–598.

Shipboard Scientific Party, 2002a. Explanatory notes. *In* Bralower, T.J., Premoli Silva, I., Malone, M.J., et al., *Proc. ODP, Init. Repts.,* 198, 1–63 [CD-ROM]. Available from: Ocean Drilling Program, Texas A&M University, College Station TX 77845-9547, USA.

Shipboard Scientific Party, 2002b. Leg 199 summary. *In* Lyle, M.W., Wilson, P.A., Janecek, T.R., et al., *Proc. ODP, Init. Repts.,* 199: College Station TX (Ocean Drilling Program), 1–87.

Sissingh, W., 1977. Biostratigraphy of Cretaceous calcareous nannoplankton. *Geol. Mijnbouw,* 56:37–65.

Street, C., and Bown, P.R., 2000. Palaeobiogeography of Early Cretaceous (Berriasian–Barremian) calcareous nannoplankton. *Mar. Micropaleontol.,* 39:265–291.

Thiede, J., Vallier, T.L., et al., 1981. *Init. Repts. DSDP,* 62: Washington (U.S. Govt. Printing Office).

Thierstein, H.R., 1971. Tentative Lower Cretaceous calcareous nannoplankton zonation. *Eclogae Geol. Helv.,* 64:458–488.

Thierstein, H.R., 1973. Lower Cretaceous calcareous nannoplankton biostratigraphy. *Abh. Geol. Bundesanst. (Austria),* 29:1–52.

Thierstein, H.R., 1974. Calcareous nannoplankton, Leg 26, Deep Sea Drilling Project. *In* Davies, T.A., Luyendyk, B.P., et al., *Init. Repts. DSDP,* 26: Washington (U.S. Govt. Printing Office), 619–667.

Thierstein, H.R., 1976. Mesozoic calcareous nannoplankton biostratigraphy of marine sediments. *Mar. Micropaleontol.,* 1:325–362.

Tremolada, F., and Erba, E., 2002. Morphometric analysis of Aptian *Assipetra infracretacea* and *Rucinolithus terebrodentarius* nannoliths: implications for taxonomy, biostratigraphy and paleoceanography. *Mar. Micropaleontol.,* 44:77–92.

van Niel, B., 1994. A review of the terminology used to describe the genus *Nannoconus* (calcareous nannofossil, *incertae sedis*). *Cah. Micropaleontol.,* 9:29–55.

Weissert, H., Lini, A., Föllmi, K.B., and Kuhn, O., 1998. Correlation of Early Cretaceous carbon isotope stratigraphy and platform drowning events: a possible link? *Palaeogeogr., Palaeoclimatol., Palaeoecol.,* 137:189–203.

Winter, A., Jordan, R.W., and Roth, P.H., 1994. Biogeography of living coccolithophores. *In* Winter, A., and Siesser, W.G. (Eds.), *Coccolithophores:* Cambridge (Cambridge Univ. Press), 161–177.

Worsley, T., 1971. Calcareous nannofossil zonation of Upper Jurassic and Lower Cretaceous sediments from the Western Atlantic. *In* Farinacci, A. (Ed.), *Proc. 2nd Planktonic Conf. Roma,* 2:1301–1322.

Young, J.R., Bergen, J.A., Bown, P.R., Burnett, J.A., Fiorentino, A., Jordan, R.W., Kleijne, A., van Niel, B.E., Ton Romein, A.J., von Salis, K., 1997. Guidelines for coccolith and calcareous nannofossil terminology. *Paleontology,* 40:875–912.

APPENDIX A

Systematic Taxonomy

The systematic paleontology section includes taxonomic discussion of key taxa, the description of one new genus (*Mattiolia furva*) and 13 new species (*Zeugrhabdotus clarus, Zeugrhabdotus petrizzoae, Helicolithus leckiei, Rhagodiscus amplus, Rhagodiscus robustus, Rhagodiscus sageri, Rhagodiscus adinfinitus, Tubodiscus bellii, Tubodiscus frankiae, Gartnerago ponticula, Haqius peltatus, Mattiolia furva*, and *Kokia stellata*). The taxonomy follows the classification and organization of Bown and Young (1997) and Bown et al. (1998). Only bibliographic references not included in Perch-Nielsen (1985) and Bown (1998) are included in the reference list. A full taxonomic list of species cited in this paper follows in "Appendix B," p. 39. Descriptive terminology follows the guidelines of Young et al. (1997), and the following abbreviations are used in taxonomic descriptions: LM = light microscope, XPL = cross-polarized light, PC = phase-contrast illumination. Holotype dimension are given in parentheses. The taxa are illustrated in Plates P1–P13.

Family Chiastozygaceae Rood et al., 1973, emend. Varol and Girgis, 1994

***Zeugrhabdotus clarus* sp. nov.**
Pl. P1, figs. 34–42

Derivation of name: From *clarus*, meaning bright, referring to the birefringent inner cycle that distinguishes this coccolith.

Diagnosis: Bicyclic murolith with a prominent bright, inner-rim cycle (LM XPL) and a central area spanned by a single bar that tapers at both ends. The two rim cycles are comparable in width, but the inner cycle may be broader and is usually complete around the inner edge of the rim. Strongly curved extinction lines cross the bright inner cycle.

Differentiation: Closest in morphology to *Zeugrhabdotus trivectis* Bergen, 1994, but *Z. clarus* has a plainer, more simply constructed bar. It is also comparable to the rim morphologies seen in the genera *Placozygus* and *Eiffellithus*.

Dimensions: length = 4.0–5.5 (5.1) µm; width = 2.5–3.6 (3.6) µm.

Holotype: Pl. P1, fig. 34 (figs. 34–36 are the same specimen).

Paratypes: Pl. P1, figs. 38, 41.

Type locality: ODP Leg 198 Hole 1207B, Shatsky Rise, northwest Pacific.

Type level: upper Albian, Sample 198-1207B-29R-CC (Subzone NC9b).

Range: lower Albian–lower Cenomanian (Subzone NC8a–Zone UC1). Found in all mid-Cretaceous Shatsky Rise sections and also in the Albian of southern France (pers. observ.).

***Zeugrhabdotus embergeri* (Noël, 1958) Perch-Nielsen, 1984**
Pl. P2, figs. 2–12

Remarks: A great variety of morphologies are classified within this species concept, most obviously in size range (5–15 µm) but also bar and spine morphology. The species name is used herein for bicyclic loxoliths possessing a broad, disjunct, birefringent, simply constructed transverse bar that bears a spine. The spine clearly divides the bar into two lateral parts.

The consistently expressed bicyclicity in this species group perhaps warrants separate generic status, as they can be clearly distinguished from the broad range of zeugrhabdotid coccoliths that range through the Cretaceous. However, this group remains poorly understood in terms of phylogeny, and therefore higher taxonomy, and we prefer to continue with the use of *Zeugrhabdotus* as a broad generic grouping until further progress is made. The genus *Gorkaea* Varol

P1. Chiastozygaceae, p. 58.

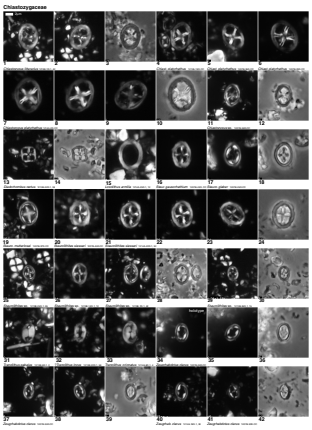

P2. Chiastozygaceae: *Zeugrhabdotus*, p. 60.

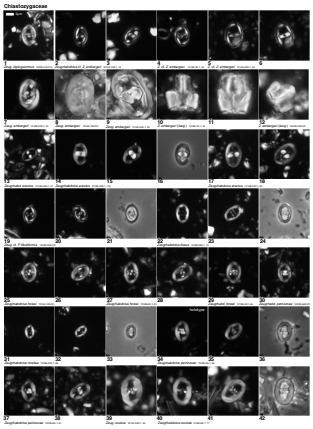

and Girgis, 1994, includes bicyclic morphologies but has a "very narrow" outer cycle rather than the near-equal width cycles seen in the *embergeri* group. In this study, smaller *embergeri* coccoliths (<6 µm) were logged as cf. *Z. embergeri* (Pl. **P2,** figs. 2–6) and forms with very broad spines as cf. *Z. kerguelenensis* (Pl. **P2,** figs. 10–12).

Range: Upper Jurassic–Cretaceous/Tertiary boundary.

Zeugrhabdotus erectus (Deflandre in Deflandre and Fert, 1954) Reinhardt, 1965

Pl. **P2,** figs. 13–18

Remarks: Used here for unicyclic loxoliths with a disjunct, birefringent, simply constructed transverse bar that bears a spine. The spine is marked by a black dot in XPL.

A wide range of zeugrhabdotid morphologies occur through the Jurassic/Cretaceous boundary interval, and the differentiation between *Z. erectus* and *Z. embergeri* has been much discussed (see review in Bralower et al., 1989). The definition adopted here, when strictly applied, results in a Berriasian last occurrence for *Z. erectus*, and they are only frequently present in the lowermost two nannofossiliferous cores of Hole 1213B (Cores 198-1213B-26R and 27R; lower Berriasian).

Range: Pliensbachian–?Berriasian; lower Berriasian (Zones NK1–NK2a) in Hole 1213B.

Zeugrhabdotus petrizzoae sp. nov.

Pl. **P2,** figs. 34–38

Derivation of name: Named for Maria Rose Petrizzo, micropaleontologist and ODP 198 shipboard scientist.

Diagnosis: Medium-sized unicyclic murolith with a central area spanned by a broad, disjunct, transverse bar. The bar is usually brighter than the rim in LM XPL and formed from two plain blocks divided by a median suture; the two blocks are offset at each end of the bar.

Differentiation: The blocks making up the bar are brighter and blockier than those of *Zeugrhabdotus diplogrammus* and offset at their ends.

Dimensions: length = 5.3 µm; width = 3.8 µm.

Holotype: Pl. **P2,** fig. 34 (figs. 34–36 are the same specimen).

Paratype: Pl. **P2,** fig. 37 (fig. 38 is the same specimen).

Type locality: ODP Leg 198 Hole 1213B, Shatsky Rise, northwest Pacific.

Type level: lower Albian, Sample 198-1213B-4R-1, 48 cm (Subzones NC8a/NC8b).

Range: Albian (Subzones NC8a/NC8b) at Site 1213.

Family Eiffellithaceae Reinhardt, 1965

Helicolithus leckiei sp. nov.

Pl. **P3,** figs. 40–42; Pl. **P4,** figs. 1, 2

Derivation of name: Named for Mark Leckie, micropaleontologist and ODP 198 shipboard scientist.

Diagnosis: Small, bicyclic murolith with a prominent bright, inner cycle (LM XPL) and central area spanned by a birefringent, diagonal cross. The two rim cycles are comparable in width but the inner cycle may be broader. The junction between the two cycles is usually distinctly scalloped.

Remarks: Three Cretaceous genera incorporate bicyclic, murolith coccoliths with diagonal crosses, *Eiffellithus*, *Tegumentum*, and *Helicolithus*, and the relationships within and between them is presently poorly understood. This new species is included within *Helicolithus*, based on the nature of the cross bars, which are straight and simply constructed.

P3. Chiastozygaceae, Eiffellithaceae, p. 62.

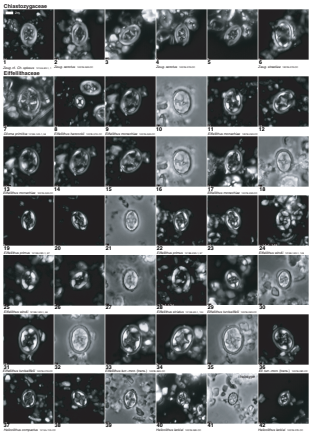

P4. Eiffellithaceae, *Rhagodiscus asper* group, p. 64.

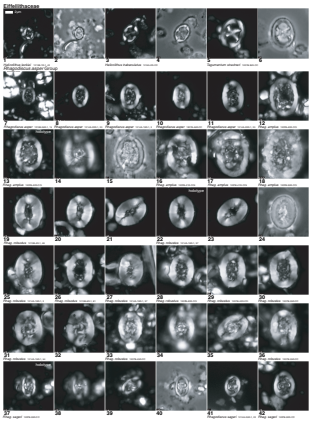

Differentiation: Close in morphology to *Corollithion*? *madagascarensis* Perch-Nielsen, 1973, but the latter has a delicate cross, does not show the distinctive scalloped cycle junction, and has a rim that shows *Corollithion*-like characteristics (i.e., a protolith-like rim) (see Bown, 1987; Young et al., 1997). In addition, it has only been recorded from much younger strata (i.e., Maastrichtian). It also resembles *Ellipsochiastus quadriserratus* Worsley, 1971, but the latter is larger with narrower bars and more open central area.

Dimensions: length = 3.4 (3.7) µm; width = 2.4 (2.5) µm.

Holotype: Pl. **P3,** fig. 41 (fig. 40 is the same specimen).

Paratype: Pl. **P3,** fig. 42.

Type locality: ODP Leg 198 Hole 1207B, Shatsky Rise, northwest Pacific.

Type level: upper Albian, Sample 198-1207B-28R-CC (Subzone NC10a).

Range: Aptian (Zone NC7)–Cenomanian (Zones UC3/UC4). Found in all mid-Cretaceous Shatsky Rise sections and also in the Albian of southern France (pers. observ.).

Family Rhagodiscaceae Hay, 1977

***Rhagodiscus asper* (Stradner, 1963) Reinhardt, 1967, Group**
Pl. **P4,** figs. 7–42; Pl. **P5,** figs. 1–6

Remarks: Murolith (loxolith) coccoliths with a relatively broad central area spanned by a granular plate that may or may not bear a spine; the rim appears unicyclic in LM.

Considerable morphological variation is observed within this species concept, and this is somewhat reflected in the number of species names that have been applied to similar but poorly defined morphotypes that in many cases may be synonyms (e.g., *Rhagodiscus reightonensis* [Taylor, 1978] Watkins in Watkins and Bowdler 1984 [wider rim]; *Rhagodiscus eboracencis* Black, 1971 [no spine]; "*Rhabdolithina" swinnertoni* Black, 1971 [large spine]; and "*Zygolithus" fenestratus* Stover, 1966 [perforate plate]). A number of distinctive morphologies were observed in the mid-Cretaceous sediments of Shatsky Rise, and these are described below as three new species.

Rhagodiscus amplus sp. nov.
Pl. **P4,** figs. 12–18

Derivation of name: From *amplus*, meaning large, and referring to the size of the coccoliths.

Diagnosis: Large (>8.0 µm) loxolith coccoliths with a wide central area (usually greater than twice as wide as the rim) that is spanned by a granular plate. A relatively large spine or spine base may or may not be present. The rim and plate usually show yellow interference colors under XPL.

Differentiation: Similar in general morphology to *Rhagodiscus asper* but distinguished by its larger size.

Dimensions: length = 9.8 µm; width = 7.2 µm.

Holotype: Pl. **P4,** fig. 13 (figs. 13–15 are the same specimen).

Paratype: Pl. **P4,** fig. 17.

Type locality: ODP Leg 198 Hole 1207B, Shatsky Rise, northwest Pacific.

Type level: Aptian, Sample 198-1207B-42R-CC (Zone NC7).

Range: Aptian (Zone NC6)–middle Albian (Subzone NC8b) at Sites 1207, 1213, and 1214.

Rhagodiscus robustus sp. nov.
Pl. **P4,** figs. 19–36

Derivation of name: From *robustus*, meaning robust, and referring to the broad, blocky rim of this species.

Diagnosis: Large (>8.0 µm) loxolith coccoliths with a broad rim (usually as broad or broader than the central area) and a central area spanned by a granular

P5. Rhagodiscaceae, ?Parhabdolithaceae, Stephanolithiaceae, p. 66.

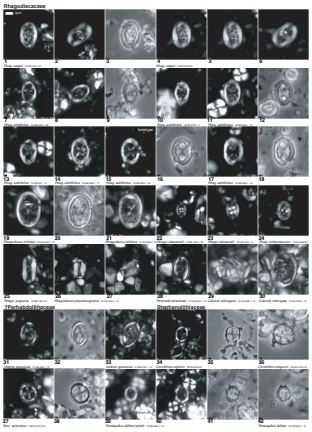

plate; a relatively large spine or spine base is usually present. The broad and blocky rim shows yellow interference colors under XPL.

Differentiation: Distinguished from other rhagodiscids by its large size and relatively closed central area, with some specimens resembling the Jurassic coccolith species *Crepidolithus crassus*. The Albian "*Crepidolithus" burwellensis* Black, 1972 (holotype scanning electron micrograph [SEM] only), displays a *Crepidolithus*-like rim but is small (~4.0 µm) and has an open central area crossed by a transverse bar.

Dimensions: length = 8.7 µm; width = 6.7 µm.

Holotype: Pl. **P4,** fig. 22 (figs. 22–24 are the same specimen).

Paratypes: Pl. **P4,** figs. 20, 29, 33.

Type locality: ODP Leg 198 Hole 1214A, Shatsky Rise, northwest Pacific.

Type level: lower Albian, Sample 198-1214A-19R-1, 37 cm (Subzones NC8A/NC8B).

Range: Barremian (Zone NC5)–upper Albian (Subzone NC10a) at Sites 1207, 1213, and 1214.

Rhagodiscus sageri sp. nov.

Pl. **P4,** figs. 37–42; Pl. **P5,** figs. 1–6

Derivation of name: Named for Will Sager, paleomagnetist and ODP Leg 198 shipboard scientist.

Diagnosis: Loxolith coccoliths with a relatively broad central area spanned by a granular plate that incorporates a transverse, raised, bridgelike structure.

Differentiation: Similar in general morphology to *Rhagodiscus asper* but distinguished by the raised ridge/bridge of the central area plate.

Dimensions: length = 9.8 µm; width = 7.2 µm.

Holotype: Pl. **P4,** fig. 37 (figs. 37–40 are the same specimen).

Paratype: Pl. **P5,** fig. 1 (figs. 1–3 are the same specimen).

Type locality: ODP Leg 198 Hole 1207B, Shatsky Rise, northwest Pacific.

Type level: Aptian, Sample 198-1207B-39R-CC (Zone NC7).

Range: Hauterivian (Zone NC4)–Cenomanian (Zones UC3/UC4) at Sites 1207, 1208, 1212, 1213, and 1214.

Other rhagodiscids

Rhagodiscus adinfinitus sp. nov.

Pl. **P5,** figs. 7–18

Derivation of name: From *ad*, meaning near or like, and referring to the similarity to the existing species *Rhagodiscus infinitus*.

Diagnosis: Medium-sized unicyclic loxolith coccoliths with a wide central area spanned by a butterfly-shaped bar with raised, birefringent edges.

Remarks: Specimens from the deepest nannofossiliferous core at Site 1213 (Core 198-1213B-27R) are slightly smaller and have less flaring bars than those higher in the hole. The raised edges of the bar make an angle of ~20°–25° with the transverse axis increasing to 40°–50° for specimens in higher cores. This may represent a shift in morphology toward the *R. infinitus* structure.

Differentiation: Comparable in general morphology to *Rhagodiscus infinitus*, with a central granular plate pierced by two large holes. However, *R. infinitus* has a plate that extends completely around the central area with distinct circular pores surrounded by raised, birefringent edges, whereas *R. adinfinitus* has only a broad, flaring bar (butterfly shaped) with raised edges that terminate against the inner edge of the rim.

Dimensions: length = 7.2 µm; width = 5.3 µm.

Holotype: Pl. **P5,** fig. 15 (fig. 16 is the same specimen).

Paratypes: Pl. **P5,** figs. 7, 18.

Type locality: ODP Leg 198 Hole 1213B, Shatsky Rise, northwest Pacific.

Type level: Berriasian, Sample 198-1213B-25R-1, 26 cm (Subzone NK2a).

Range: Berriasian (Zone NK1–Subzone NK2b) at Site 1213.

***Rhagodiscus dekaenelii* Bergen, 1994**
Pl. P5, figs. 22, 23

Remarks: Distinctive, small rhagodiscids that have a birefringent spine/spine base that almost fills the central area. Used herein as a secondary marker species approximating the base of Zone NK3 in the absence of *Calcicalathina oblongata* and *Tubodiscus verenae*.

Range: lower Valanginian (lower Subzone NK3a)–lower Hauterivian (Subzone NC4b), according to Bergen (1994) and supported herein at Site 1213.

Family Stephanolithiaceae Black, 1968

***Rotelapillus laffittei* (Noël, 1957) Noël, 1973**
Pl. P5, figs. 39–42; Pl. P6, figs. 1–9

Remarks: Circular muroliths with high walls, lateral rim spines, and central area spanned by six radial bars. This basic coccolith plan ranges throughout the Cretaceous with little change; however, a number of varieties were observed in the mid-Cretaceous material from Shatsky Rise. It is uncertain whether these morphotypes represent preservational differences or simply intraspecific variation, and until this can be better ascertained they are described here in informal nomenclature.

***Rotelapillus laffittei* (Noël, 1957) Noël, 1973, var. 1 (small)**
Pl. P5, figs. 39–42

Description: Small variety of *R. laffittei* with rim diameter <5.0 µm.

Range: upper Tithonian–Cretaceous/Tertiary boundary (Bown et al., 1998).

***Rotelapillus laffittei* (Noël, 1957) Noël, 1973, var. 2 (petaloid)**
Pl. P6, figs. 1–6

Description: Small variety of *R. laffittei* with a distal rim cycle that is strongly flaring and, at high focus, distinctly petaloid in outline.

Range: lower Aptian (Zone NC6)–Cenomanian (Zone UC4) at Site 1207.

***Rotelapillus laffittei* (Noël, 1957) Noël, 1973, var. 3 (large)**
Pl. P6, figs. 7–9

Description: Medium-sized variety of *R. laffittei* with rim diameter >5.0 µm.

Remarks: upper Hauterivian (Subzone NC4b)–lower Aptian (Zone NC6) at Sites 1207 and 1214.

Family Axopodorhabdaceae Bown and Young, 1987

***Axopodorhabdus cylindratus* (Noël, 1965) Wind and Wise in Wise and Wind, 1977**
Pl. P6, figs. 21, 22

Remarks: This species has not previously been recorded from the Early Cretaceous. It may have an extended stratigraphic range in the Pacific, or has simply not been identified due to the transitional nature of the lineage that gave rise to the typically Cretaceous species *Axopodorhabdus dietzmannii*. The latter is distinguished by a rather elongated rim with flattened sides (oblong shaped) (Pl. P6, figs. 23, 24).

Range: upper Pliensbachian–upper Tithonian (Bown and Cooper, 1998); Berriasian–upper Valanginian (Zone NK1–Subzone NK3b) at Site 1213.

P6. Stephanolithiaceae, Axopodorhabdaceae, Biscutaceae, p. 68.

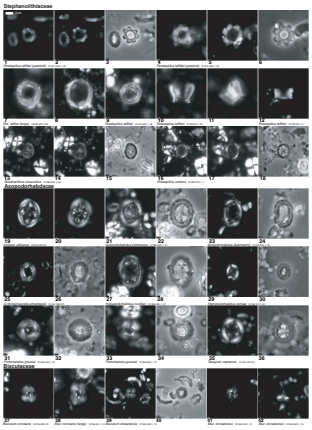

***Hexapodorhabdus cuvillieri* Noël, 1965**
Pl. P6, figs. 27, 28

Remarks: Not previously recorded from the Early Cretaceous and found here in only one Berriasian sample from Site 1213 (Sample 198-1213B-24R-1, 37 cm).
Range: upper Bajocian–upper Kimmeridgian (Bown and Cooper, 1998); Berriasian (Subzone NK2a) at Site 1213.

***Podorhabdus grassei* Noël, 1965**
Pl. P6, figs. 31–34

Remarks: Not previously recorded from the Early Cretaceous but found here consistently in the Berriasian of Site 1213 (Zone NK1–Subzone NK2a).
Range: lower Bajocian–lower Tithonian (Bown and Cooper, 1998); present in the upper Tithonian according to de Kaenel and Bergen (1996); Berriasian (Zone NK1–Subzone NK2a) at Site 1213.

Family Biscutaceae Black, 1971

***Biscutum constans* (Górka, 1957) Black in Black and Barnes, 1959 (large)**
Pl. P6, figs. 37, 38

Remarks: Large *B. constans* coccoliths (>5 µm) become conspicuous in the Albian and are shown on range charts as *B. constans* (large) (Pl. P6, fig. 38). These are probably equivalent to the *Biscutum "magnum"* of Erba (1988) that were also first recorded in the middle Albian (Subzone NC9a).
Range: Albian (Zone NC8)–Cenomanian (Zone UC2) at Sites 1207, 1213, and 1214.

***Biscutum dorsetensis* (Varol and Girgis, 1994) Bown in Bown and Cooper, 1998**
Pl. P6, figs. 39–42

Description: Circular to subcircular bicyclic *Biscutum* with a narrow central area and tall spine.
Range: upper Bathonian–Tithonian (Bown and Cooper, 1998); Berriasian–lower Valanginian (Zone NK1–Subzone NK3a) at Site 1213. Recorded for the first time in the Lower Cretaceous herein.

***Crucibiscutum bosunensis* Jeremiah, 2001**
Pl. P7, figs. 1, 2

Range: upper Aptian (Jeremiah, 2001). Observed rarely in the uppermost Aptian–lowermost Albian (top Zone NC7–base Zone NC8) at Sites 1207 and 1214.

Family Cretarhabdaceae Thierstein, 1973

***Cretarhabdus* cf. *C. conicus* Bramlette and Martini, 1964**
Pl. P7, figs. 10–13

Remarks: The name *Cretarhabdus conicus* is used here for cretarhabdid coccoliths with a distinct central area axial cross and net (Pl. P7, figs. 7–9). Similar coccoliths with slightly narrower central areas and less prominent axial crossbars were called *Cretarhabdus* cf. *C. conicus*. Possibly equivalent to "*Miravetesina" ficula* of Bralower and Bergen (1998, pl. 2, fig. 11).
Range: Not consistently differentiated in this study but recorded from the Aptian (Zones NC6–NC7) at Sites 1207 and 1214.

P7. Biscutaceae, Cretarhabdaceae, p. 70.

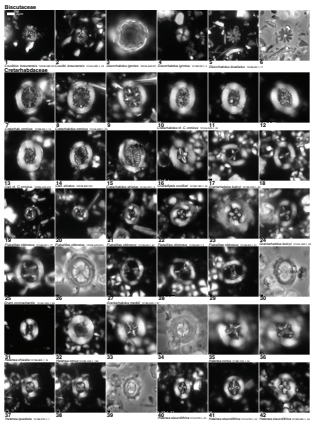

***Flabellites oblongus* (Bukry, 1969) Crux in Crux et al., 1982**
Pl. P7, figs. 19–23

Remarks: A significant size increase in this species is observed through the Aptian of the Shatsky mid-Cretaceous sections, with small sizes (3.5–5.0 µm) recorded in the lowermost Aptian (base Zone NC6) increasing to 7.0 µm at the top of Zone NC6, and reaching 10.0 µm by the lower Albian (Zone NC8).

***Grantarhabdus bukryi* Black, 1972**
Pl. P7, figs. 17, 18, 24

Remarks: Used here for medium-sized cretarhabdid coccoliths with unicyclic shield image and central area diagonal cross bars. The Albian holotype specimens have bars that make an angle of ~45° with the transverse axis of the coccolith; many of the earlier representatives included here have bars arranged at lower angles. Probably equivalent to *Grantarhabdus meddii* of many authors (e.g., Bown et al., 1998).
Range: ?Tithonian–Albian (de Kaenel and Bergen, 1996; Bown et al., 1998).

***Grantarhabdus meddii* Black, 1971**
Pl. P7, figs. 27–30

Remarks: Used here for cretarhabdid coccoliths with unicyclic shield image and central area diagonal cross bars that form a solid bar where they meet for around half of their length. They resemble both *Speetonia colligata* and *Grantarhabdus bukryi* but have distinctive cross-bar morphology.
Range: Uncertain, but Berriasian–lower Valanginian at Site 1213 (Zone NK1–Subzone NK3a).

***Helenea* Worsley, 1971, emend.**

Emended Diagnosis: Elliptical to subcircular cretarhabdid coccoliths that in LM show a change in birefringence toward the edge of the shield/rim, creating a diffuse bicyclic image; the outer cycle is narrowest. The central area structures are dominated by primary cross bars rather than lateral bars or grills, although the former may be present. Both axial and diagonal cross structures occur. The bars often flare toward their ends.
Remarks: A degree of confusion has arisen due to the description of two identical genera, *Helenea* and *Microstaurus*, in the same year by Worsley (1971) and Black (1971), which, after recombination, include one shared species name for different coccoliths. The genus *Microstaurus* is regarded here as a junior synonym of *Helenea*, and *Microstaurus quadratus* Black, 1971, a junior synonym of *Helenea staurolithina*. *Helenea quadratus* (Worsley, 1971) is included in the genus here and is distinguished by coccoliths with diagonal cross bars.

***Helenea chiastia* Worsley, 1971, emend. Bralower et al., 1989**
Pl. P7, fig. 31

Remarks: Broadly elliptical to subcircular coccoliths with a narrow central area spanned by an axial cross that bears a distinctly blocky (square) short spine. The long axis of the central area is less than one-half of the coccolith length (Bralower et al., 1989).
Range: Tithonian–lower Turonian (Bown et al., 1998).

***Helenea conus* (Worsley, 1971) Bown and Rutledge in Bown et al., 1998**
Pl. P7, figs. 32–36

Remarks: Subcircular to broadly elliptical coccoliths with a central area spanned by a vaulted axial cross that bears a spine. The bars usually display a dark median line under XPL and flare at their ends. The vaulted nature of the central structure makes focusing on the cross bars difficult.

The LM appearance of the rim of this species is not particularly typical of *Helenea*, as it is larger and shows no clear outer cycle; however, the cross bars conform to the generic characteristics, hence its inclusion here.

Range: ?upper Berriasian–?lower Barremian (Bown et al., 1998). Berriasian (Subzone NK2a)–upper Valanginian (Subzone NK3b) at Site 1213.

***Helenea quadrata* (Worsley, 1971) Bown and Rutledge in Bown et al., 1998**
Pl. P7, figs. 37–39

Remarks: Small broadly elliptical cretarhabdid coccoliths with a central area spanned by diagonal cross bars. The bars may display median black lines under XPL.

Range: lower Berriasian (grandis Tethyan Ammonite Zone)–upper Hauterivian (inversum/ligatus Ammonite Zones) (Bown et al., 1998). Restricted to the Berriasian at Site 1213 (Zone NK1–Subzone NK2a).

***Helenea staurolithina* Worsley, 1971**
Pl. P7, figs. 40–42

Remarks: Normally to broadly elliptical coccoliths with a narrow central area spanned by an axial cross. The long axis of the central area is equal to or greater than one-half of the coccolith length (Bralower et al., 1989).

In the Site 1213 material a number of specimens that resembled small *Cruciellipsis cuvillieri* coccoliths were included in this species.

Range: Tithonian–Hauterivian (Bown et al., 1998). Berriasian (Zone NK1)–lower Hauterivian (Subzone NC4b) at Site 1213.

***Pickelhaube*? sp. 1**
Pl. P8, figs. 17, 18

Remarks: Broadly elliptical placolith with relatively broad, moderately birefringent shields and an open central area.

Range: Aptian (Zone NC7)–lower Albian (lower Zone NC8) at Sites 1207 and 1214.

***Retecapsa* sp. (small)**
Pl. P8, fig. 15

Remarks: Small cretarhabdid rims (<5.0 µm) with empty central areas, but which in some cases have remnant axial crosses. They are relatively distinctive, being considerable smaller than most other cretarhabdid coccoliths, which are usually >6.0 µm.

Range: Not consistently logged in this study but lower Aptian (Zone NC6)–middle Albian (Subzone NC9a) at Site 1207.

Family Watznaueriaceae Rood et al., 1971

***Cyclagelasphaera brezae* Applegate and Bergen, 1988**
Pl. P8, figs. 30–32

Range: Berriasian (Zone NK1–Subzone NK2a) at Site 1213. Recorded from the Valanginian by Applegate and Bergen (1988).

***Cyclagelasphaera jiangii* Covington and Wise, 1987**
Pl. P8, figs. 27–29

Remarks: Medium-sized *Cyclagelasphaera* with an open central area, equivalent in width to that of the shield width. Covington and Wise (1987) described a small *Cyclagelasphaera* with an open central area spanned by radial bars, under SEM only. The rim to central area proportions are similar to those observed here

P8. Cretarhabdaceae, Watznaueriaceae, p. 72.

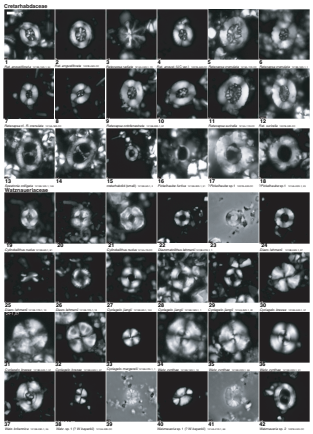

(central area equivalent in width to that of the shield), although the central area bars have not been seen. Distinguished from other species of *Cyclagelasphaera* by the large central opening.

Dimensions: length = 4.3–6.5 µm

Range: Valanginian of the North Atlantic (Covington and Wise, 1987); Berriasian (Subzone NK2a)–upper Hauterivian (Subzone NC4b) at Sites 1213 and 1214.

Watznaueria cynthae Worsley, 1971

Pl. P8, figs. 34–36

Remarks: Broadly elliptical *Watznaueria* coccoliths that have two variably developed central pores that pierce the inner cycle. These coccoliths resemble *Watznaueria biporta* Bukry, 1969, but are more subcircular in outline and do not routinely display clear pores.

Range: Berriasian (Subzone NK2a)–Albian (Zone NC8) at Sites 1207, 1213, and 1214.

Watznaueria sp. 1 (?*Watznaueria bayackii* Worsley, 1971)

Pl. P8, figs. 38–41

Remarks: Birefringent placolith coccoliths with closed central area. *Watznaueria*-like in appearance but appear flat and have relatively large, visible rim elements. They resemble *Watznaueria bayackii* Worsley, 1971, but the three holotype images provided are not good enough to allow unequivocal identification. They may represent disaggregated, isolated shields of *Watznaueria barnesiae*.

Watznaueria? sp. 2

Pl. P8, fig. 42

Remarks: Placoliths with relatively narrow shields and broad central area (central area is greater than twice the width of the rim). The LM XPL image of the rim is similar to that of *Watznaueria*, although the rim to central area proportions are not typical.

Range: Albian (Zone NC8)–Cenomanian (Zone UC4) at Sites 1207, 1208, 1212, and 1214.

Family Tubodiscaceae Bown and Rutledge in Bown and Young, 1997

Remarks: The lowermost Cretaceous assemblages of Site 1213 yield a large number of tubodiscid-like coccoliths that do not easily conform to currently described species morphologies (*Manivitella pemmatoidea*, *Tubodiscus burnettiae*, *Tubodiscus verenae*, and *Tubodiscus jurapelagicus*). The morphotypes are difficult to systematically differentiate due to the lack of characters, essentially two variably broad, contrastingly birefringent cycles. Two new species are described here, but a number of images on Pl. P9 are retained in informal nomenclature.

Tubodiscus bellii sp. nov.

Pl. P9, figs. 11–23

Derivation of name: Named for Ben Walsworth-Bell, Mesozoic nannopaleontologist.

Diagnosis: Bicyclic placolith with narrow shields and wide, open, central area. In LM XPL the two cycles have contrasting birefringence, the inner cycle being distinctly bright. The inner cycle is usually slightly narrower than the outer.

Differentiation: The shields and individual cycles are narrower than those of other tubodiscids.

Dimensions: length = 5.5–6.5 µm.

P9. Tubodiscaceae, p. 74.

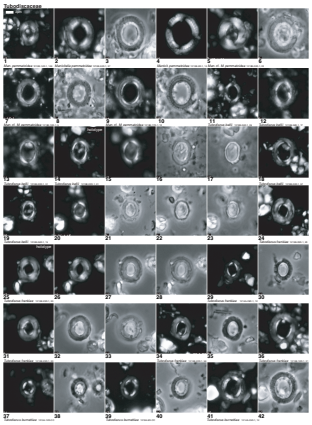

Holotype: Pl. P9, fig. 14 (figs. 14–17 are the same specimen).
Paratype: Pl. P9, fig. 19 (figs. 19–23 are the same specimen).
Type locality: ODP Leg 198 Site 1213, Shatsky Rise, northwest Pacific Ocean.
Type level: Berriasian, Sample 198-1213B-20R-1, 31 cm (Subzone NK2a).
Range: Berriasian (Zones NK1–Subzone NK2a) at Site 1213.

***Tubodiscus frankiae* sp. nov.**
Pl. P9, figs. 24–36

Derivation of name: Named for Tracy Frank, paleoceanographer and ODP 198 shipboard scientist.
Diagnosis: Bicyclic placolith with relatively broad shields and open central area. In LM XPL the two cycles have contrasting width and birefringence, the inner cycle being distinctly bright and narrow, the outer being broad and dark. The central area is usually slightly broader than the shield width.
Differentiation: The width contrast between the two rim cycles is greater than that seen in other tubodiscids. The shield morphology and LM appearance are similar to *Sollasites* coccoliths, but no central area structures have been observed.
Dimensions: length = 5.5–6.5 µm.
Holotype: Pl. P9, fig. 25 (figs. 25–28 are the same specimen).
Paratype: Pl. P9, fig. 34 (figs. 34 and 35 are the same specimen).
Type locality: ODP Leg 198 Site 1213, Shatsky Rise, northwest Pacific Ocean.
Type level: Berriasian, Sample 198-1213B-23R-1, 20 cm (Subzone NK2a).
Range: Berriasian (Subzone NK2a)–upper Hauterivian (Subzone NC4b) at Sites 1213 and 1214.

***Tubodiscus* cf. *T. verenae* Thierstein, 1973**
Pl. P10, fig. 6

Remarks: Single specimens in side view in Samples 198-1213B-19R-1, 10 cm, and 19R-1, 119–122 cm, showed *T. verenae*-like morphology (i.e., high, proximal collar). Their presence close to the first occurrence of *Percivalia fenestrata* (Subzone NK2a) conforms to the upper Berriasian first occurrence for this species reported by Bergen (1994).

Family Kamptneriaceae Bown and Hampton in Bown and Young, 1997

***Gartnerago ponticula* Bown and Hampton sp. nov.**
Pl. P10, figs. 22–24

Derivation of name: From *ponticulus*, meaning small bridge, and referring to the central structure that characterizes the coccoliths.
Diagnosis: Small- to medium-sized (usually <7.0 µm) *Gartnerago* species with an open central area spanned by a transverse, conjunct bar.
Differentiation: Similar in morphology to *Gartnerago theta* but smaller in size, has a relatively small, often diamond-shaped central area and a relatively broader inner rim cycle. The name *Gartnerago nanum* Thierstein, 1974, has previously been applied to these coccoliths (e.g., Crux, 1982; Burnett, 1998), but the holotype of the latter has a complete central area plate rather than a discrete bar.
Dimensions: length = 5.5–7.0 µm.
Holotype: Pl. P10, fig. 22 (fig. 23 is the same specimen).
Paratype: Pl. P10, fig. 24.
Type locality: ODP Leg 198 Site 1207, Shatsky Rise, northwest Pacific Ocean.
Type level: Cenomanian, Sample 198-1207B-20R-CC (Zone UC3/UC4).
Range: uppermost Albian (Zone UC0)–upper Cenomanian (Zone UC3/UC4) (Burnett in Gale et al., 1996; Burnett, 1998). Rare occurrences in the Cenomanian at Sites 1207 and 1213.

P10. Tubodiscaceae, Prediscosphaeraceae, Arkhangelskiellaceae, Kamptneriaceae, p. 76.

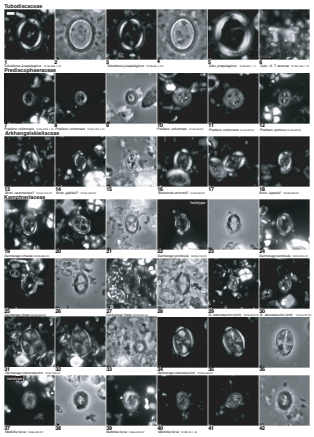

***Gartnerago stenostaurion* (Hill, 1976) Perch-Nielsen, 1984**
Pl. **P10,** figs. 29–39

Description: Small to large coccoliths characterized under LM XPL by a conspicuous, narrow, bright rim cycle and wide central area spanned by a plate. The plate is usually crossed by four radial extinction lines (two in the major axes of the coccolith ellipse and two diagonally orientated) and narrow, bright, barlike structures, which are longitudinal and near transverse (rotated by ~10°), and birefringent when the coccolith is at 45° to the polarizing directions.

Remarks: These coccoliths have an LM image that is much closer to that of *Gartnerago* than *Broinsonia*. The narrow, bright rim cycle is a unique feature of *Gartnerago*, and the dark central area plate is almost identical to those seen in *Gartnerago segmentatum* and *Gartnerago obliquum*. Small specimens of *G. stenostaurion* most closely resemble *Crucicribrum anglicum* Black, 1973 (? = *Arkhangelskiella erratica* Stover, 1966), a close ally of *Gartnerago* with a distinctly perforate central area plate. The relationships between these early *Gartnerago* taxa are not fully understood.

Range: uppermost Aptian–uppermost Albian (Burnett, 1998; Bown in Kennedy et al., 2000; Bown, 2001); mid-Albian (upper Zone NC8) to lower Cenomanian (Zone UC1/UC2) at Sites 1207, 1213, and 1214.

Heterococcoliths of uncertain affinity

***Haqius* Roth, 1978**
Pl. **P11,** figs. 1–18

Remarks: This genus comprises unicyclic placolith coccoliths with a narrow or closed central area and a characteristically dark gray (low birefringence) LM XPL image. These coccoliths are common and consistent components of the Shatsky Lower Cretaceous assemblages and show considerable variation in size. A new species is described below.

It should be noted that Worsley (1971) described the genus *Esgia* based on a specimen similar to *Haqius circumradiatus*. I have retained the use of *Haqius*, as it alone has consistently been used for coccoliths of this group. The nature of Worsley's *Esgia junior* holotype is unclear, but it may represent a transitional morphology between *H. ellipticus* and *Haqius circumradiatus*.

***Haqius ellipticus* Grün in Grün and Allemann, 1995, emend.**
Pl. **P11,** figs. 13–18

Emended diagnosis: Large (>7.0 µm) unicyclic placolith with a narrow or closed central area. Under LM XPL the shields appear gray and the numerous individual elements are usually visible. The proximal shield is significantly smaller than the distal and is often clearly distinguishable (Pl. **P11,** fig. 17).

The emendation is proposed in order to allow for the differentiation of the small species, *Haqius peltatus*, described below. The size chosen for differentiation is arbitrary, and a more appropriate figure may be forthcoming with further biometric analysis of *Haqius* populations. *H. ellipticus* coccoliths range in size from 7.0 to 14.0 µm in the Shatsky Rise material and are restricted to the Berriasian; the largest forms are particularly conspicuous.

Range: Upper Jurassic–Hauterivian/lower Barremian (Bralower et al., 1989; Bergen, 1994) but this range may include the smaller species, *H. peltatus*. Berriasian (Zone NK1–Subzone NK2b) at Site 1213.

***Haqius peltatus* sp. nov.**
Pl. **P11,** figs. 3–12

Derivation of name: From *pelta*, a small shield, referring to the size and morphology of this placolith coccolith.

P11. *Haqius,* Braarudosphaeraceae, Nannoconaceae, p. 78.

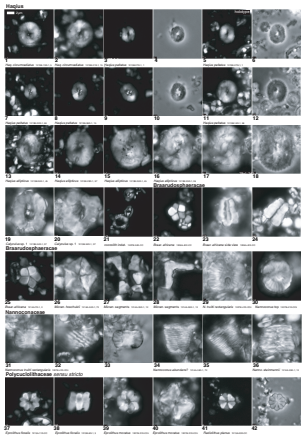

Diagnosis: Small (<6.5 µm) unicyclic placolith with a narrow or closed central area. Under LM XPL the shields appear gray and individual elements are usually visible. Some specimens possess small barlike structures that cross the narrow central area.

Differentiation: Differentiated from *Haqius ellipticus* by size and from *Haqius circumradiatus* by outline.

Dimensions: length = 3.0–6.5 µm; width = 2.4–4.5 µm.

Holotype: Pl. **P11,** fig. 5 (fig. 6 is the same specimen).

Paratypes: Pl. **P11,** fig. 8 (figs. 9 and 10 are the same specimen).

Type locality: ODP Leg 198 Site 1213, Shatsky Rise, northwest Pacific Ocean.

Type level: Berriasian, Sample 198-1213B-27R-1, 1 cm (Zone NK1).

Range: Berriasian (Zone NK1)–Albian (Subzone NC8a). Small elliptical *Haqius* coccoliths have not previously been reported from the Albian, and this may be a species that developed restricted paleobiogeographic distribution in the mid-Cretaceous.

Calyculus? sp. 1

Pl. **P11,** figs. 19, 20

Description/Remarks: Large coccoliths (>10 µm) with low birefringence, blocky, flaring rim, and open central area. Most closely resemble coccoliths of the Jurassic genus *Calyculus,* but they have not been recorded in sediments younger than Tithonian (de Kaenel and Bergen, 1996; Bown and Cooper, 1999).

Range: Recorded in a single Berriasian sample from Site 1213 (Sample 198-1213B-24R-1, 37 cm).

Mattiolia gen. nov.

Pl. **P10,** figs. 37–42

Type species: *Mattiolia furva* sp. nov.

Derivation of name: Named for Emanuela Mattioli, Mesozoic nannopaleontologist.

Diagnosis: Placoliths with a distinctly dark image under XPL. The type species has broadly elliptical shields and a narrow central area, filled with a broad plate/axial cross; the plate is also dark under XPL but is crossed by at least four extinction lines.

Differentiation: The new genus is proposed because the coccoliths are quite unlike any other Cretaceous taxa. Other Cretaceous placolith coccoliths appear dark under XPL (e.g., *Haqius* and *Repagulum*); however, the rim outline, rim to central area proportions, and central area structures are quite different in *Mattiolia furva*. Until SEM images are forthcoming we cannot comment further on the taxonomic affinities of the genus.

Mattiolia furva sp. nov.

Pl. **P10,** figs. 37–42

Derivation of name: From *furvus*, meaning dark, and referring to the appearance of this species under XPL.

Diagnosis: Medium-sized (~5.5 µm), broadly elliptical placoliths with a distinctly dark image under XPL and a central area equivalent in width to the shield. The central area is filled by a broad axial cross that may form a complete plate. The central area plate, like the shields, has a dark appearance under XPL but is crossed by at least four extinction lines, axially and diagonally orientated.

Differentiation: See remarks for the genus.

Dimensions: length = 5.1–5.9 µm; width = 4.1–4.9 µm

Holotype: Pl. **P10,** fig. 37 (fig. 38 is the same specimen).

Paratype: Pl. **P10,** fig. 42 (figs. 40–42 are the same specimen).

Type locality: ODP Leg 198 Site 1208, Shatsky Rise, northwest Pacific Ocean.

Type level: Albian, Sample 198-1208A-42X-CC (Subzones NC8c–NC9a).

Range: Albian (Subzones NC8a/NC8b–Zone NC9) at Sites 1208, 1213, and 1214.

Nannoliths

***Assipetra terebrodentarius* (Applegate et al. in Covington and Wise, 1987) Rutledge and Bergen in Bergen, 1994**
Pl. P12, figs. 1–18

Description: Blocky, globular nannoliths formed from six or more complexly intergrown calcite blocks that are joined along broadly radial sutures; roughly circular in plan and rectangular in side view.

Remarks: Tremolada and Erba (2002) recognized considerable size variation within the species and proposed a division into two subspecies with the limit at 7.5 µm. Unfortunately, they renamed the larger morphotype, which was already represented by the original holotype of Applegate et al. in Covington and Wise, 1987 (holotype = 7.7 µm). We have emended the diagnosis of the subspecies here, raising the size limit between them to 8.0 µm. This represents a clearer cutoff point between the two morphotypes and brings the original species holotype into the smaller subspecies, thus avoiding the need for renaming.

Assipetra terebrodentarius* (Applegate et al. in Covington and Wise, 1987) Rutledge and Bergen in Bergen, 1994, ssp. *terebrodentarius
Pl. P12, figs. 3–12

Description: Small- to medium-sized (<8.0 µm diameter) subspecies of *A. terebrodentarius*.

Dimensions: diameter = 4.0–7.6 µm.

Range: The first occurrence is usually considered to be upper Hauterivian (Bergen, 1994; Channell et al., 1995; Gardin et al., 2000) but is slightly earlier in this material, where its range overlaps with *Cruciellipsis cuvillieri*, in sediments assigned to upper Subzone NC4b. This range overlap has also been reported by Erba et al. (1999) and Lozar and Tremolada (2003). The upper range is uncertain but specimens have been observed as high as the Campanian (pers. observ.; Lees and Bown, this volume; Lozar and Tremolada, 2003).

***Assipetra terebrodentarius* (Applegate et al. in Covington and Wise, 1987) Rutledge and Bergen in Bergen, 1994, *youngii* Tremolada and Erba, 2002, emend.**
Pl. P12, figs. 13–18

Diagnosis: A large (>8.0 µm diameter) subspecies of *A. terebrodentarius*.

Remarks: A number of the specimens named *Assipetra infracretacea larsonii* by Tremolada and Erba (2002) are considered to be side views of *A. terebrodentarius*.

Range: Aptian, according to Tremolada and Erba (2002), and particularly abundant in sediments associated with OAE 1a. Recorded well into the Upper Cretaceous (Campanian: herein, pers. observ., and Lees and Bown, this volume), but the last common and consistent occurrence may be toward the top of the Aptian.

***Braarudosphaera africana* Stradner, 1961**
Pl. P11, figs. 22–25

Remarks: *Braarudosphaera* was practically absent in the Shatsky Rise sections; however, the single mid-Cretaceous sample at Site 1208 yielded relatively frequent *B. africana*, including specimens tall enough to be orientated on their sides. Such tall pentaliths are common in the Eocene but have rarely been documented in the Cretaceous; the best known were published by Lambert (1986), who documented spectacular specimens from the upper Albian of Cameroon.

P12. Polycylolithaceae s.l., p. 80.

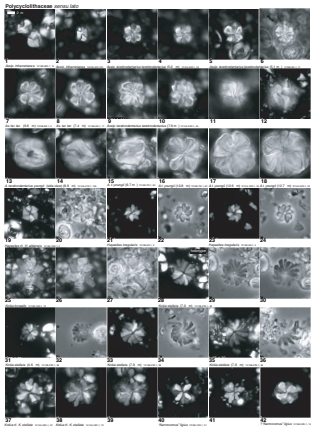

***Hayesites* Manivit, 1971, emend. Applegate et al. in Covington and Wise, 1987**

***Hayesites* cf. *H. albiensis* Manivit, 1971**
Pl. **P12,** figs. 19, 20

Remarks: Of the genus *Hayesites*, only *H. irregularis* was unequivocally identified from the Shatsky Rise mid-Cretaceous sections (Pl. **P12,** figs. 21–24). Forms with five or six radially arranged rays were logged as *Hayesites* cf. *H. albiensis* but did not have the long, symmetrically arranged free rays characteristic of the species. The problematic nature of *H. albiensis* prevents the identification of Subzone NC8b (see discussion in Kennedy et al., 2000).

Range: *Hayesites* cf. *H. albiensis* was logged in the Albian at Sites 1207, 1213, and 1214.

***Kokia borealis* Perch-Nielsen, 1998**
Pl. **P12,** figs. 25, 26

Description: Stellate, multiradiate, rosette-shaped nannolith constructed from 8–10 single crystal-unit radial rays that show low birefringence under XPL (van Niel, 1994).

Range: Mostly reported from the Berriasian to lowermost Valanginian of the Boreal North Sea Basin (Bown et al., 1998), but Lozar and Tremolada (2003) recorded it (unillustrated) from the Hauterivian of the northwest Pacific Ocean. It was found herein in one Berriasian (Subzone NK2a) sample from Site 1213.

***Kokia stellata* sp. nov.**
Pl. **P12,** figs. 28–36

Derivation of name: From *stellata*, meaning starry, referring to the stellate morphology of this nannolith.

Diagnosis: Stellate, multiradiate, rosette-shaped nannolith constructed from 10–15 single crystal-unit rays joined for most of their length along curved sutures; low birefringence under XPL.

Differentiation: *Kokia borealis* has fewer rays joined along straight sutures, and *Kokia curvata* has fewer rays that are overlapping.

Dimensions: diameter = 4.5–8.0 µm

Holotype: Pl. **P12,** fig. 28 (figs. 28–30 are the same specimen).

Paratypes: Pl. **P12,** figs. 32, 35.

Type locality: ODP Leg 198 Site 1213, Shatsky Rise, northwest Pacific Ocean.

Type level: Berriasian, Sample 198-1213B-27R-1, 38 cm (Zone NK1).

Range: Berriasian (Zone NK1) at Site 1213.

***Kokia* cf. *K. stellata* sp. nov.**
Pl. **P12,** figs. 31–33

Description: Stellate, multiradiate, rosette-shaped nannolith (7.0–8.5 µm) constructed from ~12 single crystal-unit rays joined for most of their length along straight sutures; low birefringence under XPL.

Differentiation: Less uniform in birefringence than other species of *Kokia*, with near-radial c-axis orientation in the rays but resembles *Kokia stellata* in general morphology. Less regularly constructed, more rays, and less free-ray than cretarhabdid spine tops (calyxes) such as *Retecapsa radiata* (Worsley, 1971) Applegate and Bergen, 1988.

Range: upper Hauterivian (Subzone NC4b) at Site 1213.

***Rucinolithus wisei* Thierstein, 1971**
Pl. **P13,** figs. 1–6

Remarks: Stellate, six-rayed nannoliths that in this study ranged in size from 2.5 to 5.5 µm. Specimens in the lowermost part of the range (Cores 198-1213B-22R to 21R) were smaller than 3.0 µm, and size increased upsection.

Range: upper Berriasian (Subzone NK2a)–upper Valanginian (Subzone NK3a) (Bralower et al., 1989; Bergen, 1994) at Site 1213.

P13. Polycyclolithaceae s.l., Lapideacassaceae, p. 82.

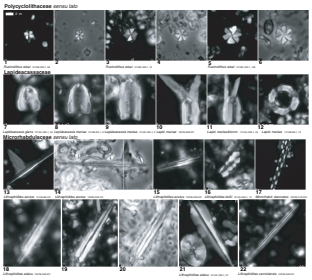

APPENDIX B

Taxonomic List

A full list of all taxa cited in the text, figures, and range charts is given below. Most bibliographic references can be found in Perch-Nielsen (1985) and Bown (1998).

Assipetra infracretacea (Thierstein, 1973) Roth, 1973
Assipetra terebrodentarius (Applegate et al. in Covington and Wise, 1987) Rutledge and Bergen in Bergen, 1994, ssp. *terebrodentarius* emend.
Assipetra terebrodentarius (Applegate et al. in Covington and Wise, 1987) Rutledge and Bergen in Bergen, 1994, *youngii* Tremolada and Erba, 2002, emend.
Axopodorhabdus albianus (Black, 1967) Wind and Wise in Wise and Wind, 1977
Axopodorhabdus cylindratus (Noël, 1965) Wind and Wise in Wise and Wind, 1977
Axopodorhabdus dietzmannii (Reinhardt, 1965) Wind and Wise, 1983
Biscutum constans (Górka, 1957), Black, 1959
Biscutum dorsetensis (Varol and Girgis, 1994) Bown in Bown and Cooper, 1998
Braarudosphaera africana Stradner, 1961
Braarudosphaera hockwoldensis Black, 1973
Braloweria boletiformis (Black, 1972) Crux, 1991
Broinsonia cenomanica (Black, 1973) Bown, 2001
Broinsonia enormis (Shumenko, 1968) Manivit, 1971
Broinsonia galloisii (Black, 1973) Bown in Kennedy et al., 2000
Broinsonia matalosa (Stover, 1966) Burnett in Gale et al., 1996
Broinsonia signata (Noël, 1969) Noël, 1970
Broinsonia viriosa (Jeremiah, 1996) Bown in Kennedy et al., 2000
Bukrylithus ambiguus Black, 1971
Calcicalathina alta Perch-Nielsen, 1979
Calcicalathina oblongata (Worsley, 1971) Thierstein, 1971
Calciosolenia fossilis (Deflandre in Deflandre and Fert, 1954) Bown in Kennedy et al., 2000
Calyculus Noël, 1973
Ceratolithina Perch-Nielsen, 1988
Chiastozygus litterarius (Górka, 1957) Manivit, 1971
Chiastozygus platyrhethus Hill, 1976
Chiastozygus spissus Bergen in Bralower and Bergen, 1998
Cleistorhabdus williamsii Black, 1972
Clepsilithus maculosus Rutledge and Bown, 1996
Conusphaera Trejo, 1969
Conusphaera mexicana Trejo, 1969
Conusphaera rothii (Thierstein, 1971) Jakubowski, 1986
Corollithion exiguum Stradner, 1961
Corollithion kennedyi Crux, 1981
Corollithion signum Stradner, 1963
"Crepidolithus" burwellensis Black, 1972
Crepidolithus crassus (Deflandre in Deflandre and Fert, 1954) Noël, 1965
Crepidolithus parvulus de Kaenel and Bergen, 1996
Cretarhabdus conicus Bramlette and Martini, 1964
Cretarhabdus striatus (Stradner, 1963) Black, 1973
Cribrosphaerella ehrenbergii (Arkhangelsky, 1912) Deflandre in Piviteau, 1952
Crucibiscutum bosunensis Jeremiah, 2001
Crucibiscutum hayi (Black, 1973) Jakubowski, 1986
Crucibiscutum salebrosum (Black, 1971) Jakubowski, 1986
Cruciellipsis cuvillieri (Manivit, 1966) Thierstein, 1971, emend. Wind and Cepek, 1979
Crucicribrum anglicum Black, 1973
Cyclagelosphaera brezae Applegate and Bergen, 1988
Cyclagelosphaera jiangii Covington and Wise, 1987

Cyclagelosphaera margerelii Noël, 1965
Cyclagelosphaera rotaclypeata Bukry, 1969
Cylindralithus nudus Bukry, 1969
Cylindralithus sculptus Bukry, 1969
Diadorhombus rectus Worsley, 1971
Diazomatolithus lehmanii Noël, 1965
Diloma primitiva (Worsley, 1971) Wind and Cepek, 1979
Discorhabdus biradiatus (Worsley, 1971) Thierstein, 1973
Discorhabdus ignotus (Gorka, 1957) Perch-Nielsen, 1968
Eiffellithus eximius (Stover, 1966) Perch-Nielsen, 1968
Eiffellithus hancockii Burnett, 1998
Eiffellithus monechiae Crux, 1991
Eiffellithus primus Applegate and Bergen, 1988
Eiffellithus striatus (Black, 1971) Applegate and Bergen, 1988
Eiffellithus turriseiffelii (Deflandre in Deflandre and Fert, 1954) Reinhardt, 1965
Eiffellithus windii Applegate and Bergen, 1988
Ethmorhabdus hauterivianus (Black, 1971) Applegate, Covington, and Wise, 1987
Eprolithus floralis (Stradner, 1962) Stover, 1966
Eprolithus moratus (Stover, 1966) Burnett, 1998
Eprolithus octopetalus Varol, 1992
Flabellites oblongus (Bukry, 1969) Crux in Crux et al., 1982
Florisphaera profunda Okada and Honjo, 1973
Gaarderella granulifera Black, 1973
Gartnerago chiasta Varol, 1991
Gartnerago nanum Thierstein, 1974
Gartnerago ponticula sp. nov.
Gartnerago praeobliquum Jakubowski, 1986
Gartnerago segmentatum (Stover, 1966) Thierstein, 1974
Gartnerago stenostaurion (Hill, 1976) Perch-Nielsen, 1984
Gartnerago theta (Black in Black and Barnes, 1959) Jakubowski, 1986
Grantarhabdus bukryi Black, 1972
Grantarhabdus coronadventis (Reinhardt, 1966a) Grün in Grün and Allemann, 1975
Grantarhabdus meddii Black, 1971
Haqius circumradiatus (Stover, 1966) Roth, 1978
Haqius ellipticus (Grün in Grün and Allemann, 1975) Bown, 1992
Haqius peltatus sp. nov.
Hayesites albiensis Manivit, 1971
Hayesites irregularis (Thierstein in Roth and Thierstein, 1972) Applegate et al. in Covington and Wise, 1987
Helenea chiastia Worsley, 1971
Helenea conus (Worsley, 1971) Rutledge and Bown, 1998
Helenea staurolithina Worsley, 1971
Helenea quadrata (Worsley, 1971) Rutledge and Bown, 1998
Helicolithus compactus (Bukry, 1969) Varol and Girgis, 1994
Helicolithus leckiei sp. nov.
Helicolithus trabeculatus (Górka, 1957) Verbeek, 1977
Hemipodorhabdus gorkae (Reinhardt, 1969) Grün in Grün and Allemann, 1975
Hexapodorhabdus cuvillieri Noël, 1965
Kokia borealis Perch-Nielsen, 1988
Kokia curvata Perch-Nielsen, 1988
Kokia stellata sp. nov.
Laguncula dorotheae Black, 1971
Lapideacassis glans Black, 1971
Lapideacassis mariae Black, 1971
Lithraphidites acutus Verbeek and Manivit in Manivit et al., 1977
Lithraphidites alatus Thierstein in Roth and Thierstein, 1972
Lithraphidites bollii (Thierstein, 1971) Thierstein, 1973
Lithraphidites carniolensis Deflandre, 1963
Loxolithus armilla (Black, 1959) Noël, 1965
Manivitella pemmatoidea (Deflandre, 1965) Thierstein, 1971, emend. Black, 1973

Mattiolia furva gen. et sp. nov.
Micrantholithus Deflandre in Deflandre and Fert, 1954
Micrantholithus hoschulzii (Reinhardt, 1966) Thierstein, 1971
Micrantholithus obtusus Stradner, 1963
Microrhabdulus decoratus Deflandre, 1959
Micula staurophora (Gardet, 1955) Stradner, 1963
Miravetesina favula Grün in Grün and Allemann, 1975
"Miravetesina" ficula (Stover, 1966) Bralower and Bergen, 1998
Nannoconus Kamptner, 1931
Nannoconus abundans Stradner and Grün, 1973
Nannoconus ligius Applegate and Bergen, 1988
Nannoconus truitti Brönnimann, 1955, *rectangularis* Deres and Achéritéguy, 1980
Nannoconus steinmannii Kamptner, 1931
Percivalia fenestrata (Worsley, 1971) Wise, 1983
Perissocyclus plethotretus (Wind and Cepek, 1979) Crux, 1989
Pickelhaube furtiva (Roth, 1983) Applegate et al. in Covington and Wise, 1987
Pleurochrysis Pringsheim, 1955
Podorhabdus grassei Noël, 1965
Prediscosphaera cretacea (Arkhangelsky, 1912) Gartner, 1968
Prediscosphaera columnata (Stover, 1966) Perch-Nielsen, 1984
Prediscosphaera spinosa (Bramlette and Martini, 1964) Gartner, 1968
Quadrum gartneri Prins and Perch-Nielsen in Manivit et al., 1977
Quadrum intermedium Varol, 1992
Radiolithus hollandicus Varol, 1992
Radiolithus planus Stover, 1966
Radiolithus undosus (Black, 1973) Varol, 1992
Repagulum parvidentatum (Deflandre and Fert, 1954) Forchheimer, 1972
Retecapsa angustiforata Black, 1971
Retecapsa crenulata (Bramlette and Martini, 1964) Grün, 1975
Retecapsa cf. *P. madingleyensis* Black, 1973
Retecapsa octofenestrata (Bralower, 1989) Bown, 1998
Retecapsa radiata (Worsley, 1971) Applegate and Bergen, 1988
Retecapsa surirella (Deflandre and Fert, 1954) Grün in Grün and Allemann, 1975
"Rhabdolithina" swinnertoni Black, 1971
Rhagodiscus achlyostaurion (Hill, 1976) Doeven, 1983
Rhagodiscus adinfinitus sp. nov.
Rhagodiscus amplus sp. nov.
Rhagodiscus angustus (Stradner, 1963) Reinhardt, 1971
Rhagodiscus asper (Stradner, 1966) Reinhardt, 1967
Rhagodiscus dekaenelii Bergen, 1994
Rhagodiscus gallagheri Rutledge and Bown, 1996
Rhagodiscus infinitus (Worsley, 1971) Applegate et al. in Covington and Wise, 1987
Rhagodiscus pseudoangustus Crux, 1987
Rhagodiscus reniformis Perch-Nielsen, 1973
Rhagodiscus robustus sp. nov.
Rhagodiscus sageri sp. nov.
Rhagodiscus splendens (Deflandre, 1953) Verbeek, 1977
Rotelapillus laffittei (Noël, 1956) Noël, 1973
Rotelapillus radians Noël, 1973
Rucinolithus wisei Thierstein, 1971
Seribiscutum primitivum (Thierstein, 1974) Filewicz et al. in Wise and Wind, 1977
Sollasites Black, 1967
Sollasites horticus (Stradner et al., 1966) Black, 1968
Speetonia colligata Black, 1971
Staurolithites Caratini, 1963
Staurolithites aenigma Burnett, 1998
Staurolithites crux (Deflandre and Fert, 1954) Caratini, 1963
Staurolithites gausorhethium (Hill, 1976) Varol and Girgis, 1994
Staurolithites glaber (Jeremiah, 1996) Burnett, 1998
Staurolithites mutterlosei Crux, 1989

Staurolithites rotatus Jeremiah, 1996
Staurolithites siesseri Bown in Kennedy et al., 2000
Stoverius achylosus (Stover, 1966) Perch-Nielsen, 1986
Stradnerlithus silvaradius (Filewicz et al., 1976) Rahman and Roth, 1991
Tegulalithus tesselatus (Stradner in Stradner et al., 1968) Crux, 1986
Tegumentum stradneri Thierstein in Roth and Thierstein, 1972
Tetrapodorhabdus coptensis Black, 1971
Tranolithus gabalus Stover, 1966, emend. Köthe, 1981
Tranolithus incus de Kaenel and Bergen, 1996
Tranolithus minimus (Bukry, 1969) Perch-Nielsen, 1984
Tranolithus orionatus (Reinhardt, 1966) Reinhardt, 1966
Tubodiscus Thierstein, 1973
Tubodiscus bellii sp. nov.
Tubodiscus burnettiae Bown in Kennedy et al., 2000
Tubodiscus frankiae sp. nov.
Tubodiscus jurapelagicus (Worsley, 1971) Roth, 1973
Tubodiscus verenae Thierstein, 1973, emend. Grün, 1975
Umbria granulosa Bralower and Thierstein in Bralower et al., 1989
Watznaueria Reinhardt, 1964
Watznaueria barnesiae (Black, 1959) Perch-Nielsen, 1968
Watznaueria bayackii Worsley, 1971
Watznaueria biporta Bukry, 1969
Watznaueria britannica (Stradner, 1963) Reinhardt, 1964
Watznaueria cynthae Worsley, 1971
Watznaueria fossacincta (Black, 1971) Bown, 1989
Zeugrhabdotus Reinhardt, 1965
Zeugrhabdotus bicrescenticus (Stover, 1966) Burnett in Gale et al., 1996
Zeugrhabdotus burwellensis (Black, 1972) Burnett, 1998
Zeugrhabdotus clarus sp. nov.
Zeugrhabdotus diplogrammus (Deflandre in Deflandre and Fert, 1954) Burnett in Gale et al., 1996
Zeugrhabdotus embergeri (Noël, 1958) Perch-Nielsen, 1984
Zeugrhabdotus erectus (Deflandre in Deflandre and Fert, 1954) Reinhardt, 1965
Zeugrhabdotus fissus Grün and Zweili, 1980
Zeugrhabdotus howei Bown in Kennedy et al., 2000
Zeugrhabdotus kerguelenensis Watkins, 1992
Zeugrhabdotus noeliae Rood et al., 1971
Zeugrhabdotus petrizzoae sp. nov.
Zeugrhabdotus scutula (Bergen, 1994) Rutledge and Bown, 1996
Zeugrhabdotus streetiae Bown in Kennedy et al., 2000
Zeugrhabdotus xenotus (Stover, 1966) Burnett in Gale et al., 1996
Zeugrhabdotus cf. *P. fibuliformis* (Reinhardt, 1964) Hoffmann, 1970

Figure F1. Bathymetric map of Shatsky Rise and the location of Shatsky Rise in the Pacific Ocean (inset). The main map indicates the location of ODP and DSDP sites on Shatsky Rise, whereas the inset shows the location of Shatsky Rise in the Pacific Ocean relative to other Cretaceous volcanic features. Modified from Bralower, Premoli Silva, Malone, et al. (2002), Klaus and Sager (2002), and Robinson et al. (2004).

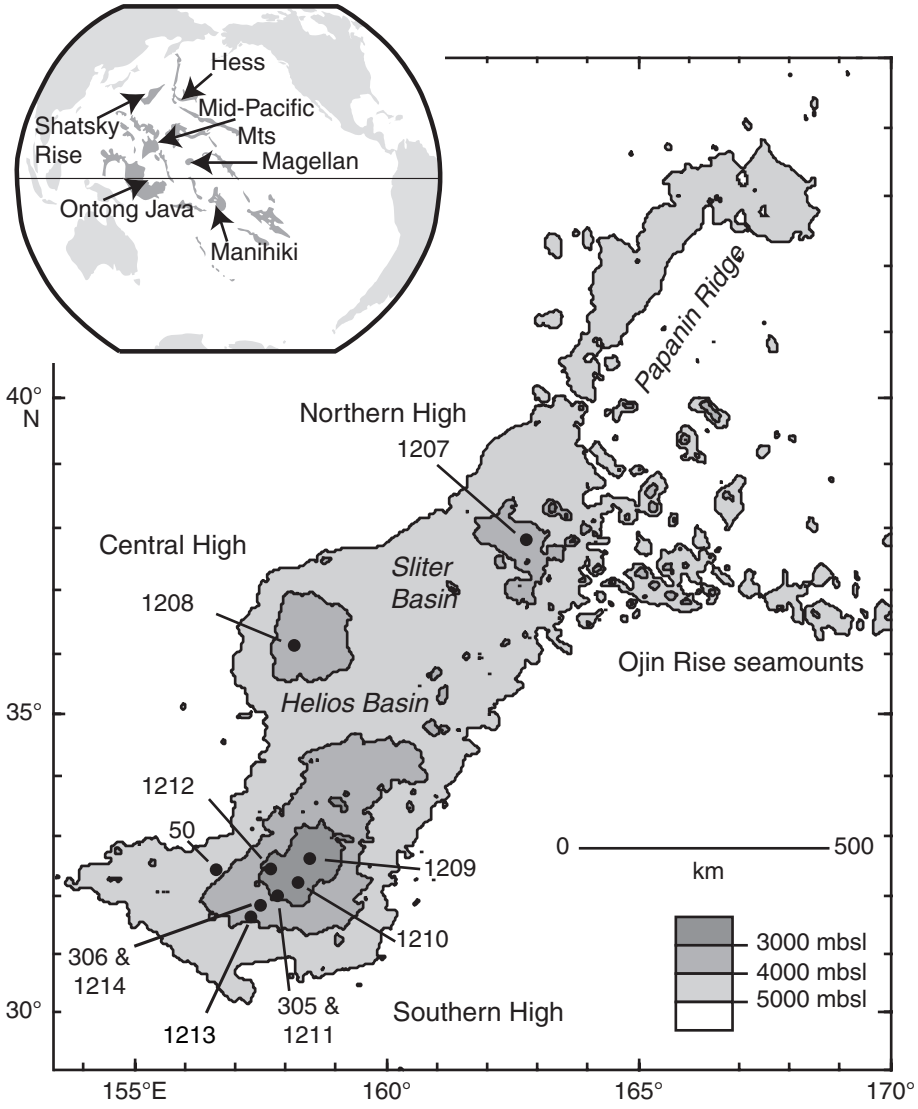

Figure F2. Age-depth plot of calcareous nannofossil datums from Site 1213. Red squares = nannofossil datums: actual depth in core (mbsf) vs. age from the Bralower, Premoli Silva, Malone, et al. (2002) time-scale. Red lines = plots of a single or few occurrences. Red square = total depth and age range for *U. granulosa*. OAE1a is also included in the plots. Horizontal black lines = hiatuses. FO = first occurrence, LO = last occurrence.

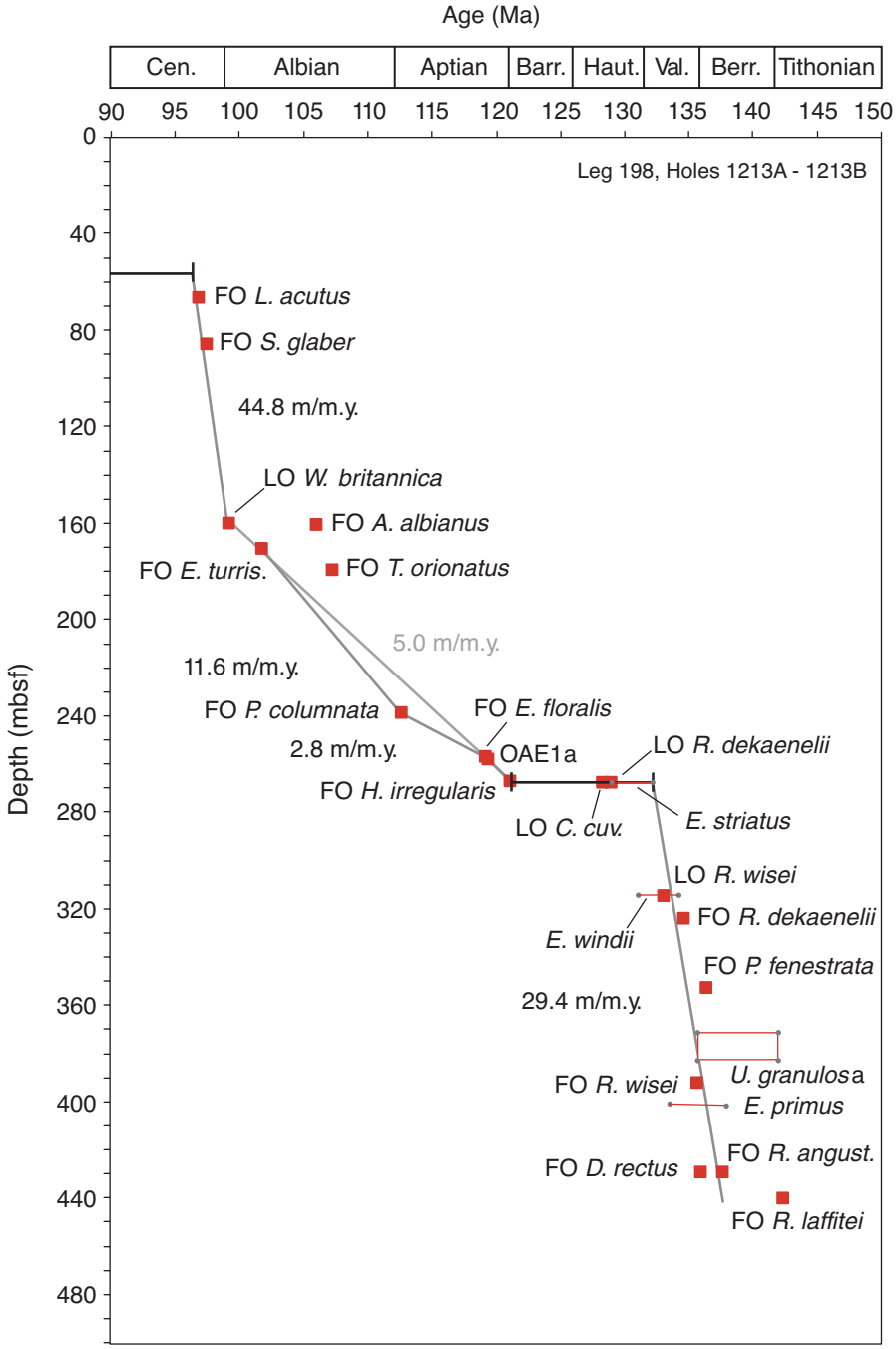

Figure F3. Biostratigraphy and chronostratigraphy for Sites 1207, 1213 and 1214 with core numbers, selected nannofossil datum events, and correlation lines. Blue stars = cores with enhanced siliceous content, as inferred from wireline logs (after Robinson et al., 2004). Organic-rich sediments are marked in red, and hiatuses are shown in green. Marker species are in larger bold text. Non-standard marker species are in bold text.

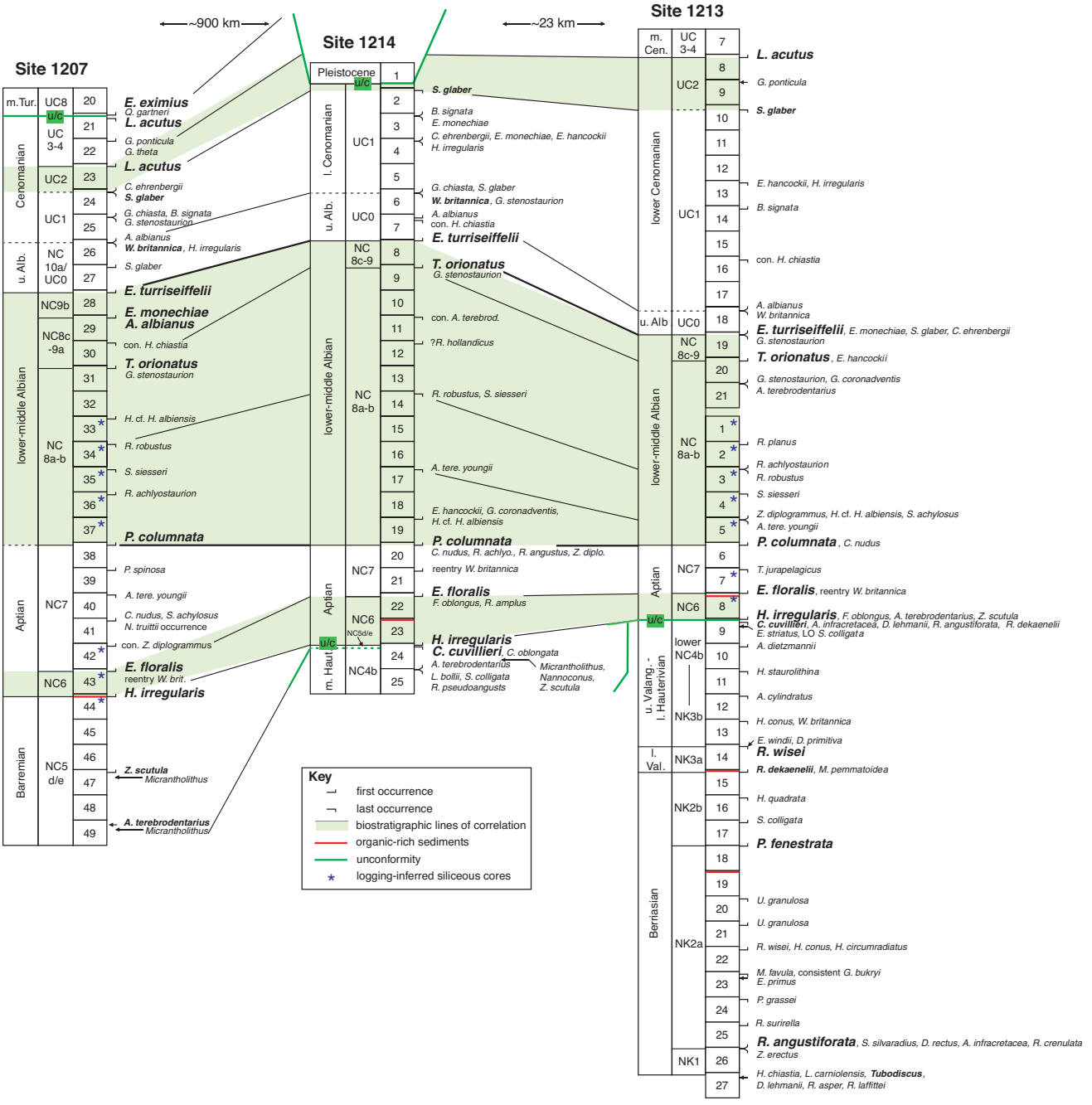

Figure F4. Age-depth plot of calcareous nannofossil datums from Site 1214. Red squares = nannofossil datums: actual depth in core (mbsf) vs. age from the Bralower, Premoli Silva, Malone, et al. (2002) timescale. OAE1a is also included in the plots. Horizontal black lines = hiatuses. FO = first occurrence, LO = last occurrence.

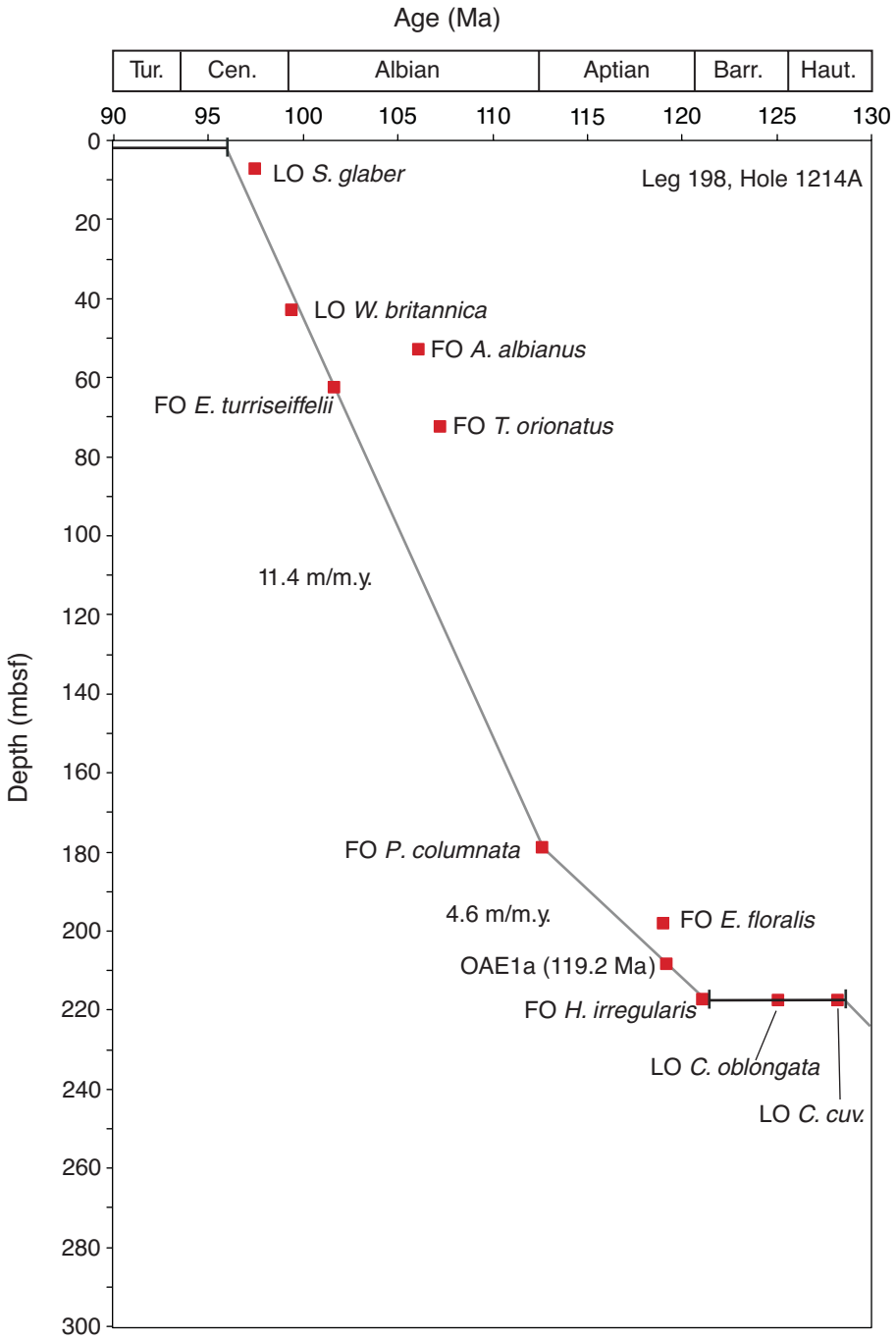

Figure F5. Age-depth plot of calcareous nannofossil datums from Site 1207. Red squares = nannofossil datums: actual depth in core (mbsf) vs. age from the Bralower, Premoli Silva, Malone, et al. (2002) timescale. OAE1a is also included in the plots. Horizontal black lines = hiatuses. FO = first occurrence, LO = last occurrence.

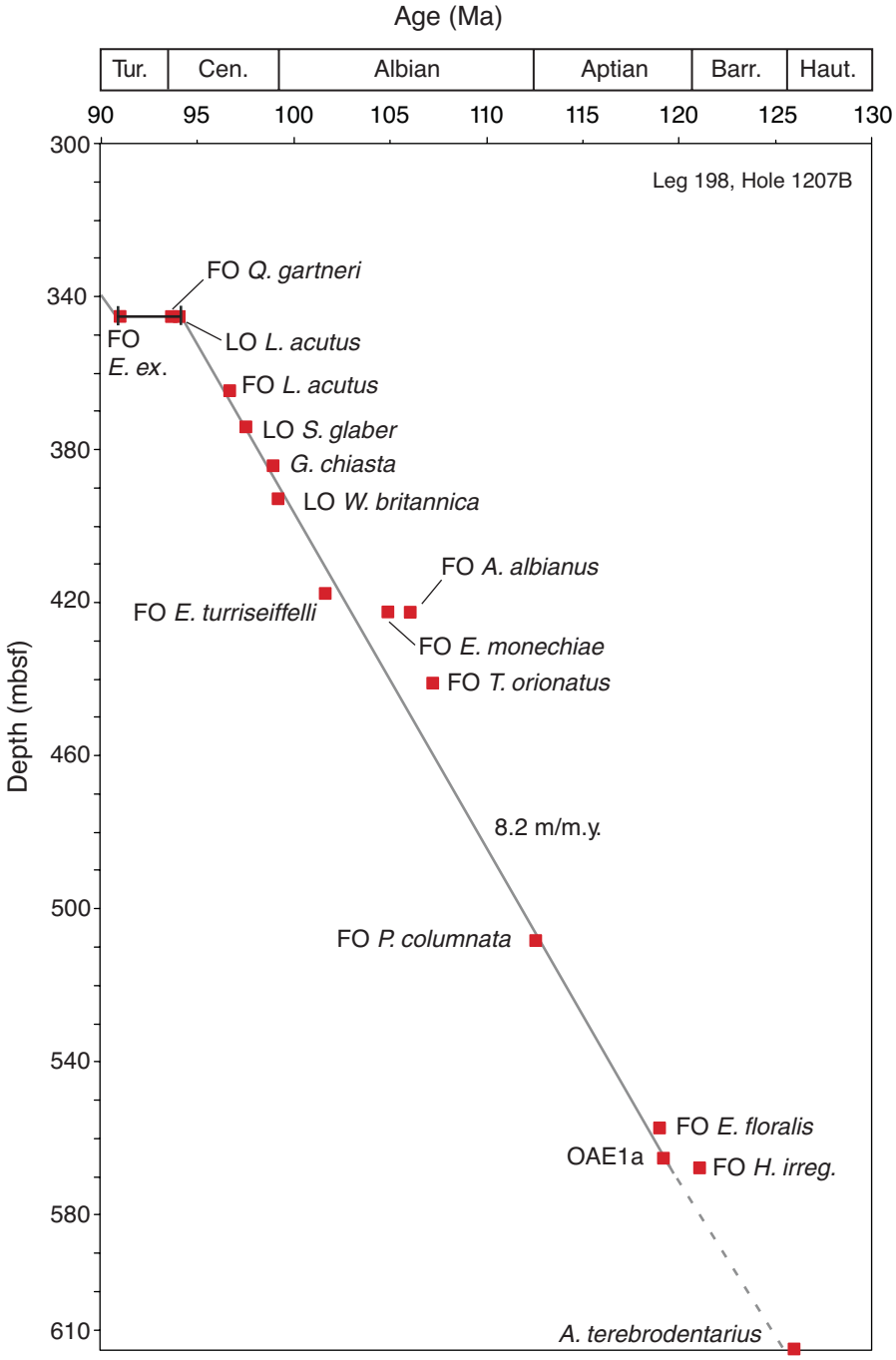

Table T1. Calcareous nannofossil stratigraphic range chart, Site 1213. (This table is available in an **oversized format.**)

Table T2. Calcareous nannofossil stratigraphic range chart, Site 1214. (This table is available in an **oversized format.**)

Table T3. Calcareous nannofossil stratigraphic range chart, Site 1207. (This table is available in an **oversized format.**)

Table T4. Calcareous nannofossil stratigraphic range chart, Site 1208.

Stage	Nannofossil zone	Core, section	Depth (mbsf)	Preservation	Abundance	*Axopodorhabdus dietzmannii*	*Biscutum constans*	*Braarudosphaera africana*	*Bukrylithus ambiguus*	*Chiastozygus litterarius*	*Chiastozygus platyrhethus*	*Chiastozygus* sp.	*Cretarhabdus striatus*	*Cribrosphaerella ehrenbergii*	*Cyclagelosphaera margerelii*	*Cylindralithus nudus*	*Discorhabdus ignotus*	*Eprolithus floralis*	*Flabellites oblongus*	*Gartnerago stenostaurion*	*Grantarhabdus bukryi*	*Haqius circumradiatus*	*Hayesites irregularis*	*Helenea chiastia*	*Helicolithus leckiei*	*Hemipodorhabdus gorkae*	*Lapideacassis mariae*	*Lithraphidites carniolensis*	*Loxolithus armilla*	*Manivitella pemmatoidea*	*Manivitella* cf. *M. pemmatoidea*	*Mattiolia furva*	*Nannoconus truitti rectangularis*	*Nannoconus* (top view)	*Prediscosphaera columnata* (circular)
m. Albian	NC8c–NC9a	198-1208A-42X-CC	382.90	G	A	F	C	F	R	R	•	R	R	R	R	F	C	•	F	F	•	R	F	F	F	C	•	C	F	F	F	F	R	R	C

Preservation: G = good, M = moderate, P = poor. Species abundance: A = abundant (>10%), C = common (1%–10%), F = few (0.1%–1%), R = rare (<0.1%), B = barren. Total abundance: A = abundant (>10 per field of view [FOV]), C = common (1–10 per FOV), F = few (1 per 2–10 FOV), R = rare (1 per 11–100 FOV), dot = 1 or 2 specimens. ? = questionable occurrence. Shading = age-diagnostic taxa.

Stage	Nannofossil zone	Core, section	Depth (mbsf)	Preservation	Abundance	*Prediscosphaera spinosa*	*Retecapsa crenulata*	*Retecapsa surirella*	*Rhagodiscus achylostaurion*	*Rhagodiscus angustus*	*Rhagodiscus asper*	*Rhagodiscus sageri*	*Rotelapillus laffittei*	*Rotelapillus laffittei* (petaloid)	*Staurolithites mutterlosei*	*Staurolithites* (small, bicyclic)	*Tegumentum stradneri*	*Tetrapodorhabdus coptensis*	*Tranolithus gabalus*	*Tranolithus orionatus*	*Watznaueria barnesae*	*Watznaueria britannica*	*Watznaueria* sp. 1	*Zeugrhabdotus diplogrammus*	*Zeugrhabdotus clarus*	*Zeugrhabdotus embergeri*	*Zeugrhabdotus* cf. *P. fibuliformis*	*Zeugrhabdotus howei*	*Zeugrhabdotus noeliae*	*Zeugrhabdotus xenotus*
m. Albian	NC8c–NC9a	198-1208A-42X-CC	382.90	G	A	•	F	F	C	C	F	•	C	•	•	R	F	F	R	•	A	R	•	•	•	R	R	C	A	R

Table T5. Stratigraphic range chart for calcareous nannofossils from Site 1212.

Stage	Nannofossil zone	Core, section, interval (cm)	Depth (mbsf)	Preservation	Abundance	*Axopodorhabdus albianus*	*Axopodorhabdus dietzmannii*	*Biscutum constans*	*Biscutum constans* (large)	*Broinsonia galloisii*	*Bukrylithus ambiguus*	*Calciosolenia fossilis*	*Chiastozygus litterarius*	*Chiastozygus platyrhethus*	*Cretarhabdus striatus*	*Cribrosphaerella ehrenbergii*	*Cyclagelosphaera margerelii*	*Cylindralithus nudus*	*Discorhabdus ignotus*	*Eiffellithus hancockii*	*Eiffellithus monechiae*	*Eiffellithus turriseiffelii*	*Eiffellithus turriseiffelii* (small)	*Eiffellithus turriseiffelii* (rotated X)	*Eprolithus floralis*	*Flabellites oblongus*	*Gartnerago stenostaurion*	*Gartnerago* cf. *G. theta*	*Grantarhabdus coronadventis*	*Haqius circumradiatus*	*Hayesites irregularis*	*Helenea chiastia*	*Helicolithus compactus*	*Helicolithus leckiei*	*Hemipodorhabdus gorkae*	*Lapideacassis mariae*	*Lithraphidites alatus*	*Lithraphidites carniolensis*	*Loxolithus armilla*	*Manivitella pemmatoidea*
u. Albian	NC10a	198-1212B-																																					
		24H-6, 40	197.40	M-G	A	F	•	A	C				•	•	•	•		F	F			C			•	R				•	•		•	F		R	C	F	F
		24H-6, 51	197.51	M-G	A	F	F	A	C			•	•	•				F	C		?•	C	F		•	•	•							C		•	C	F	F
		25H-CC	199.90	G	A	R	R	A			F	R	R	R	R	•	•	R	A	R		C	C		R	R	R	•					R	C	•	R	C		
		26H-CC	204. 29	M	C			F						•		R		R	F	•		F	F			•	•							R			F		R
		27H-CC	207.35	M-G	A			A	C	•	R		•	•	•		•	R	C			C	F	R		R	R				•		•	•	C		•	C		F

Note: Preservation: G = good, M = moderate, P = poor. Species abundance: A = abundant (>10%), C = common (1%–10%), F = few (0.1%–1%), R = rare (<0.1%), B = barren. Total abundance: A = abundant (>10 per field of view [FOV]), C = common (1–10 per FOV), F = few (1 per 2–10 FOV), R = rare (1 per 11–100 FOV), dot = 1 or 2 specimens. ? = questionable occurrence. Shading = age-diagnostic taxa.

Stage	Nannofossil zone	Core, section, interval (cm)	Depth (mbsf)	Preservation	Abundance	*Manivitella* cf. *M. pemmatoidea*	*Nannoconus* (top view)	*Prediscosphaera columnata* (circular)	*Prediscosphaera columnata* (large)	*Prediscosphaera cretacea*	*Prediscosphaera spinosa*	*Retecapsa angustiforata* (UC morph.)	*Retecapsa crenulata*	*Retecapsa surirella*	*Rhagodiscus achylostaurion*	*Rhagodiscus angustus*	*Rhagodiscus angustus* (robust)	*Rhagodiscus asper*	*Rhagodiscus sageri*	*Rotelapillus laffittei*	*Staurolithites gausorhethium*	*Staurolithites glaber*	*Staurolithites* spp.	*Tegumentum stradneri*	*Tetrapodorhabdus coptensis*	*Tranolithus gabalus*	*Tranolithus orionatus*	*Tubodiscus burnettiae*	*Watznaueria barnesae*	*Watznaueria* sp. 1	*Zeugrhabdotus diplogrammus*	*Zeugrhabdotus clarus*	*Zeugrhabdotus embergeri*	*Zeugrhabdotus howei*	*Zeugrhabdotus* cf. *Z. kerguelenensis*	*Zeugrhabdotus noeliae*	*Zeugrhabdotus* cf. *Chiastozygus spissus*
u. Albian	NC10a	198-1212B-																																			
		24H-6, 40	197.40	M-G	A	•	1	C	F	R				R	R	R		R		F	R	•			R	F			A	C	F	F	C		A		
		24H-6, 51	197.51	M-G	A	R		A		R			F	R	R			R		C	•	•		F	F	•	R	C	A	C	F	F	F	R	C			
		25H-CC	199.90	G	A	R		A					R	R	C	C		R	F	F		•	R	C	F	F	C		A	F	F	F	R	R	R			
		26H-CC	204. 29	M	C			F					R	R	F				R	R				R	F			•	C	R	F				F		•	
		27H-CC	207.35	M-G	A		1	C			A	R	F		C	F		F	F	C				F	C	•	F		A		F	F			A			

Table T6. Early Cretaceous marginal sea/neritic taxa.

Author	Marginal/neritic taxa
Thierstein (1976)	*Nannoconus* spp., *Calcicalathina oblongata,* *Lithraphidites bollii,* *Micrantholithus obtusus,* *Braarudosphaera bigelowii,* holococcoliths
Roth and Bowdler (1981), Roth and Krumbach (1986)	*Nannoconus,* *Micrantholithus,* *Braarudosphaera,* *Broinsonia,* *Biscutum constans,* *Zeugrhabdotus* spp. NB. Oceanic taxa: *Watznaueria,* *Rhagodiscus asper,* *Rhagodiscus splendens,* *Lithraphidites carniolensis*
Applegate et al. (1989)	*Nannoconus,* *Micrantholithus,* *Pickelhaube,* *Zebrashapka,* *Lithraphidites bollii,* *Lithraphidites alatus*

Table T7. Early Cretaceous nannoplankton with Boreal, Tethyan, or bipolar distributions but which are rare or absent at Shatsky Rise.

Tethyan taxa rare or absent	Boreal taxa rare or absent	Bipolar species rare or absent
Calcicalathina oblongata	***Kokia borealis***	*Repagulum parvidentatum*
Conusphaera mexicana	*Kokia curvata*	*Crucibiscutum salebrosum*
Conusphaera rothii	*Sollasites arcuatus*	*Laguncula dorotheae*
Nannoconus spp.	*Sollasites horticus*	*Seribiscutum primitivum*
Micrantholithus spp.	*Sollasites falklandensis* (austral)	***Broinsonia*** spp.
Lithraphidites bollii	*Micrantholithus speetonensis*	Ceratolithina spp.
Tubodiscus verenae	*Triquetrorhabdulus? shetlandensis*	
Calcicalathina? alta	*Eprolithus? antiquus*	
holococcoliths	*Tegulalithus septentrionalis*	
	Tegulalithus tesselatus	
	Braarudosphaera spp.	
	Braloweria boletiformis	
	Broinsonia viriosa	
	holococcoliths	
	Farhania varolii	
	Lithraphidites moray-firthensis	
	Crucibiscutum hayi	
	Garderella granulifera	

Note: Those that are present, although usually rarely, are in bold.

Table T8. Compilation of presence/absence data for *Nannoconus, Micrantholithus* (Berriasian–Aptian), and *Braarudosphaera* (Aptian–Upper Cretaceous) from Cretaceous DSDP and ODP sites from the Pacific and Indian oceans. (**See table notes.** Continued on next page.)

Location	Leg	Site	Setting	Stratigraphy	*Nannoconus*	*Micrantholithus*/ *Braarudosphaera*	Reference
Pacific Ocean							
Shatsky Rise	6	49	Oceanic igneous province	Lower Cretaceous (Albian)			Bukry (1971), Hay (1971)
Shatsky Rise		50	Oceanic igneous province	Lower Cretaceous (Albian)			
Shatsky Rise	32	305	Oceanic igneous province	Valanginian–Upper Cretaceous			Bukry (1975a)
Shatsky Rise		306	Oceanic igneous province	Berriasian–Cenomanian			
Shatsky Rise	198	1207	Oceanic igneous province	Lower Cretaceous	X(2)	X(2)	This study
Shatsky Rise		1208	Oceanic igneous province	Lower Cretaceous	X(1)	X(1)	
Shatsky Rise		1212	Oceanic igneous province	Lower Cretaceous	X(2)		
Shatsky Rise		1213	Oceanic igneous province	Lower Cretaceous	X(2)		
Shatsky Rise		1214	Oceanic igneous province	Lower Cretaceous	X(3)	X(4)	
Hess Rise	32	310	Oceanic igneous province	upper Albian–Cenomanian			Bukry (1975a)
N. Hess Rise	62	464	Oceanic igneous province	upper Aptian–Cenomanian	X(1)		Thiede, Vallier, et al. (1981), Cepek (1981), Roth (1981)
S. Hess Rise		465	Oceanic igneous province + s.w. debris	upper Albian–Upper Cretaceous	4	X(3)	
S. Hess Rise		466	Oceanic igneous province	upper Albian–Upper Cretaceous			
Ontong Java Plateau	30	288	Oceanic igneous province	Aptian–Upper Cretaceous			Bukry (1975b), Shafik (1975)
Ontong Java Plateau		289	Oceanic igneous province	Aptian			
Ontong Java Plateau	130	807	Oceanic igneous province	lower Aptian	X(1)	X(2)	Erba (1994), Mao and Wise (1993)
Ontong Java Plateau		803	Oceanic igneous province	Albian–Cenomanian			
Hawaiian magnetic lineations		164	Ridge-abyssal	Barremian–Aptian			Roth (1973), Bukry (1973a)
Nr. Magellan Rise		166	Ridge-abyssal	Hauterivian–Cenomanian	X(1)		
Magellan Rise	17	167	Oceanic rise	Tithonian/Berriasian–Upper Cretaceous	X(2)	X(2)	
Near Marshall Islands		169	Abyssal	upper Albian–Upper Cretaceous			
Central Pacific Basin		170	Abyssal	upper Albian–Upper Cretaceous			
Japanese magnetic lineations	20	195	Ridge-abyssal	Valanginian–Hauterivian			Bukry (1973b), Hekel (1973)
Japanese magnetic lineations		196	Ridge-abyssal	Valanginian–Hauterivian			
Japanese magnetic lineations	32	303	Ridge-abyssal	Valanginian–Cenomanian			Bukry (1975a)
Japanese magnetic lineations		304	Ridge-abyssal	Valanginian–Albian			
Japanese magnetic lineations		307	Ridge-abyssal	Berriasian–Upper Cretaceous			
Manihiki Plateau	33	317	Oceanic igneous province	Barremian–Aptian			Martini (1976), Bukry (1976)
Mid-Pacific Mountains	62	463	Guyot: shallow + turbidites + s.w. debris	Barremian–UpperCretaceous	4	X(2)	Thiede, Vallier, et al. (1981), Cepek (1981), Roth (1981), Erba (1994)
N. Pigafetta Basin	129	800	Redeposited volcaniclastics, cherts, and lmsts	Aptian–Cenomanian	X(3)	X(3)	Erba and Covington (1992), Larson, Lancelot, et al. (1992)
Pigafetta Basin		801	Abyssal + turbidites + s.w. debris	Tithonian, upper Aptian–Cenomanian	X(3)		
Mariana Basin		802	Abyssal + turbidites + s.w. debris	upper Aptian–Upper Cretaceous	X(5)	4	
Lo-En Guyot	144	872	Guyot: inner to middle neritic (200 m)	upper Coniacian–Santonian	X(3)		Erba et al. (1995)
MIT Guyot		878	Guyot: carbonate platform, photic zone	lower Aptian–upper Albian	X(4)	X(1)	
Takuyo-Daisan Guyot		879	Guyot: carbonate platform, photic zone	upper Aptian–Albian	X(5)	4	
Nadezhda Basin	185	1149	Abyssal	upper Valanginian–upper Hauterivian		X(1)	Lozar and Tremolada (2003)
Indian Ocean							
Wharton Basin	26	256	Ridge-abyssal	Albian			Pers. observ., Thierstein (1974)
Wharton Basin		257	Ridge-abyssal	Albian			
Naturaliste Plateau		258	Oceanic rise: with clastics	Albian–Upper Cretaceous		4	

Table T8 (continued).

Location	Leg	Site	Setting	Stratigraphy	*Nannoconus*	*Micrantholithus*/ *Braarudosphaera*	Reference
Perth Abyssal Plain	27	259	Ridge-abyssal	Albian			Pers. observ., Proto Decima (1974)
Gascoyne Abyssal Plain		260	Ridge-abyssal	Valanginian–Upper Cretaceous			Pers. observ., Proto Decima (1974)
Argo Abyssal Plain		261	Ridge-abyssal	Tithonian–Hauterivian			Pers. observ., Bown (1992), Proto Decima (1974)
Cuvier Abyssal Plain		263	Ridge-abyssal + turbidites + s.w. debris	Valanginian–Aptian			Pers. observ., Proto Decima (1974)
Wombat Plateau	122	761	Deep shelf	Lower Cretaceous			Bralower and Siesser (1992), Bralower (1992)
Exmouth Plateau		762	Deep shelf	Lower Cretaceous–Upper Cretaceous	X(1)		Bralower and Siesser (1992)
Exmouth Plateau		763	Deep shelf	Lower Cretaceous–Upper Cretaceous			Bralower and Siesser (1992)
Argo Abyssal Plain	123	765	Ridge-abyssal + turbidites	Tithonian–Upper Cretaceous	X(1)	4	Pers. observ., Bown (1992), Mutterlose (1992b)
Gascoyne Abyssal Plain		766	Ridge-abyssal + turbidites + s.w. debris	Valanginian–Upper Cretaceous	X(3)	4	

Notes: The presence of turbidites and shallow-water (s.w.) debris, when recorded in DSDP/ODP publications, is noted in the Setting column. Absence is denoted by a shaded box. Presence in more than five samples is denoted by a tick. Sporadic or limited occurrences in less than five samples are shown with an X, followed by the number of samples in which the taxon was recorded.

Table T9. Biostratigraphic datums.

Bioevent	Depth (mbsf)		
	Hole 1207B	Site 1213	Site 1214
FO *Lithraphidites acutus*	364.27	66.34	0
FO *Gartnerago ponticula*	354.50	76.04	0
FO *Gartnerago chiasta*	383.63	0	43.2
FO *Cribrosphaerella ehrenbergii*	373.92	170.13	25.9
LO *Staurolithites glaber*	373.92	85.43	6.90
FO *Broinsonia signata*	383.63	124.93	16.4
LO *Gartnerago stenostaurion*	383.63	170.13	43.2
LO *Watznaueria britannica*	393.05	160.45	43.2
FO *Axopodorhabdus albianus*	393.05	160.45	52.64
FO *Staurolithites glaber*	402.62	170.13	43.2
LO *Hayesites irregularis*	393.05	114.83	25.9
FO *Eiffellithus turriseiffelii*	417.34	170.13	63.37
FO *Eiffellithus monechiae*	422.12	170.13	25.9
LO con *Helenea chiastia*	431.49	143.24	52.64
FO *Tranolithus orionatus*	440.78	179.61	72.09
FO *Gartnerago stenostaurion*	440.78	189.3	72.09
FO *Hayesites* cf. *H. albiensis*	460.33	228.3	168.77
LO con. *Assipetra terebrodentarius*	526.55	179.61	91.98
LO con *Rhagodiscus robustus*	469.50	209.04	120.64
LO *Staurolithites siesseri*	478.87	189.30	120.64
FO *Prediscosphaera columnata*	507.77	238.63	178.33
FO *Prediscosphaera spinosa*	517.27	209.04	178.33
FO con *Zeugrhabdotus diplogrammus*	545.93	228.3	178.33
LO con *Assipetra terebrodentarius youngii*	526.55	228.3	149.58
FO *Cylindralithus nudus*	536.25	238.63	178.33
FO *Stoverius achylosus*	536.25	228.3	168.77
FO *Eprolithus floralis*	557.02	256.83	198.02
Reentry *Watznaueria britannica*	557.02	256.83	188.38
FO *Hayesites irregularis*	566.90	266.57	217.03

Note. FO = first occurrence, LO = last occurrence.

Plate P1. Chiastozygaceae. Images with black background are cross-polarized light images; those with light backgrounds are phase contrast images. **1–3.** *Chiastozygus litterarius* (Sample 198-1213B-1R-1, 42 cm). **4–10.** *Chiastozygus platyrhethus;* (4) Sample 198-1213A-19R-CC, (5) Sample 198-1207B-35R-CC, (6) Sample 198-1207B-23R-CC, (7–10) Sample 198-1214A-2R-CC. **11, 12.** *Chiastozygus* sp. (Sample 198-1207B-36R-CC). **13, 14.** *Diadorhombus rectus* (Sample 198-1213B-22R-1, 38 cm). **15.** *Loxolithus armilla* (Sample 198-1214A-25R-1, 12 cm). **16.** *Staurolithites gausorhethium* (Sample 198-1207B-43R-CC). **17, 18.** *Staurolithites glaber* (Sample 198-1207B-25R-CC). **19.** *Staurolithites mutterlosei* (Sample 198-1207B-37R-CC). **20–24.** *Staurolithites siesseri;* (20) Sample 198-1207B-45R-CC), (21–24) Sample 198-1214A-22R-1, 32 cm. **25–30.** *Staurolithites* sp.; (25) Sample 198-1213B-25R-1, 26 cm, (26) Sample 198-1213B-14R-1, 12 cm, (27, 28) Sample 198-1213B-1R-1, 42 cm, (29, 30) Sample 198-1213B-26R-1, 15 cm. **31.** *Tranolithus gabalus* (Sample 198-1213B-5R-1, 2 cm). **32.** ?*Tranolithus incus* (Sample 198-1213B-22R-1, 58 cm). **33.** *Tranolithus orionatus* (Sample 198-1214A-6R-1, 4 cm). **34–42.** *Zeugrhabdotus clarus;* (34) holotype (Sample 198-1207B-29R-CC) (35, 36) Sample 198-1207B-29R-CC, (37–39) Sample 198-1207B-35R-CC, (40) Sample 198-1214A-18R-1, 30 cm, (41, 42) Sample 198-1207B-30R-CC. (**Plate shown on next page.**)

Plate P1 (continued). (Caption shown on previous page.)

Chiastozygaceae

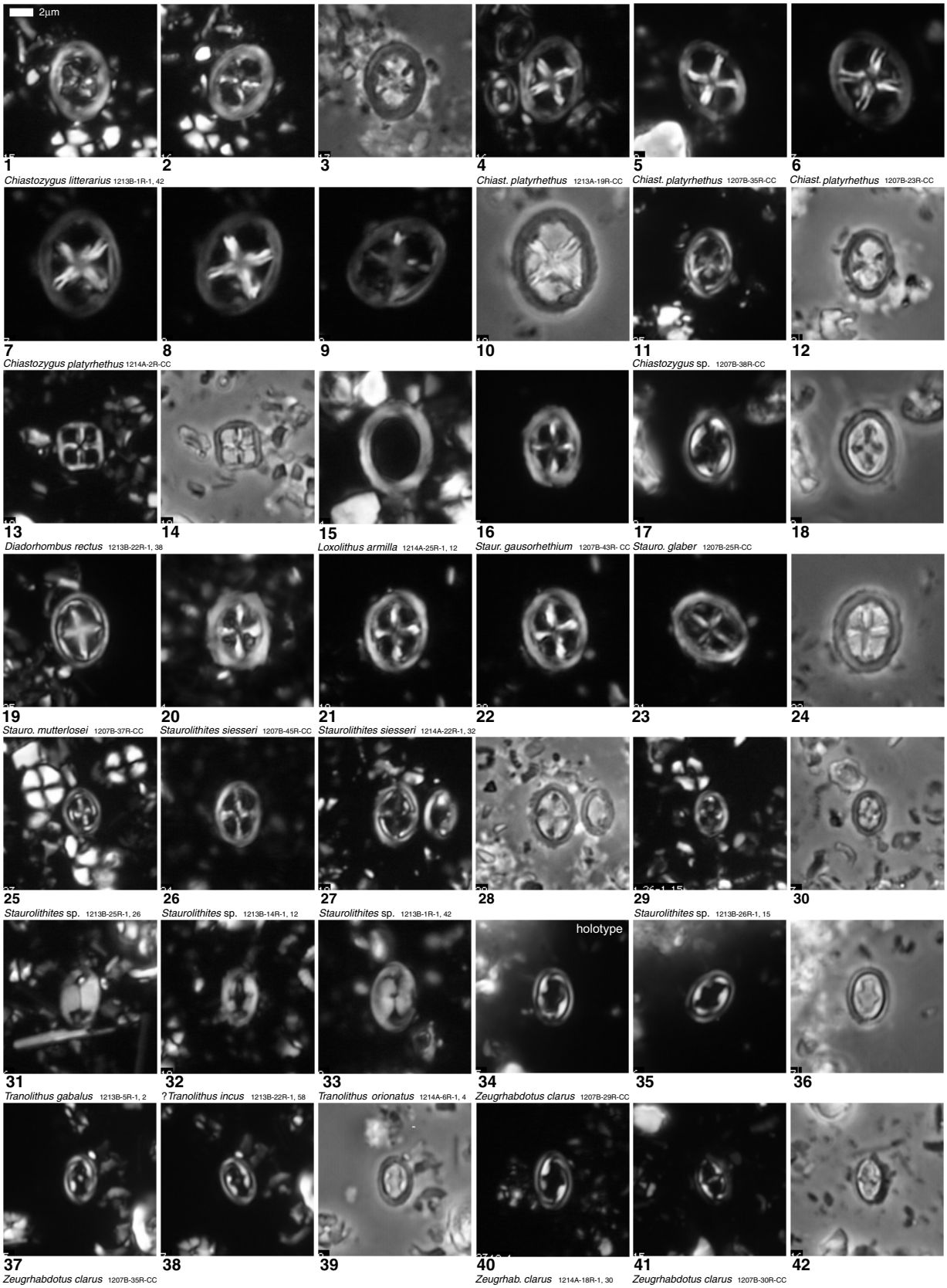

Plate P2. Chiastozygaceae: *Zeugrhabdotus*. Images with black background are cross-polarized light images; those with light backgrounds are phase contrast images. **1.** *Zeugrhabdotus diplogrammus* (Sample 198-1207B-41R-CCi). **2–6.** *Zeugrhabdotus* cf. *Z. embergeri;* (2, 3) Sample 198-1214A-10R-1, 13 cm, (4) Sample 198-1213B-1R-1, 42 cm, (5, 6) Sample 198-1214A-25R-1, 22 cm. **7–9.** *Zeugrhabdotus embergeri;* (7) Sample 198-1213B-27R-1, 22 cm, (8) Sample 198-1213A-19R-CC, (9) Sample 198-1214A-25R-1, 22 cm. **10–12.** *Zeugrhabdotus embergeri* (*kerguelenensis*); (10, 11) Sample 198-1213B-1R-1, 42 cm, (12) Sample 198-1207B-24R-CC. **13–18.** *Zeugrhabdotus erectus;* (13) Sample 198-1213B-24R-1, 37 cm, (14–16) Sample 198-1213B-19R-1, 115 cm, (17, 18) Sample 198-1213B-27R-1, 22 cm. **19–21.** *Zeugrhabdotus* cf. *Placozygus fibuliformis* (Sample 198-1207B-22R-CC). **22–24.** *Zeugrhabdotus fissus* (Sample 198-1213B-26R-1, 15 cm). **25–29.** *Zeugrhabdotus howei;* (25, 26) Sample 198-1213A-13R-CC, (27, 28) Sample 198-1213B-6R-1, 81 cm, (29) Sample 198-1213B-4R-1, 48 cm. **30, 34–38.** *Zeugrhabdotus petrizzoae*; (30) Sample 198-1207B-36R-CC, (34) holotype (Sample 198-1213B-4R-1, 48 cm), (35, 36) Sample 198-1213B-4R-1, 48 cm, (37, 38) Sample 198-1213B-6R-1, 81 cm. **31–33.** *Zeugrhabdotus noeliae* (Sample 198-1213B-27R-1, 38 cm). **39–42.** *Zeugrhabdotus scutula;* (30) Sample 198-1214A-24R-1, 46 cm, (40–42) Sample 198-1213B-9R-1, 17 cm. (**Plate shown on next page.**)

Plate P2 (continued). (Caption shown on previous page.)

Chiastozygaceae

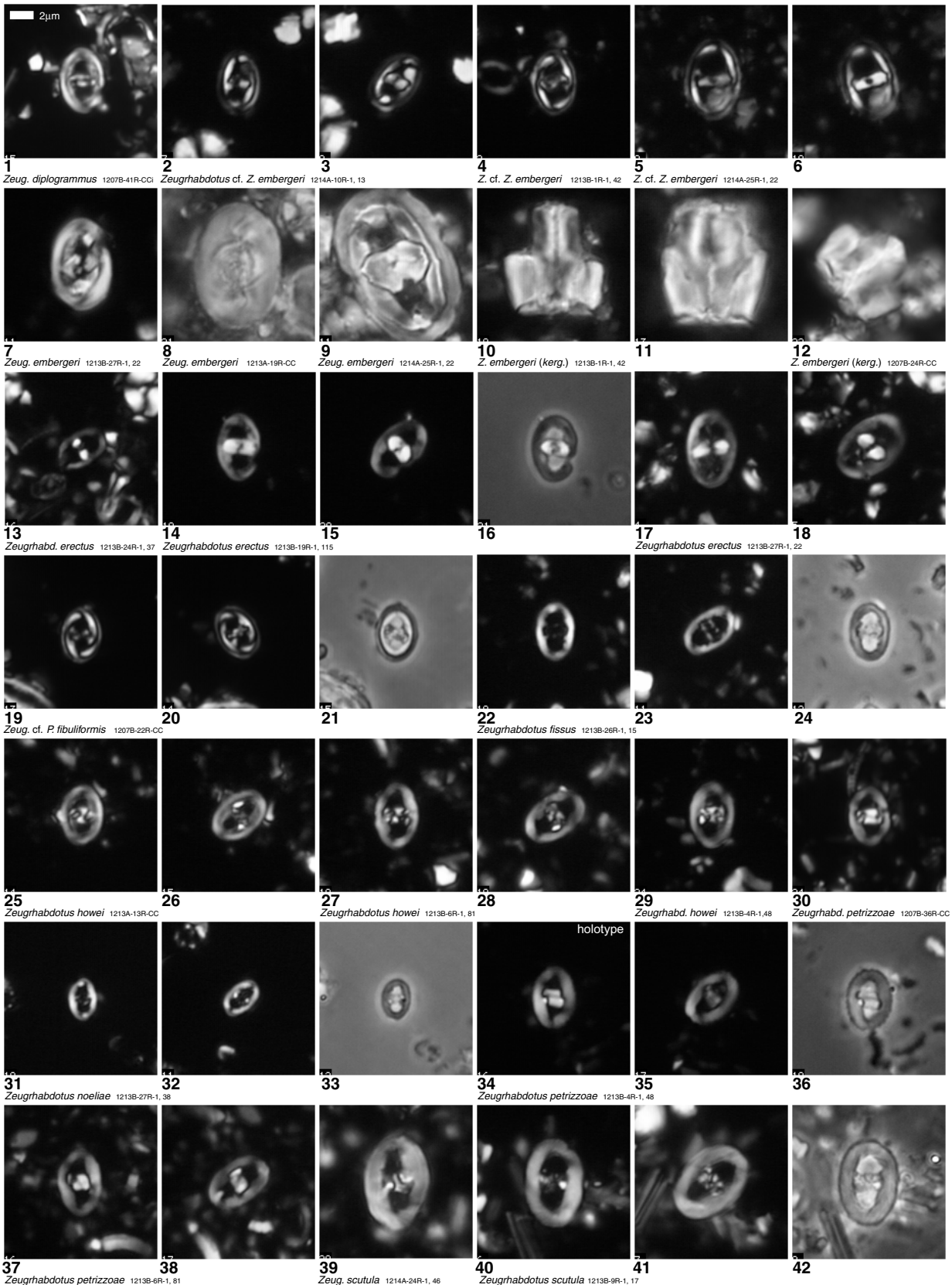

Plate P3. Chiastozygaceae, Eiffellithaceae. Images with black background are cross-polarized light images; those with light backgrounds are phase contrast images. **1.** *Zeugrhabdotus* cf. *Chiastozygus spissus* (Sample 198-1214A-8R-1, 1 cm). 2–*5. Zeugrhabdotus xenotus* (2, 3) Sample 198-1207B-28R-CC, (4, 5) Sample 198-1207B-27R-CC. **6.** *Zeugrhabdotus streetiae* (Sample 198-1207B-27R-CC). **7.** *Diloma primitiva* (Sample 198-1213B-14R-1, 58 cm). **8.** *Eiffellithus hancockii* (Sample 198-1207B-37R-CC). **9–18.** *Eiffellithus monechiae* (Sample 198-1270B-29R-CC). **19–23.** *Eiffellithus primus* (Sample 198-1213B-23R-1, 97 cm). **24–27.** *Eiffellithus windii;* (24) Sample 198-1213B-14R-1, 148 cm, (25–27) Sample 198-1213B-14R-1, 58 cm. **28.** *Eiffellithus striatus* (Sample 198-1213B-9R-1, 124 cm). **29–32.** *Eiffellithus turriseiffelii;* (29, 30) Sample 198-1207B-28R-CC, (31, 32) Sample 198-1207B-27R-CC. **33–36.** *Eiffellithus turriseiffelii-monechiae* (trans.) (Sample 198-1207B-28R-CC). **37–39.** *Helicolithus compactus* (Sample 198-1213A-11R-CC). **40–42.** *Helicolithus leckiei;* (40) Sample 198-1207B-28R-CC, (41) holotype (Sample 198-1207B-28R-CC), (42) Sample 198-1207B-27R-CC. (**Plate shown on next page.**)

Plate P3 (continued). (Caption shown on previous page.)

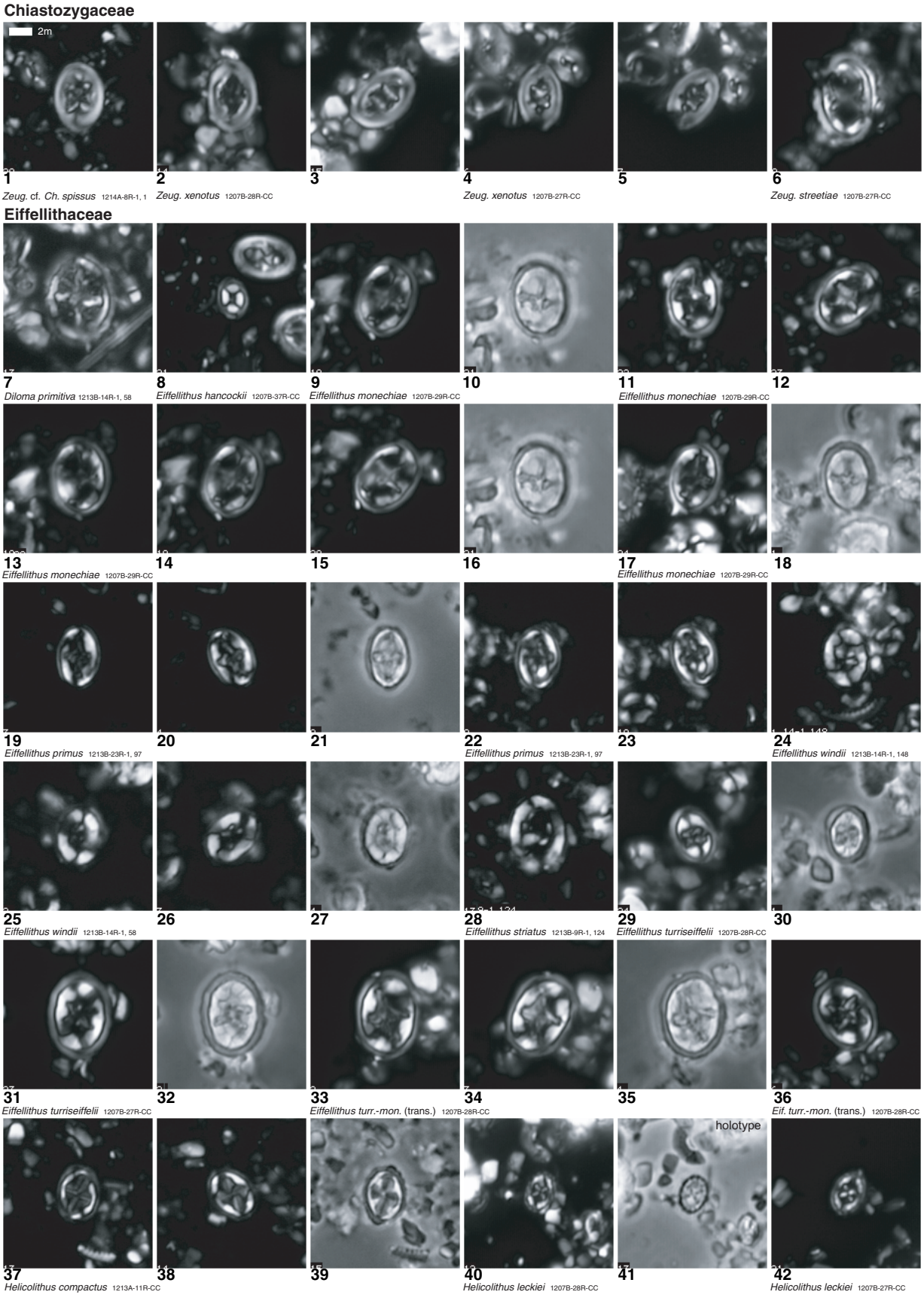

Plate P4. Eiffellithaceae, *Rhagodiscus asper* group. Images with black background are cross-polarized light images; those with light backgrounds are phase contrast images. **1, 2.** *Helicolithus leckiei* (Sample 198-1213B-1R-1, 42 cm). **3, 4.** *Helicolithus trabeculatus* (Sample 198-1214A-2R-CC). **5, 6.** *Tegumentum stradneri* (Sample 198-1207B-35R-CC). **7–11.** *Rhagodiscus asper;* (7) Sample 198-1213B-26R-1, 15 cm, (8, 11) Sample 198-1214A-20R-1, 23 cm, (9) Sample 198-1214A-19R-1, 2 cm, (10) Sample 198-1207B-46R-CC. **12–18.** *Rhagodiscus amplus;* (12) Sample 198-1207B-40R-CCi, (13) holotype (Sample 198-1270B-42R-CCi), (14, 15) Sample 198-1207B-42R-CCi), (16, 17) Sample 198-1207B-41R-CCii, (18) Sample 198-1207B-39R-CCi. **19–36.** *Rhagodiscus robustus;* (19–21) Sample 198-1213B-4R-1, 48 cm, (22) holotype (Sample 198-1214A-19R-1 37 cm), (23, 24, 27) Sample 198-1214A-19R-1, 37 cm, (25) Sample 198-1214A-19R-1, 2 cm, (26) Sample 198-1213B-6R-1, 81 cm, (28, 29) Sample 198-1207B-40R-CCi, (30, 36) Sample 198-1207B-35R-CC, (31, 32) Sample 198-1214A-15R-1, 54 cm, (33–35) Sample 198-1207B-45R-CC. **37–42.** *Rhagodiscus sageri;* (37) holotype (Sample 198-1207B-39R-CC), (38–40) Sample 198-1207B-39R-CC, (41) Sample 198-1214A-25R-1, 22 cm, (42) Sample 198-1207B-30R-CC. (**Plate shown on next page.**)

Plate P4 (continued). (Caption shown on previous page.)

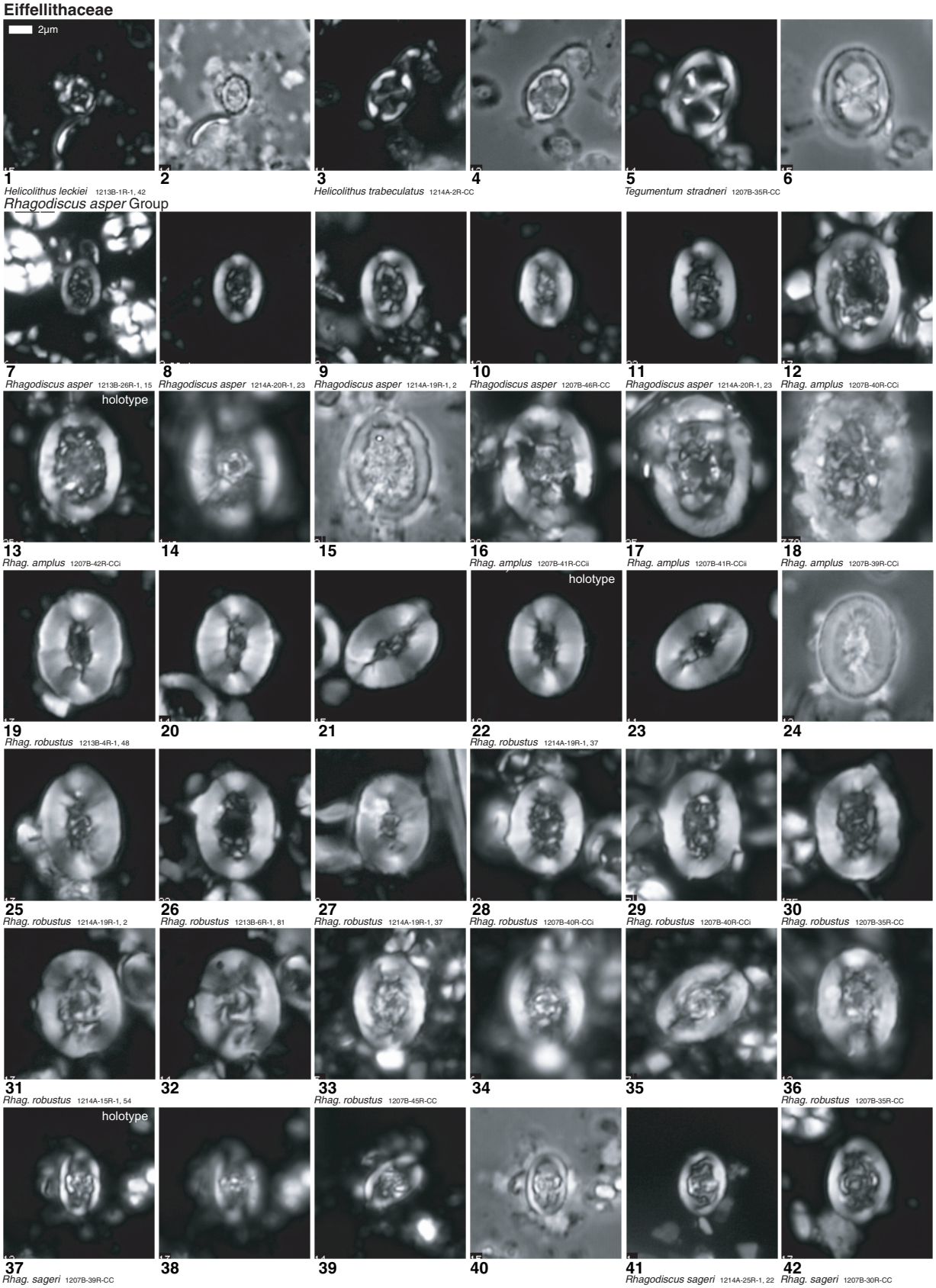

Plate P5. Rhagodiscaceae, ?Parhabdolithaceae, Stephanolithiaceae. Images with black background are cross-polarized light images; those with light backgrounds are phase contrast images. **1–6.** *Rhagodiscus sageri;* (1–3) Sample 198-1213B-1R-1, 42 cm, (4–6) Sample 198-1270B-30R-CC. **7–18.** *Rhagodiscus adinfinitus;* (7–9) Sample 198-1213B-27R-1, 38 cm, (10) Sample 198-1213B-27R-1, 1 cm, (11–13, 17, 18) Sample 198-1213B-26R-1, 15 cm, (14) Sample 198-1213B-26R-1, 17 cm, (15) holotype (Sample 198-1213B-25R-1, 26 cm), (16) Sample 198-1213B-25R-1, 26 cm. **19–21.** *Rhagodiscus infinitus;* (19, 20) Sample 198-1214A-24R-1, 72 cm, (21) Sample 198-1214A-25R-1, 22 cm. **22, 23.** *Rhagodiscus dekaenelii;* (22) Sample 198-1213B-15R-1, 34 cm, (23) Sample 198-1213B-12R-1, 9 cm. **24.** *Rhagodiscus achlyostaurion* (Sample 198-1213A-20R-CC). **25.** *Rhagodiscus angustus* (Sample 198-1213B-13R-CC). **26, 27.** *Rhagodiscus pseudoangustus* (Sample 198-1214A-25R-1, 12 cm). **28.** *Percivalia fenestrata* (Sample 198-1214A-25R-1, 12 cm). **29, 30.** *Calcicalathina oblongata* (Sample 198-1214A-25R-1, 12 cm). **31–33.** *Umbria granulosa;* (31, 32) Sample 198-1213B-20R-1, 31 cm, (33) Sample 198-1213B-21R-1, 15 cm. **34, 35.** *Corollithion signum* (Sample 198-1207B-24R-CC). **36.** *Corollithion exiguum* (Sample 198-1207B-21R-CCii). **37, 38.** *Stoverius achylosus* (Sample 198-1207B-41R-CCii). **39–41.** *Rotelapillus laffittei* (Sample 198-1213B-26R-1, 15 cm); (39, 40) small. (**Plate shown on next page.**)

Plate P5 (continued). (Caption shown on previous page.)

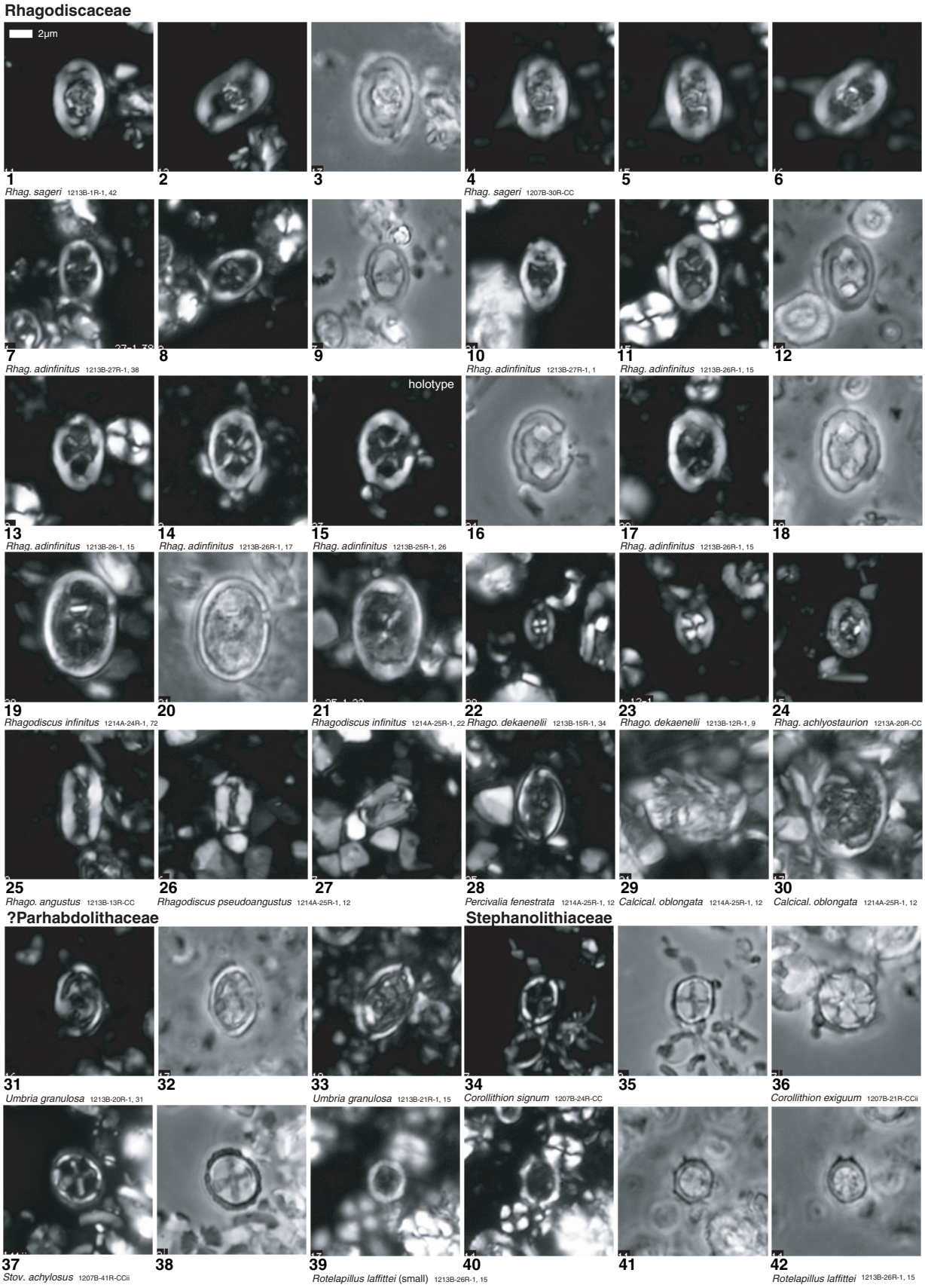

Plate P6. Stephanolithiaceae, Axopodorhabdaceae, Biscutaceae. Images with black background are cross-polarized light images; those with light backgrounds are phase contrast images. **1–6.** *Rotelapillus laffittei* (petaloid) (Sample 198-1214A-16R-1, 29 cm). **7, 8.** *Rotelapillus laffittei* (large) (Sample 198-1270B-44R-CCii). **9–12.** *Rotelapillus laffittei;* (9) Sample 198-1214A-24R-1, 46 cm, (10, 11) Sample 198-1213B-6R-1, 81 cm, (12) Sample 198-1213B-5R-1, 2 cm. **13–15.** *Stradnerlithus silvaradius* (Sample 198-1213B-25R-1, 26 cm). **16–18.** *Rotelapillus radians* (Sample 198-1213B-27R-1, 1 cm). **19, 20.** *Axopodorhabdus albianus* (Sample 198-1207B-23R-CC). **21, 22.** *Axopodorhabdus cylindratus* (Sample 198-1213B-24R-1, 37 cm). **23, 24.** *Axopodorhabdus dietzmannii* (Sample 198-1214A-20R-1, 23 cm). **25, 26.** *Cribrosphaerella ehrenbergii* (Sample 198-1213A-18R-CC). **27, 28.** *Hexapodorhabdus cuvillieri* (Sample 198-1213B-24R-1, 37 cm). **29, 30.** *Hemipodorhabdus gorkae* (Sample 198-1213B-1R-1, 42 cm). **31–34.** *Podorhabdus grassei;* (31, 32) Sample 198-1213B-27R-1, 22 cm, (33, 34) Sample 198-1213B-26R-1, 15 cm. **35, 36.** *Tetrapodorhabdus coptensis* (Sample 198-1213A-13R-CC). **37.** *Biscutum constans* (Sample 198-1207B-29R-CC). **38.** *Biscutum constans* (large) (Sample 198-1213B-3R-1, 14 cm). **39–42.** *Biscutum dorsetensis;* (39, 40, 42) Sample 198-1213B-26R-1, 15 cm, (41) Sample 198-1213B-24R-1, 37 cm. (**Plate shown on next page.**)

Plate P6 (continued). (Caption shown on previous page.)

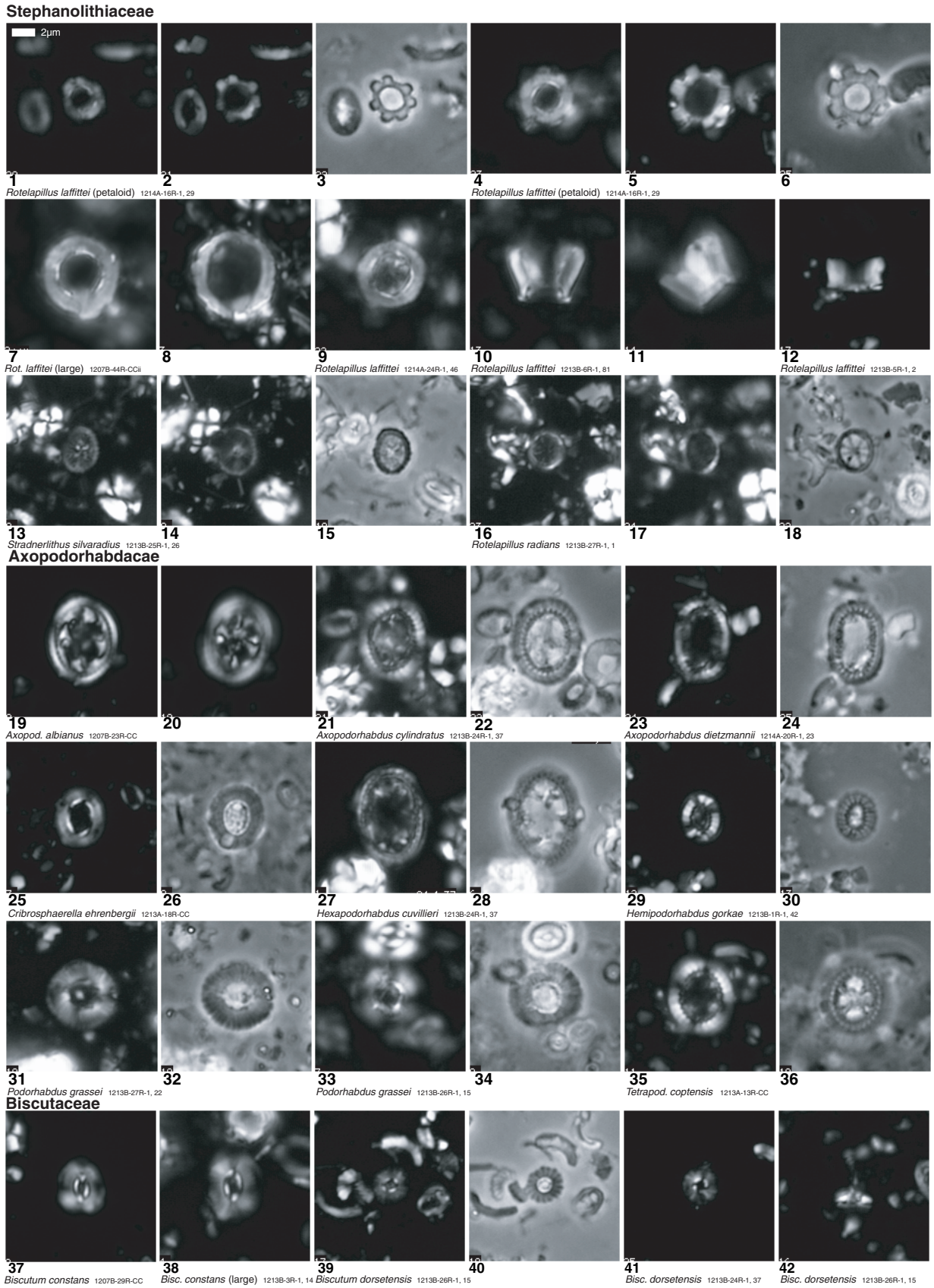

Plate P7. Biscutaceae, Cretarhabdaceae. Images with black background are cross-polarized light images; those with light backgrounds are phase contrast images. **1, 2.** *Crucibiscutum bosunensis;* (1) Sample 198-1207B-39R-CC, (2) Sample 198-1214A-20R-1, 23 cm. **3, 4.** *Discorhabdus ignotus;* (3) Sample 198-1207B-45R-CC, (4) Sample 198-1213B-5R-1, 2 cm. **5, 6.** *Discorhabdus biradiatus* (Sample 198-1213B-9R-1, 17 cm). **7–9.** *Cretarhabdus conicus;* (7) Sample 198-1213B-3R-1, 14 cm, (8, 9) Sample 198-1214A-20R-1, 23 cm. **10–13.** *Cretarhabdus* cf. *C. conicus;* (10–12) Sample 198-1214A-22R-1, 32 cm, (13) Sample 198-1207B-44R-CCi. **14, 15.** *Cretarhabdus striatus;* (14) Sample 198-1207B-40R-CCi, (15) Sample 198-1214A-7R-1, 2 cm. **16.** *Cruciellipsis cuvillieri* (Sample 198-1213B-15R-1, 34 cm). **17, 18, 24.** *Grantarhabdus bukryi* (17, 18) Sample 198-1213B-23R-1, 20 cm, (24) Sample 198-1214A-16R-1, 29 cm. **19–23.** *Flabellites oblongus;* (19) Sample 198-1213B-9R-1, 17 cm, (20) Sample 198-1207B-44R-CCii, (21, 23) Sample 198-1213B-6R-1, 81 cm, (22) Sample 198-1213B-8R-1, 3 cm. **25, 26.** *Grantarhabdus coronadventis* (Sample 198-1214A-16R-1, 29 cm). **27–30.** *Grantarhabdus meddii* (Sample 198-1213B-24R-1, 37 cm). **31.** *Helenea chiastia* (Sample 198-1213B-26R-1, 15 cm). **32–36.** *Helenea conus;* (32–34) Sample 198-1213B-14R-1, 148 cm, (35, 36) Sample 198-1213B-15R-1, 34 cm. **37–39.** *Helenea quadrata* (Sample 198-1213B-27R-1, 1 cm). **40–42.** *Helenea staurolithina;* (40) Sample 198-1213B-27R-1, 22 cm, (41) Sample 198-1213B-27R-1, 24 cm, (42) Sample 198-1213B-25R-1, 45 cm. (**Plate shown on next page.**)

Plate P7 (continued). (Caption shown on previous page.)

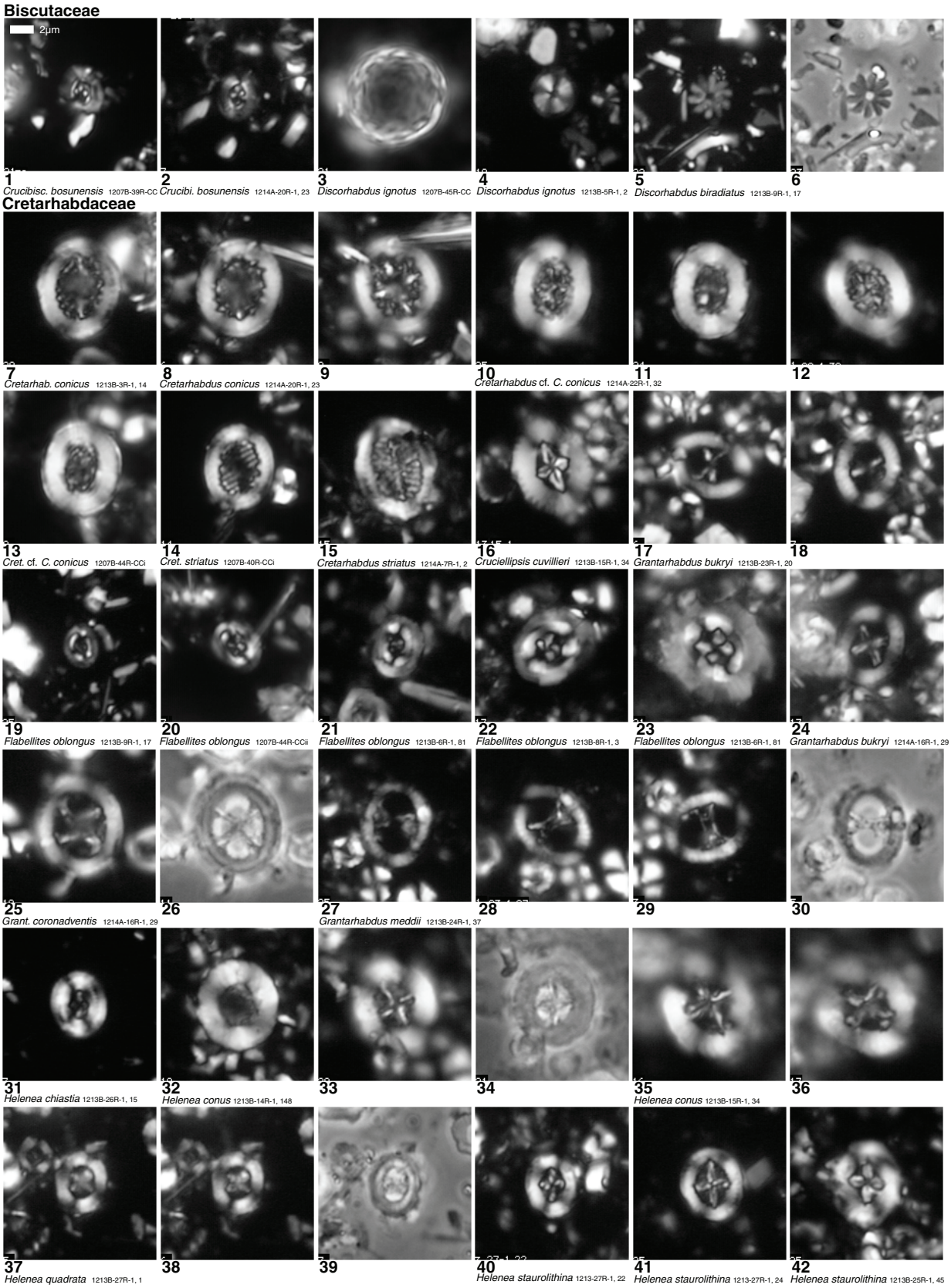

Plate P8. Cretarhabdaceae, Watznaueriaceae. Images with black background are cross-polarized light images; those with light backgrounds are phase contrast images. **1, 2.** *Retecapsa angustiforata;* (1) Sample 198-1213B-15R-1, 34 cm, (2) Sample 198-1207B-49R-CC. **3.** *Retecapsa radiata* (Sample 198-1214A-24R-1, 72 cm). **4.** *Retecapsa angustiforata* (Upper Cretaceous variety) (Sample 198-1207B-46R-CC). **5, 6.** *Retecapsa crenulata;* (5) Sample 198-1213A-11R-CC, (6) Sample 198-1213B-18R-1, 1 cm. **7, 8.** *Retecapsa* cf. *R. crenulata* (Sample 198-1213A-18R-CC). **9, 10.** *Retecapsa octofenestrata* (Sample 198-1213B-23R-1, 97 cm). **11, 12.** *Retecapsa surirella;* (11) Sample 198-1213A-11R-CC, (12) Sample 198-1207B-32R-CC. **13, 14.** *Speetonia colligata* (Sample 198-1213B-14R-1, 148 cm). **15.** Cretarhabdid (small) (Sample 198-1213B-5R-1, 2 cm). **16.** *Pickelhaube furtiva* (Sample 198-1213B-20R-1, 31 cm). **17, 18.** ?*Pickelhaube* sp. 1; (17) Sample 198-1207B-43R-CC, (18) Sample 198-1214A-20R-1, 23 cm. **19–21.** *Cylindralithus nudus;* (19, 20) Sample 198-1213B-6R-1, 81 cm, (21) Sample 198-1213A-7R-CC. **22–26.** *Diazomatolithus lehmanii;* (22, 23) Sample 198-1213B-27R-1, 1 cm, (24) Sample 198-1213B-24R-1, 37 cm, (25, 26) Sample 198-1213B-17R-1, 10 cm. **27–29.** *Cyclagelosphaera jiangii;* (27) Sample 198-1213B-9R-1, 124 cm, (28) Sample 198-1213B-18R-1, 1 cm, (20) Sample 198-1214A-25R-1, 22 cm. **30–32.** *Cyclagelosphaera brezae* (Sample 198-1213B-24R-1, 37 cm). **33.** *Cyclagelosphaera margerelii* (Sample 198-1213B-27R-1, 1 cm). 3**4–36.** *Watznaueria cynthae;* (34) Sample 198-1213B-19R-1, 10 cm, (35) Sample 198-1213B-22R-1, 58 cm, (36) Sample 198-1213B-20R-1, 31 cm. **37.** *Watznaueria britannica* (Sample 198-1213B-25R-1, 26 cm). **38–41.** *Watznaueria* sp. 1 (?*W. bayackii*); (38, 39) Sample 198-1213A-20R-CC, (40, 41) Sample 198-1214A-21R-1, 68 cm. **42.** *Watznaueria* sp. 2 (Sample 198-1207B-24R-CC). (**Plate shown on next page.**)

Plate P8 (continued). (Caption shown on previous page.)

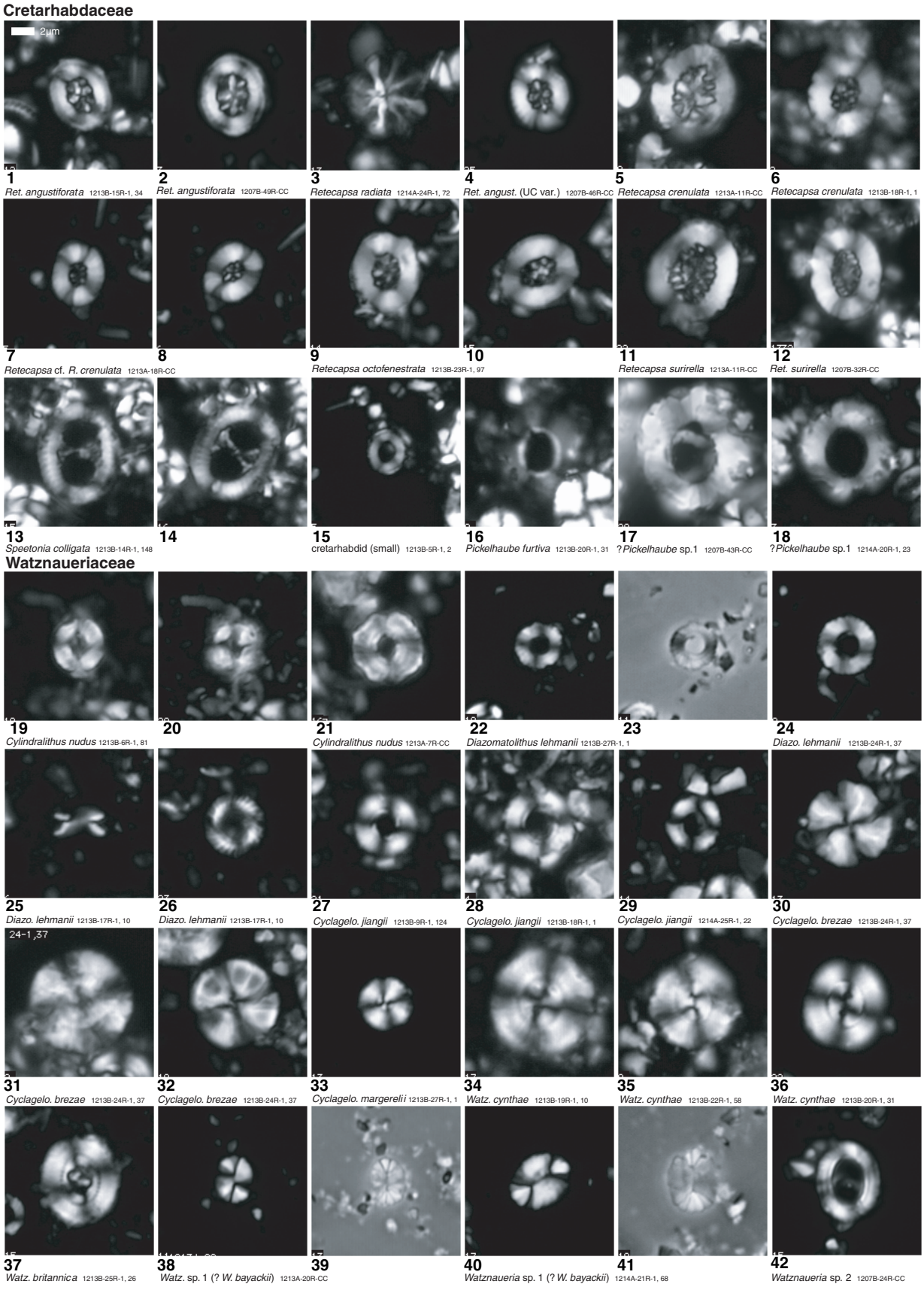

Plate P9. Tubodiscaceae. Images with black background are cross-polarized light images; those with light backgrounds are phase contrast images. **1–4.** *Manivitella pemmatoidea;* (1) Sample 198-1213B-14R-1, 148 cm, (2, 3) Sample 198-1213B-24R-1, 37 cm, (4) Sample 198-1213B-3R-1, 14 cm. **5–10.** *Manivitella* cf. *M. pemmatoidea;* (5, 6) Sample 198-1213B-23R-1, 20 cm, (7, 8) Sample 198-1213B-13R-1, 5 cm, (9, 10) Sample 198-1213B-17R-1, 10 cm. **11–23.** *Tubodiscus bellii;* (11) Sample 198-1213B-25R-1, 26 cm, (12) Sample 198-1213B-26R-1, 17 cm, (13, 15–17) Sample 198-1213B-20R-1, 31 cm, (14) holotype (Sample 198-1213B-20R-1, 31 cm), (18) Sample 198-1213B-23R-1, 97 cm, (19–23) Sample 198-1213B-26R-1, 15 cm. **24–36.** *Tubodiscus frankiae;* (24, 26–28, 31–33) Sample 198-1213B-23R-1, 20 cm, (25) holotype (Sample 198-1213B-23R-1, 20 cm), (29, 30) Sample 198-1214A-25R-1, 12 cm, (34, 35) Sample 198-1213B-22R-1, 58 cm, (36) Sample 198-1213B-10R-1, 21 cm. **37–42.** *Tubodiscus burnettiae;* (37, 38) Sample 198-1213A-12R-CC, (39, 40) Sample 198-1213A-9R-CC, (41, 42) Sample 198-1214A-25R-1, 12 cm. (**Plate shown on next page.**)

Plate P9 (continued). (Caption shown on previous page.)

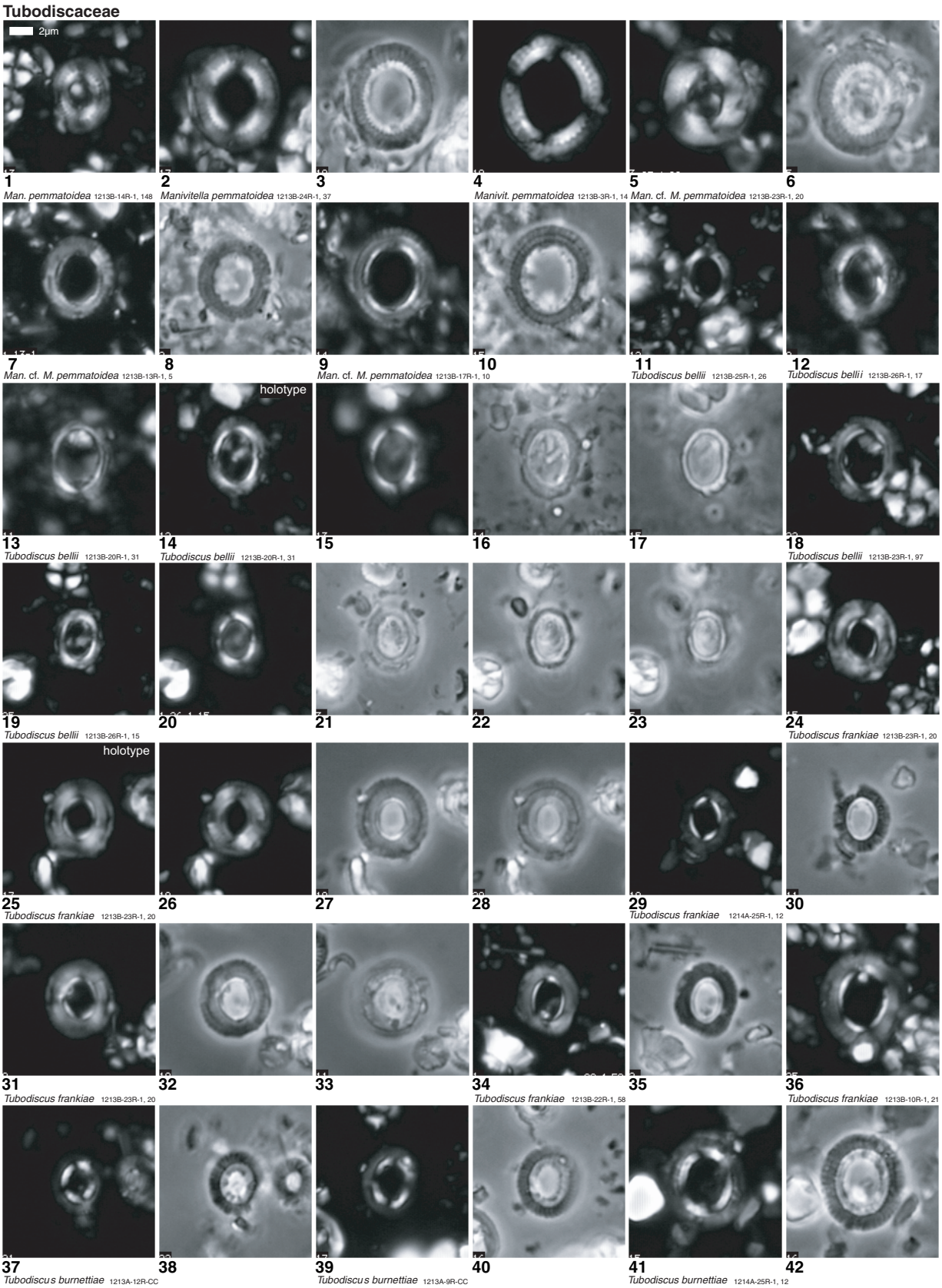

Plate P10. Tubodiscaceae, Prediscosphaeraceae, Arkhangelskiellaceae, Kamptneriaceae. Images with black background are cross-polarized light images; those with light backgrounds are phase contrast images. **1–5.** *Tubodiscus jurapelagicus;* (1, 2) Sample 198-1214A-25R-1, 22 cm, (3, 4) Sample 198-1213B-9R-1, 124 cm, (5) Sample 198-1213B-9R-1, 17 cm. 6. *Tubodiscus* cf. *T. verenae* (Sample 198-1213B-19R-1, 10 cm. **7–11.** *Prediscosphaera columnata;* (7) Sample 198-1214A-20R-1, 23 cm, (8, 9) Sample 198-1214A-17R-1, 27 cm, (10) Sample 198-1214A-2R-CC, (11) Sample 198-1213A-9R-CC. **12.** *Prediscosphaera spinosa* (Sample 198-1213A-9R-CC). **13.** *Broinsonia cenomanica*? (Sample 198-1213A-11R-CC). **14, 15.** *Broinsonia galloisii*? (Sample 198-1213A-13R-CC). **16, 17.** *Broinsonia enormis*? (Sample 198-1213A-9R-CC). **18.** *Broinsonia signata*? (Sample 198-1207B-25R-CC). **19–21.** *Gartnerago chiasta* (Sample 198-1207B-25R-CC). **22–24.** *Gartnerago ponticula;* (22) holotype (Sample 198-1207B-21R-CC), (23, 24) Sample 198-1207B-21R-CC. **25–28.** *Gartnerago theta* (Sample 198-1207B-22R-CC). **29, 30.** *Gartnerago stenostaurion* (small); (29) Sample 198-1207B-30R-CC, (30) Sample 198-1213A-21R-CC. **31–33.** *Gartnerago stenostaurion* (Sample 198-1213A-19R-CC). **34–36.** *Gartnerago stenostaurion* (Sample 198-1207B-25R-CC). **37–42.** *Mattiolia furva;* (37) holotype (Sample 198-1208A-42X-CC), (38, 39) Sample 198-1208A-42X-CC, (40–42) Sample 198-1213B-1R-1, 42 cm. (**Plate shown on next page.**)

Plate P10 (continued). (Caption shown on previous page.)

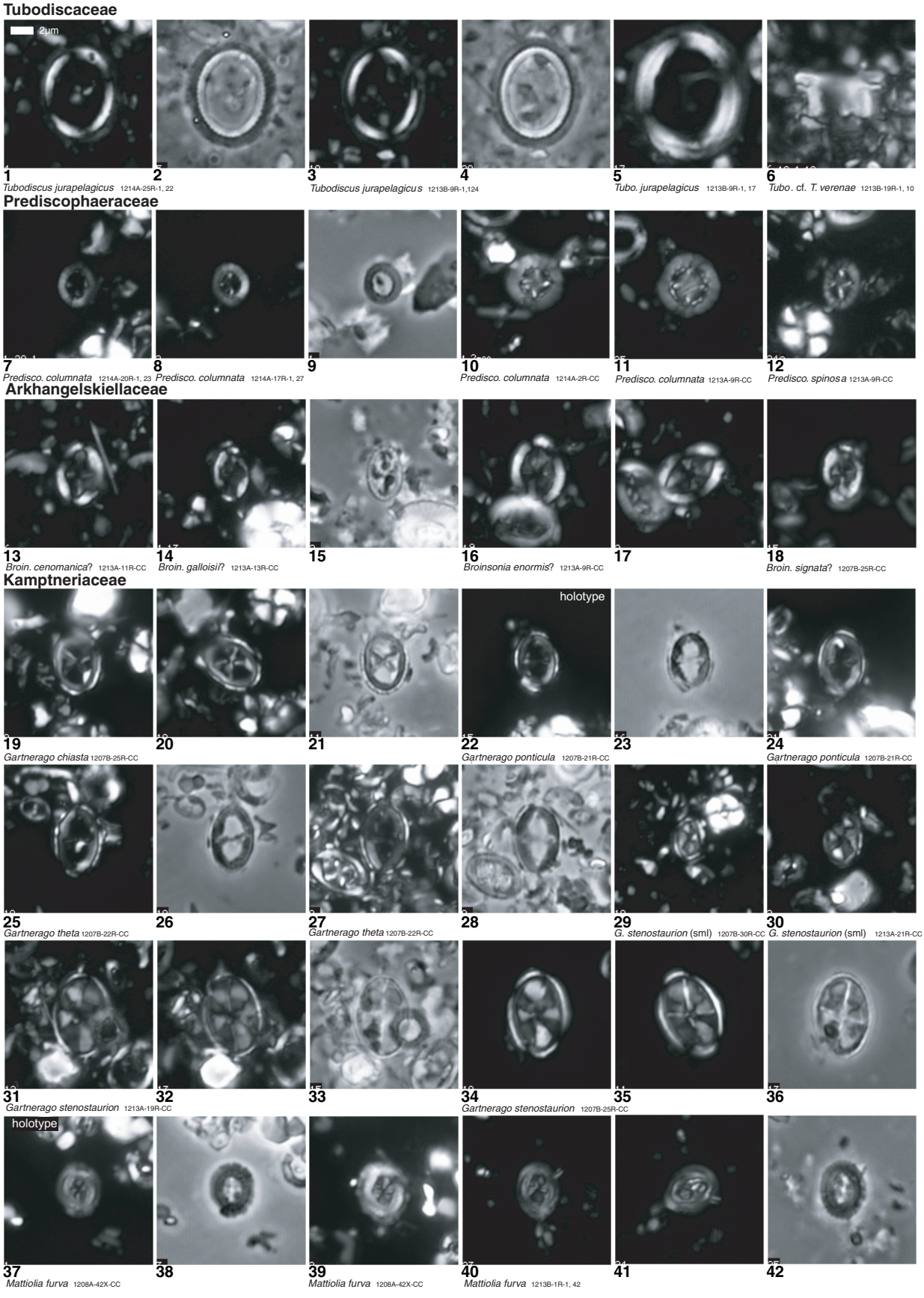

Plate P11. Haqius, Braarudosphaeraceae, Nannoconaceae. Images with black background are cross-polarized light images; those with light backgrounds are phase contrast images. **1, 2.** *Haqius circumradiatus;* (1) Sample 198-1213B-13R-1, 5 cm, (2) Sample 198-1213B-21R-1, 15 cm. **3–12.** *Haqius peltatus;* (3, 4, 6) Sample 198-1213B-27R-1, 1 cm, (5) holotype (Sample 198-1213B-27R-1, 1 cm), (7) Sample 198-1213B-22R-1, 58 cm, (8–10) Sample 198-1213B-26R-1, 15 cm, (11, 12) Sample 198-1213B-14R-1, 58 cm. **13–18.** *Haqius ellipticus;* (13, 15) Sample 198-1213B-25R-1, 45 cm, (14) Sample 198-1213B-23R-1, 97 cm, (16–18) Sample 198-1213B-25R-1, 26 cm. **19, 20.** *Calyculus* sp. 1 (Sample 198-1213B-24R-1, 37 cm). **21.** Coccolith indeterminate (Sample 198-1207B-24R-CC). **22–25.** *Braarudosphaera africana;* (22) Sample 198-1208A-42X-CC, (23, 24) Sample 198-1208A-42X-CC (side view), (25) Sample 198-1214A-7R-1, 2 cm. **26.** *Micrantholithus hoschulzii* (Sample 198-1214A-24R-1, 72 cm). **27, 28.** *Micrantholithus* segments (Sample 198-1214A-25R-1, 12 cm). **29, 31–33.** *Nannoconus truitti rectangularis* (Sample 198-1207B-41R-CCii). **30.** *Nannoconus* top (Sample 198-1207B-41R-CCii). **34, 35.** *Nannoconus abundans*? (Sample 198-1214A-24R-1, 72 cm). **36.** *Nannoconus steinmannii* (Sample 198-1214A-25R-1, 12 cm). **37, 38.** *Eprolithus floralis;* (37) Sample 198-1213A-11R-CC, (38) Sample 198-1213B-8R-1, 3 cm. **39, 40.** *Eprolithus moratus* (Sample 198-1207B-21R-CCii). **41, 42.** *Radiolithus planus* (Sample 198-1213A-20R-CC). (**Plate shown on next page.**)

Plate P11 (continued). (Caption shown on previous page.)

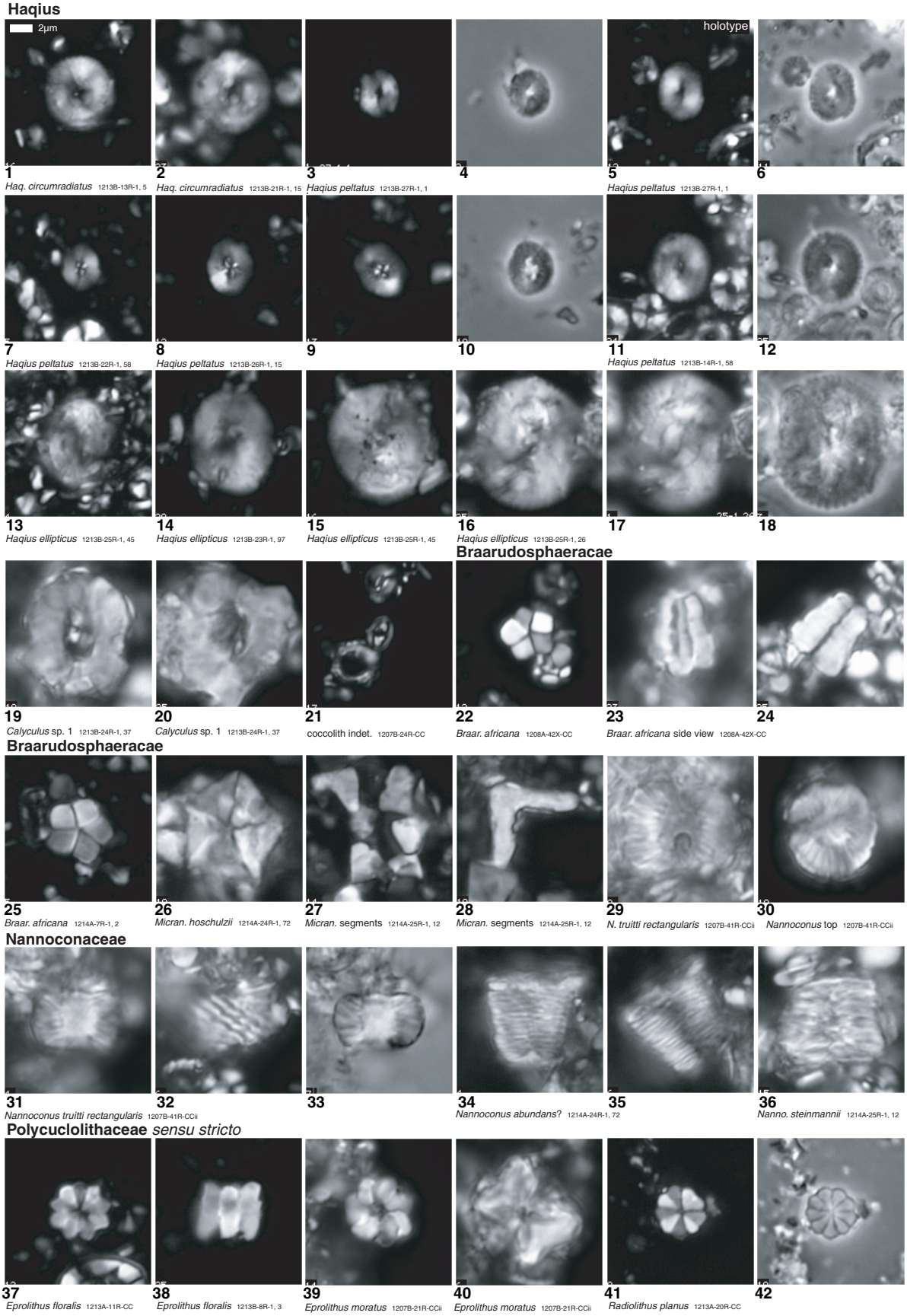

Plate P12. Polycylolithaceae sensu lato. Images with black background are cross-polarized light images; those with light backgrounds are phase contrast images. **1, 2.** *Assipetra infracretacea;* (1) Sample 198-1213B-26R-1, 15 cm, (2) Sample 198-1207B-44R-CCi. **3–12.** *Assipetra terebrodentarius terebrodentarius;* (3, 4) 5.0 µm (Sample 198-1214A-25R-1, 22 cm), (5, 6) 5.1 µm (Sample 198-1213B-9R-1, 17 cm), (7) 6.6 µm (Sample 198-1213B-8R-1, 3 cm), (8) 7.4 µm (Sample 198-1213B-9R-1, 17 cm), (9–12) 7.6 µm (Sample 198-1214A-24R-1, 46 cm). **13–18.** *Assipetra terebrodentarius youngii;* (13, 14) side view; 8.9 µm (Sample 198-1214A-21R-1, 103 cm), (15) 9.7 µm (Sample 198-1213B-7R-1, 93 cm), (16) 10.8 µm (Sample 198-1213B-7R-1, 93 cm), (17) 12.6 µm (Sample 198-1214A-18R-1, 30 cm), (18) 12.7 µm (Sample 198-1214A-22R-1, 32 cm). **19, 20.** *Hayesites* cf. *H. albiensis* (Sample 198-1214A-19R-1, 2 cm). **21–24.** *Hayesites irregularis* (Sample 198-1213B-5R-1, 2 cm). **25–27.** *Kokia borealis* (Sample 198-1213B-19R-1, 10 cm). **28–36.** *Kokia stellata* (Sample 198-1213B-27R-1, 38 cm) (28) holotype (7.0 µm), (29, 30) 7.0 µm, (31, 32) 4.6 µm, (33–36) 7.9 µm. **37–39.** *Kokia* cf. *K. stellata;* (37) Sample 198-1214A-25R-1, 22 cm, (38, 39) Sample 198-1214A-24R-1, 72 cm. **40, 41.** *"Nannoconus" ligius* (Sample 198-1213B-10R-1, 21 cm). **42.** ?*"Nannoconus" ligius* (Sample 198-1213B-22R-1, 15 cm). (**Plate shown on next page.**)

Plate P12 (continued). (Caption shown on previous page.)

Polycyclolithaceae *sensu lato*

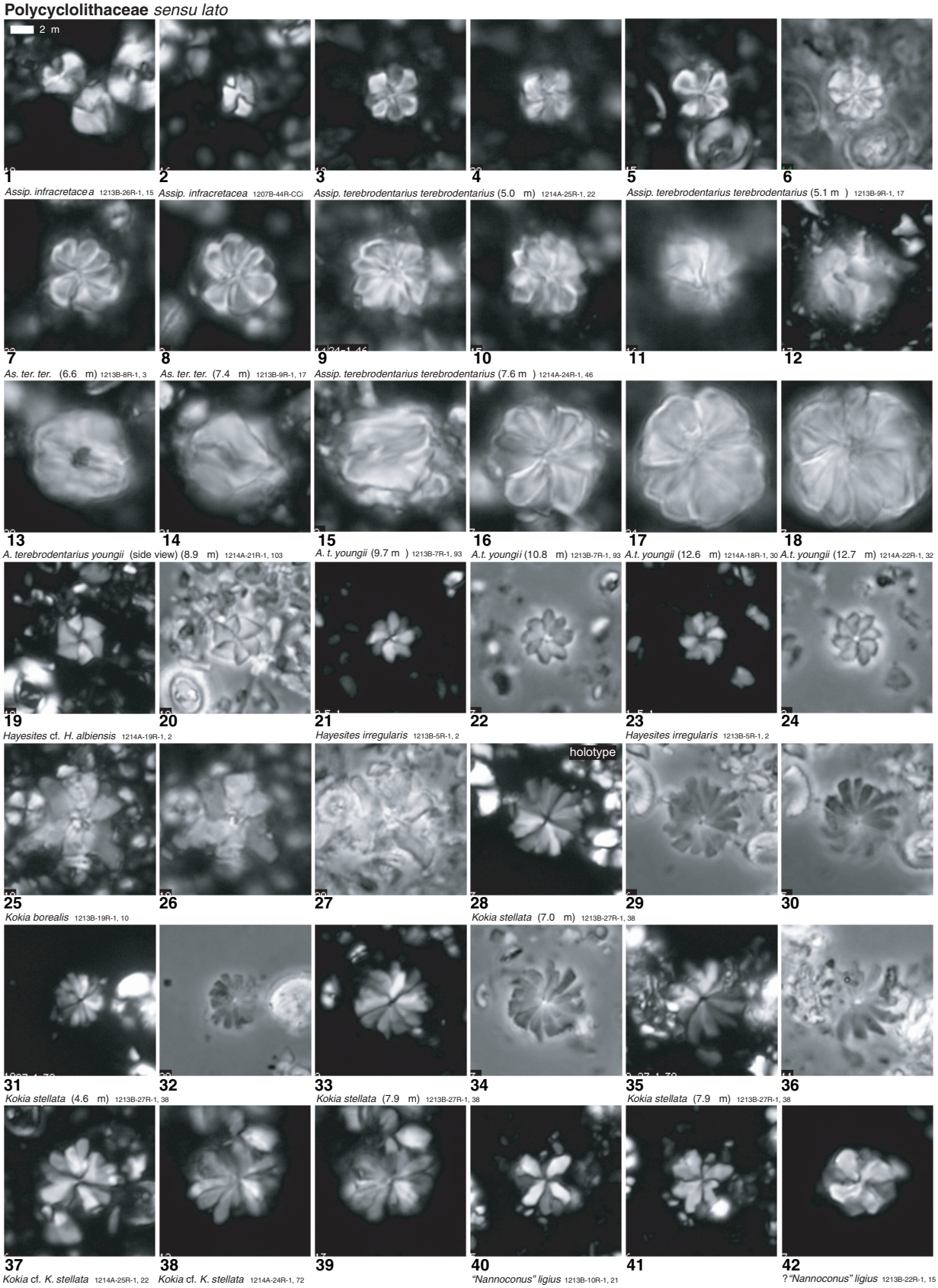

1 *Assip. infracretacea* 1213B-26R-1, 15
2 *Assip. infracretacea* 1207B-44R-CCi
3 *Assip. terebrodentarius terebrodentarius* (5.0 m) 1214A-25R-1, 22
4
5 *Assip. terebrodentarius terebrodentarius* (5.1 m) 1213B-9R-1, 17
6
7 *As. ter. ter.* (6.6 m) 1213B-8R-1, 3
8 *As. ter. ter.* (7.4 m) 1213B-9R-1, 17
9 *Assip. terebrodentarius terebrodentarius* (7.6 m) 1214A-24R-1, 46
10
11
12
13 *A. terebrodentarius youngii* (side view) (8.9 m) 1214A-21R-1, 103
14
15 *A. t. youngii* (9.7 m) 1213B-7R-1, 93
16 *A.t. youngii* (10.8 m) 1213B-7R-1, 93
17 *A.t. youngii* (12.6 m) 1214A-18R-1, 30
18 *A.t. youngii* (12.7 m) 1214A-22R-1, 32
19 *Hayesites* cf. *H. albiensis* 1214A-19R-1, 2
20
21 *Hayesites irregularis* 1213B-5R-1, 2
22
23 *Hayesites irregularis* 1213B-5R-1, 2
24
25 *Kokia borealis* 1213B-19R-1, 10
26
27
28 *Kokia stellata* (7.0 m) 1213B-27R-1, 38
29
30
31 *Kokia stellata* (4.6 m) 1213B-27R-1, 38
32
33 *Kokia stellata* (7.9 m) 1213B-27R-1, 38
34
35 *Kokia stellata* (7.9 m) 1213B-27R-1, 38
36
37 *Kokia* cf. *K. stellata* 1214A-25R-1, 22
38 *Kokia* cf. *K. stellata* 1214A-24R-1, 72
39
40 *"Nannoconus" ligius* 1213B-10R-1, 21
41
42 ? *"Nannoconus" ligius* 1213B-22R-1, 15

Plate P13. Polycyclolithaceae sensu lato, Lapideacassaceae. Images with black background are cross-polarized light images; those with light backgrounds are phase contrast images. **1–6.** *Rucinolithus wisei;* (1, 2) Sample 198-1213B-22R-1, 58 cm, (3, 4) Sample 198-1213B-19R-1, 10 cm, (5, 6) Sample 198-1213B-14R-1, 148 cm. **7.** *Lapideacassis glans* (Sample 198-1214A-16R-1, 29 cm). **8–10, 12.** *Lapideacassis mariae;* (8) Sample 198-1213B-9R-1, 47 cm, (9) Sample 198-1214A-19R-1, 2 cm, (10) Sample 198-1207B-30R-CC, (12) Sample 198-1213B-9R-1, 73 cm. **11.** *Lapideacassis mariae/biocornutus* (Sample 198-1214A-16R-1, 29 cm). **13–15.** *Lithraphidites acutus;* (13) Sample 198-1213A-8R-CC, (14, 15) Sample 198-1207B-23R-CC. **16.** *Lithraphidites bollii* (Sample 198-1214A-25R-1, 12 cm). **17.** *Microrhabdulus decoratus* (Sample 198-1207B-21R-CCii). **18–21.** *Lithraphidites alatus;* (18–20) Sample 198-1207B-45R-CC, (21) Sample 198-1214A-19R-1, 37 cm. **22.** *Lithraphidites carniolensis* (Sample 198-1207B-45R-CC).